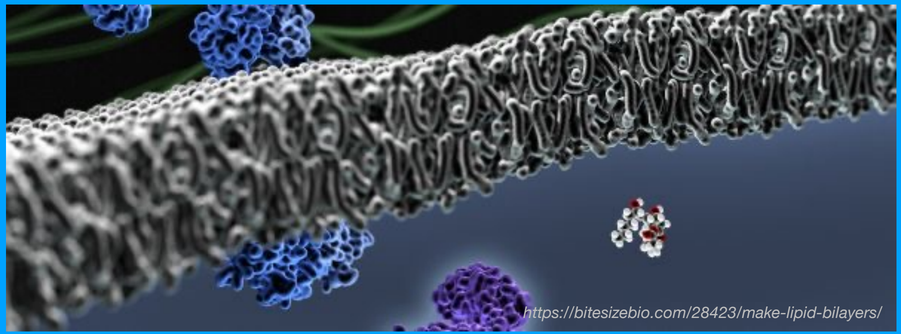

Structure of model biological membranes with neutron scattering: present developments and future perspectives

Giovanna Fragneto
European Spallation Source ERIC

Uncharged, subatomic particles found in atomic nuclei
Approx. mass of neutron 1.67×10^{-27} kg, v = 2.2 km/s at RT
energy ~ 0.025 eV, wave-particle duality, ***λ = 0.18 nm at RT***

Neutrons: An ideal probe at the atomic scale

- Like X-rays thermal neutrons possess the right wavelengths.
- In addition neutrons possess the ideal energies for spectroscopy of thermal fluctuations.

From 1000 nm

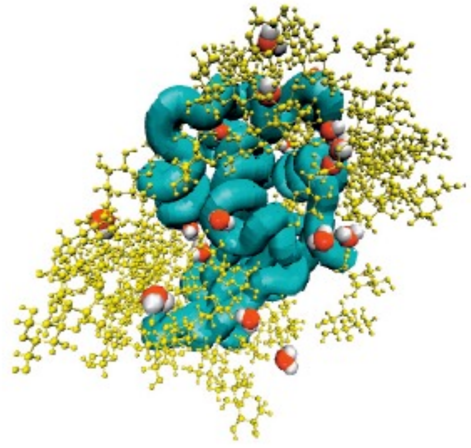

Cold Neutrons

$$\Delta\phi = \frac{\Delta y}{D} = \frac{\lambda}{d}$$

The information is encoded in the change of direction and speed of the neutrons as they path through the material.

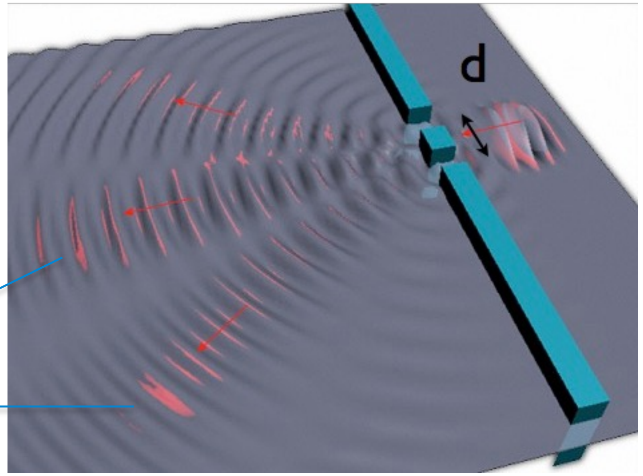

Up to 0.001 nm

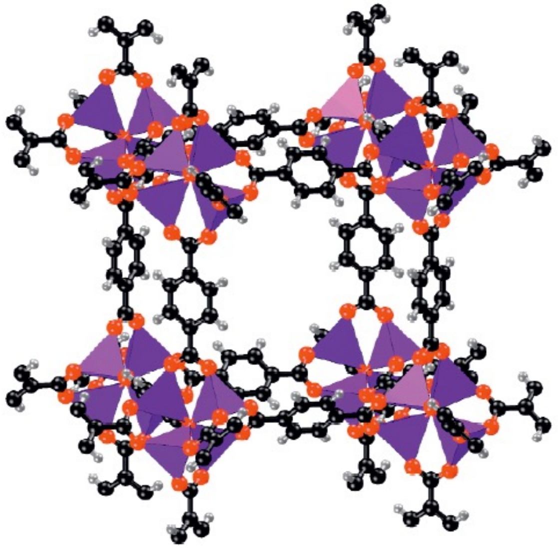

Hot Neutrons

Why use neutrons to study soft an biological material?

Neutrons interact with nuclei

- are sensitive to light atoms, particularly hydrogen
- can exploit isotopic substitution, especially H/D
- ‘see‘ materials differently to X-rays, complementary

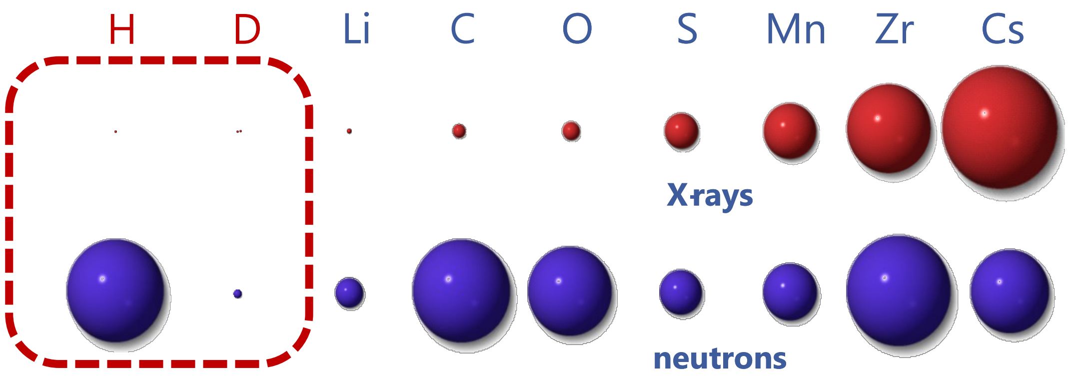

Polyelectrolyte + surfactant complex

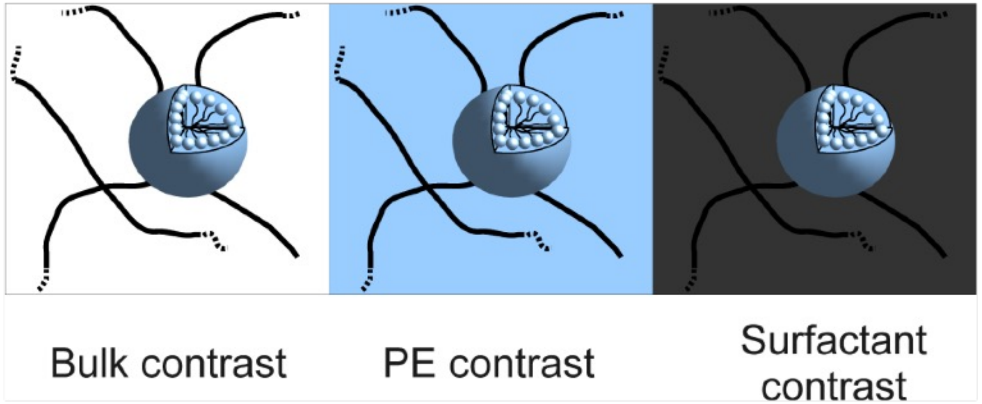

Hoffmann et al. J. Chem. Phys. 2015.

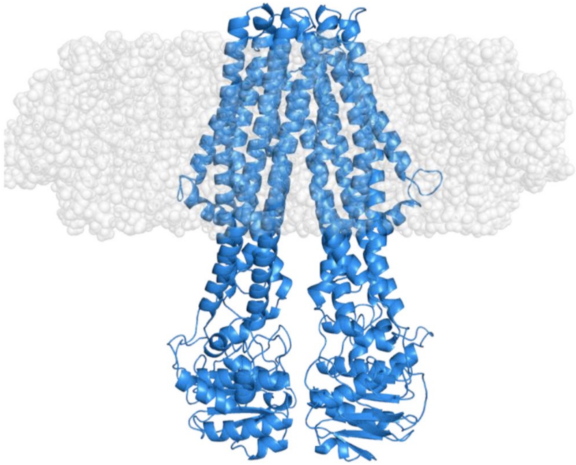

Josts et al. Structure 2018

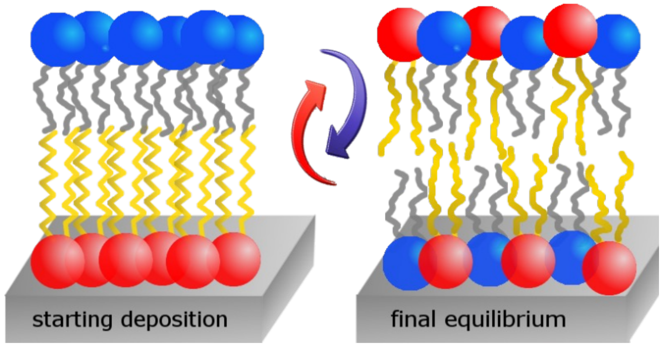

Gerelli Y., et al., Langmuir 2012

Neutrons are a neutral particle

- are highly penetrating → *buried interfaces*
- can be used as non-destructive probes
- can be used to study samples in extreme environments

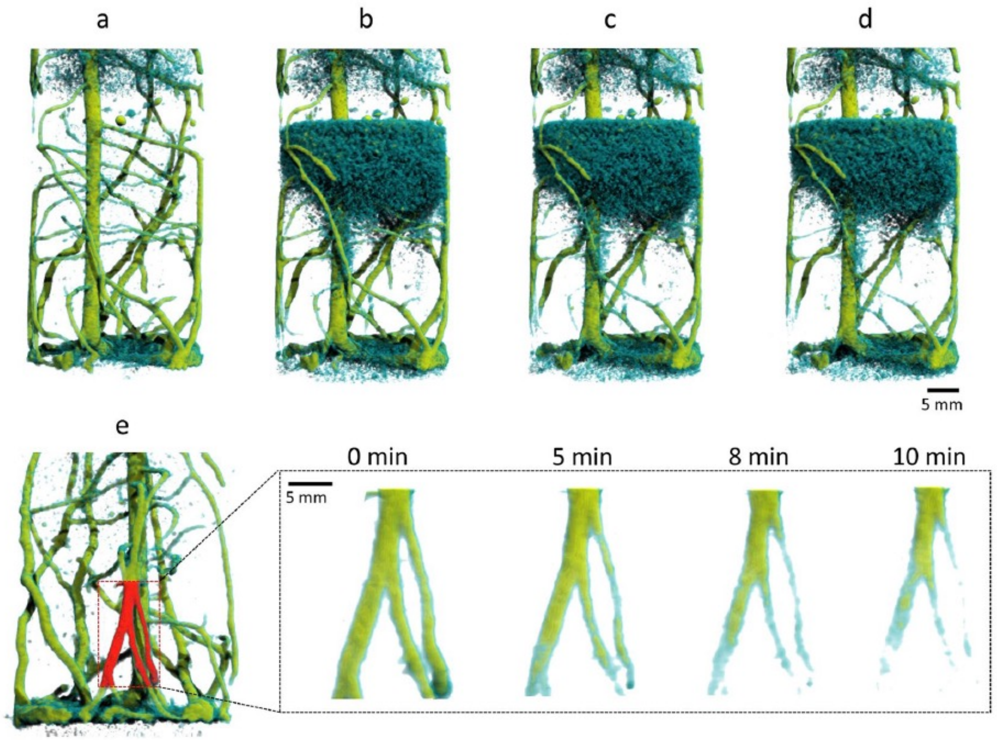

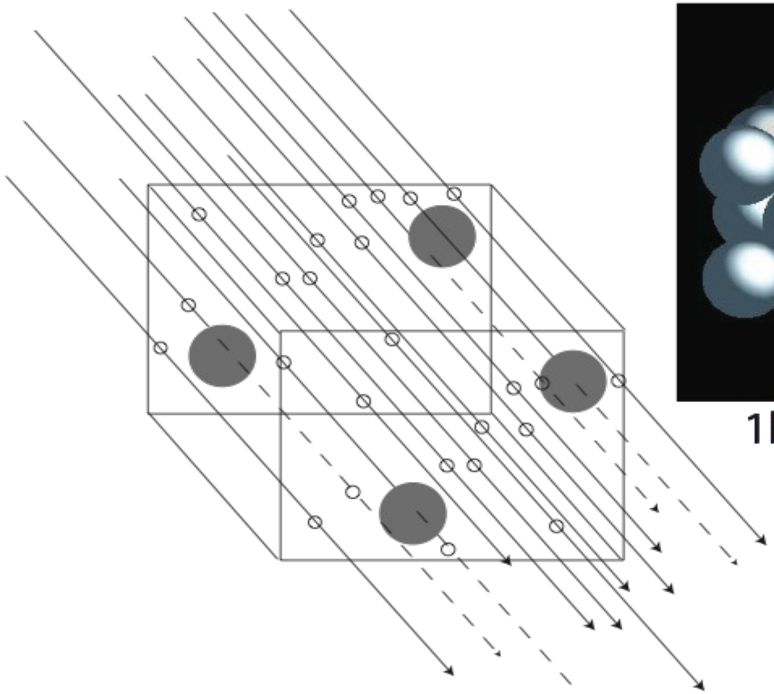

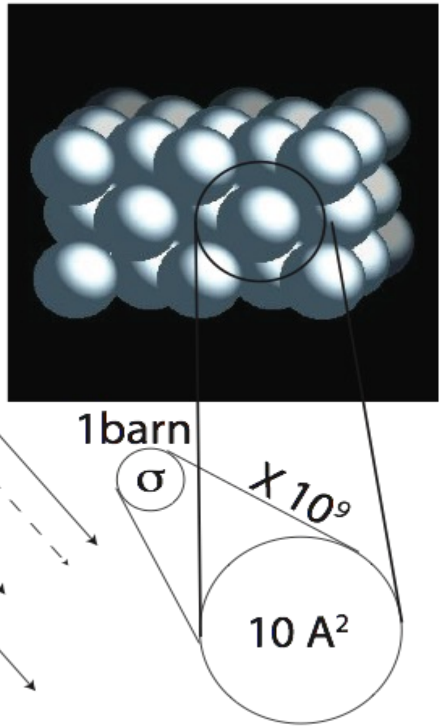

Neutrons have a spin, therefore a sensitivity to magnetic properties

Beams of polarized neutrons (in which all the spins are aligned)

allow the characterization of exotic materials with complex structure and behavior

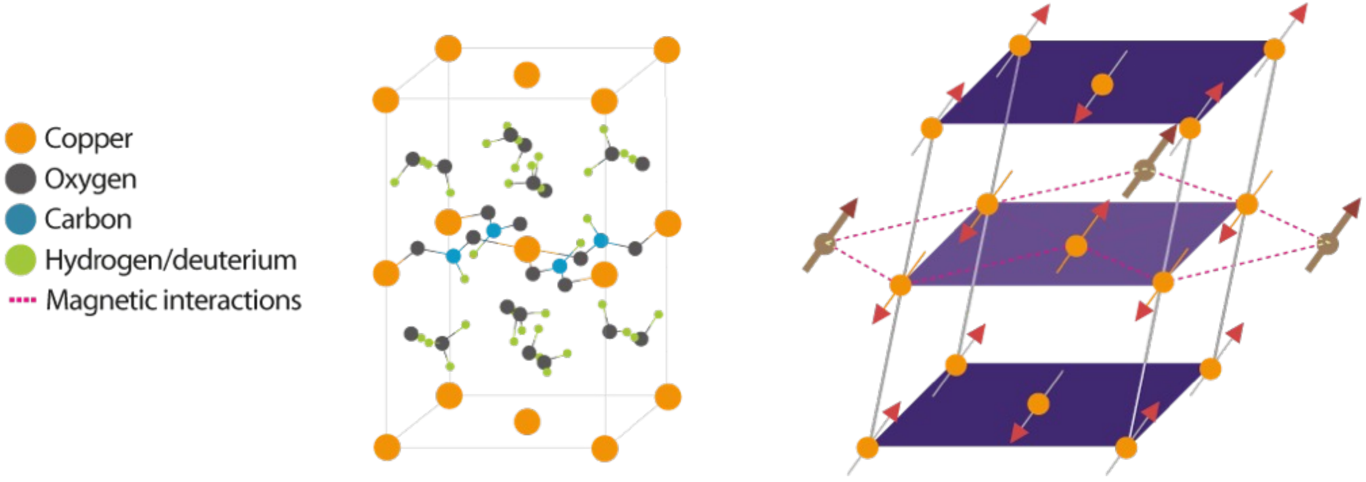

Copper formate:
crystal structure vs magnetic structure

Arrangement of spins in two different types of skyrmions

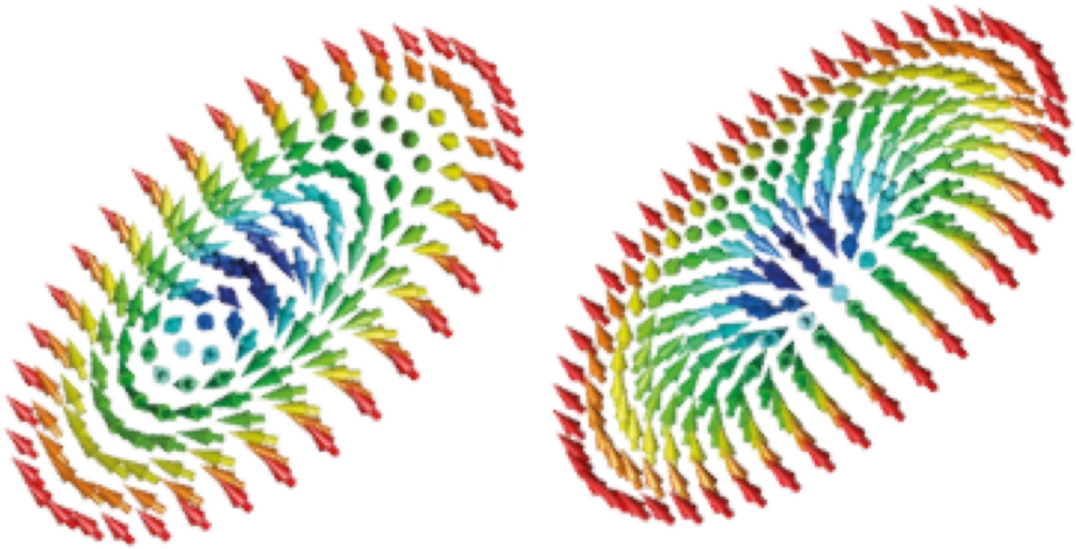

I. Kezsmarki et al., Nature Materials, 2015, **14**, 1116; DOI: 10.1038/nmat4402ptions.

Schematic view of elastic neutron scattering spectra

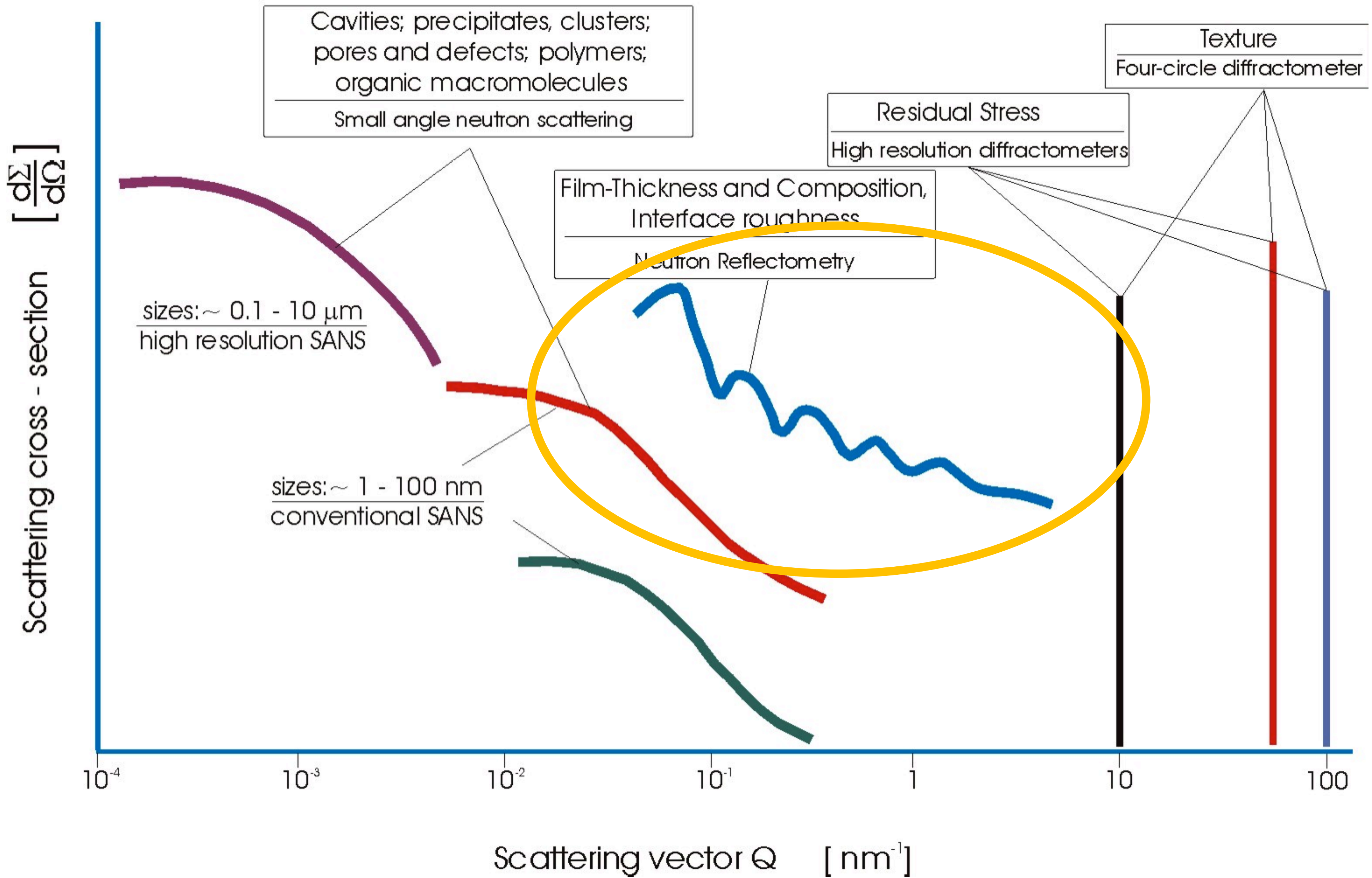

Specular Reflectivity

- Thickness of layers at interfaces
- Roughness/interdiffusion
- Composition in the direction normal to the interface

$\theta_i = \theta_f$

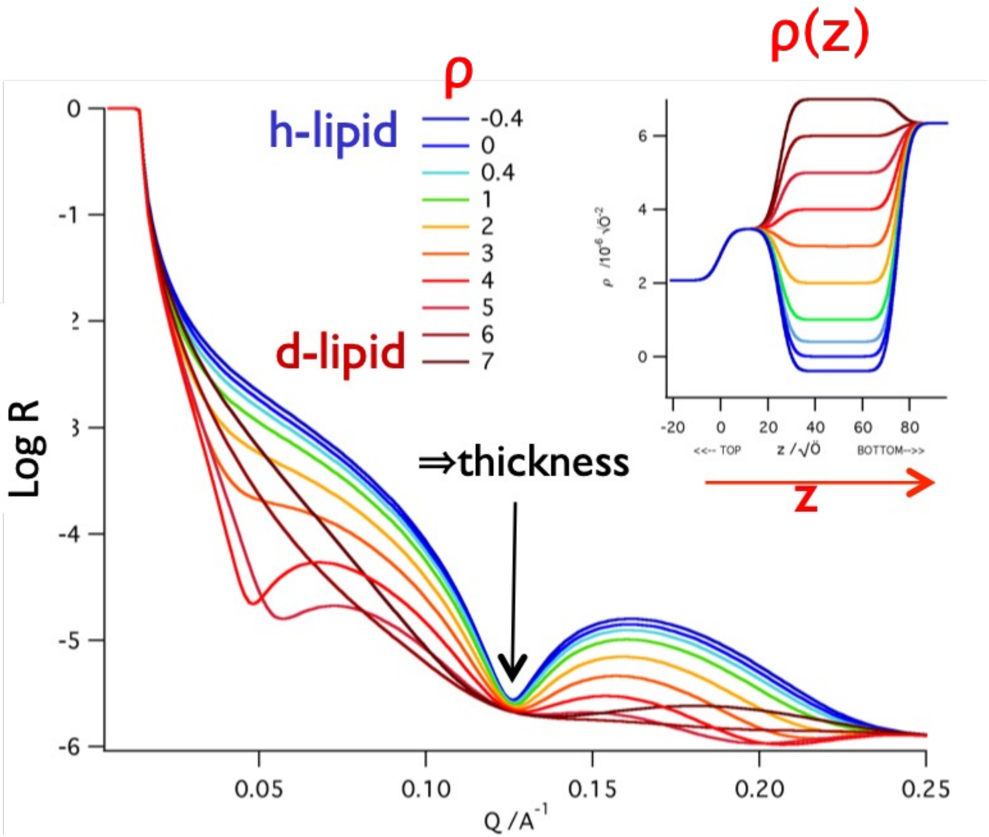

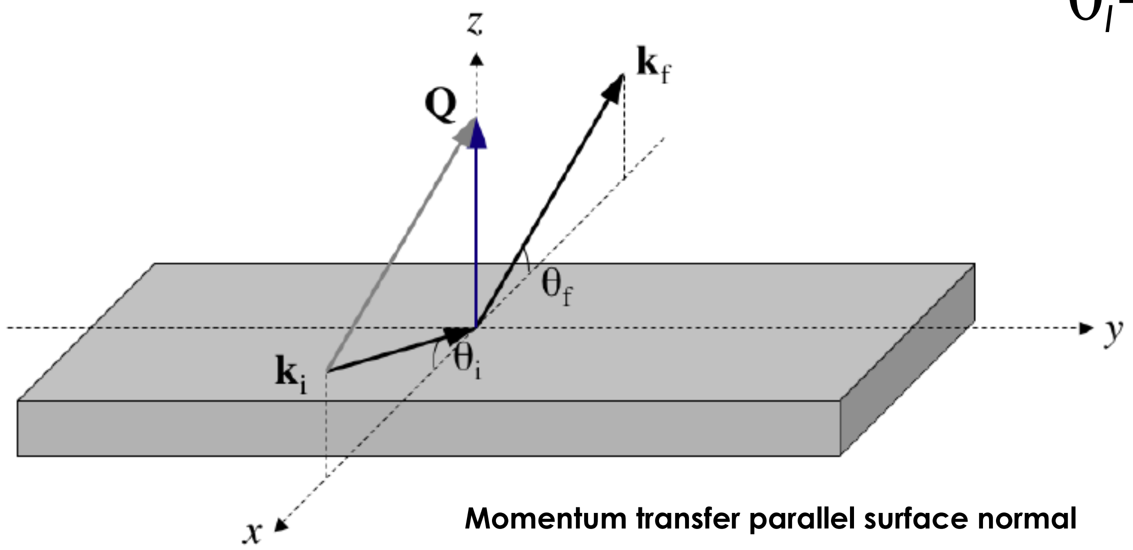

Momentum transfer parallel surface normal

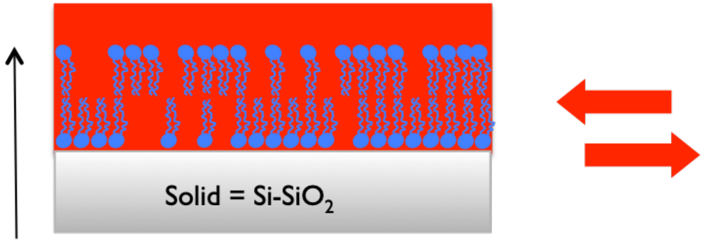

Model structure of lipid membrane
= layered model of structure & composition

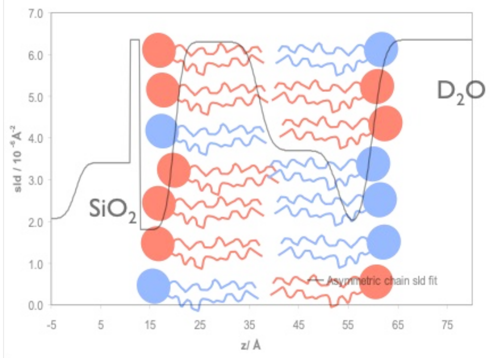

Scattering Length Density Profile

Off-specular Reflectivity

In-plane features (height fluctuations, domains, holes …) can be probed by ***off-specular*** *measurements: for thin films synchrotron radiation is more suitable*

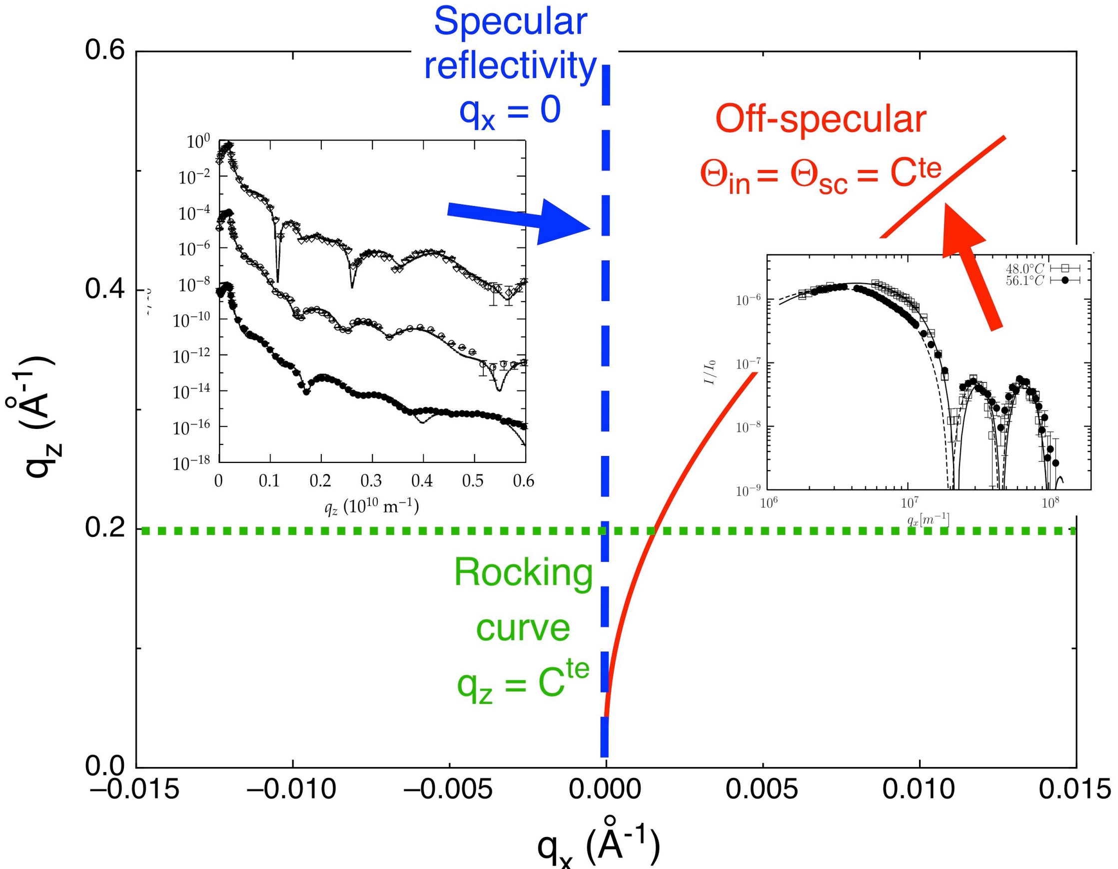

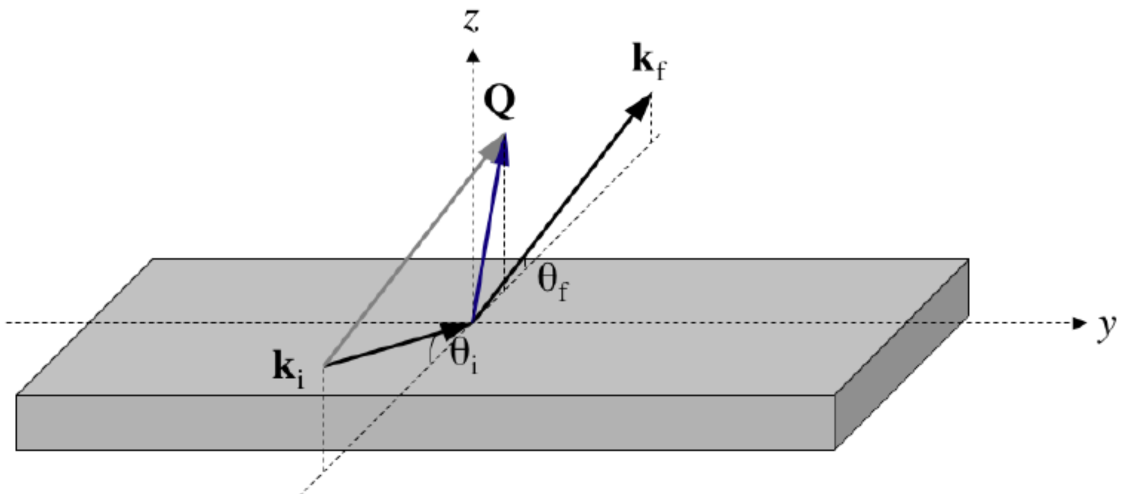

Momentum transfer in xz plane

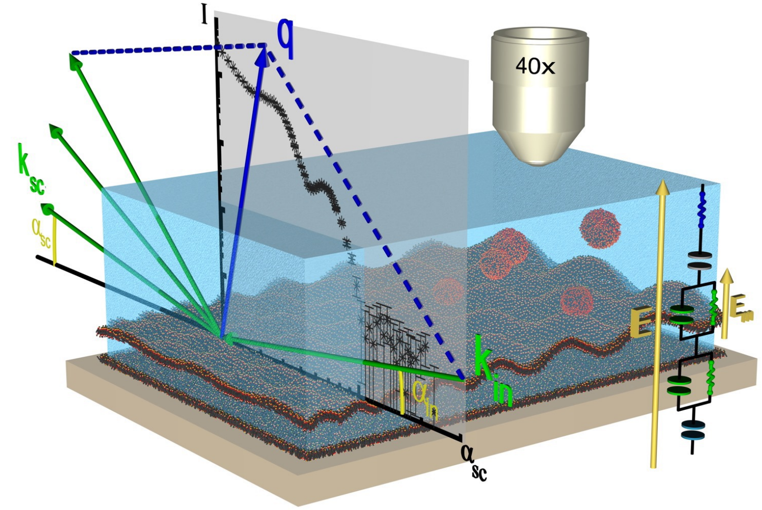

Specular reflectivity measurements

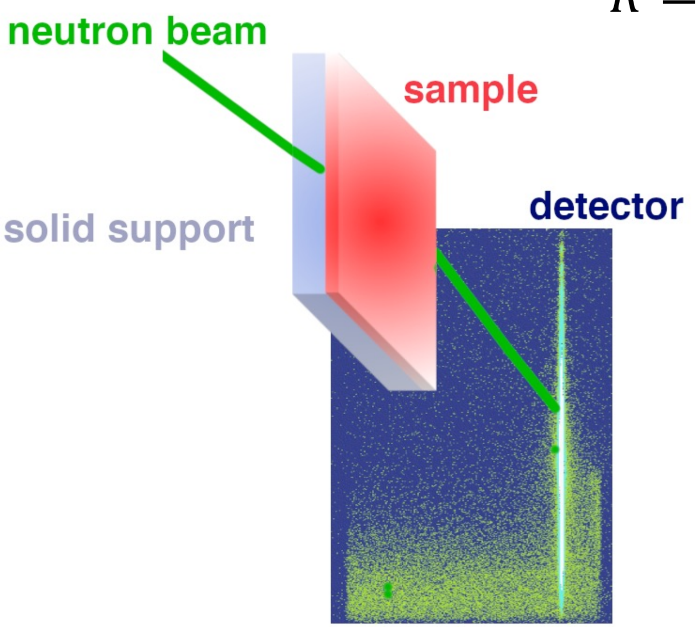

$$R = \frac{I_r}{I_0}$$

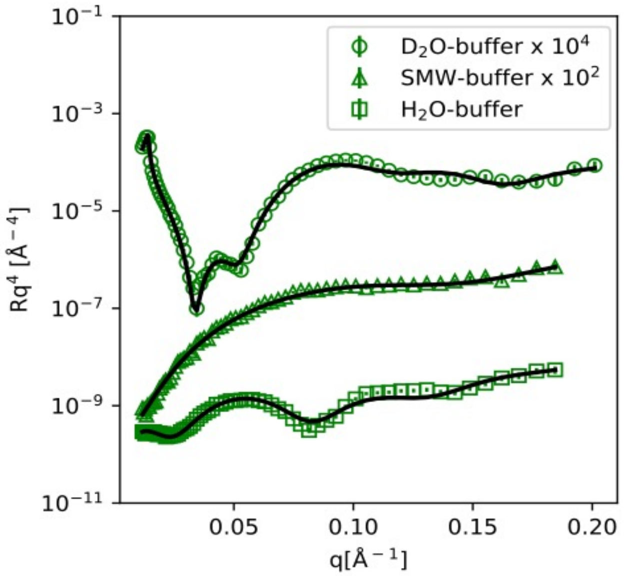

$$q = \frac{4\pi}{\lambda} sin\theta$$

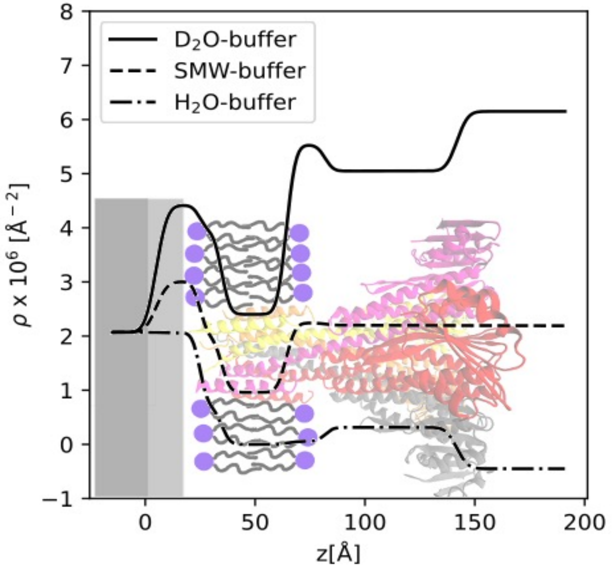

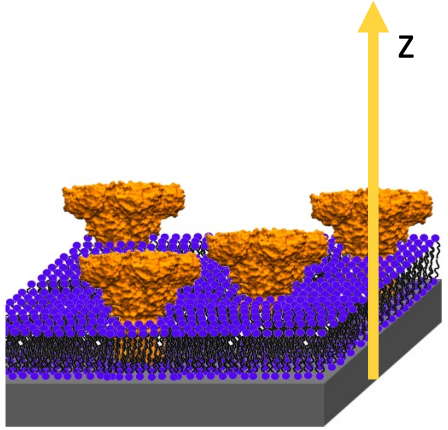

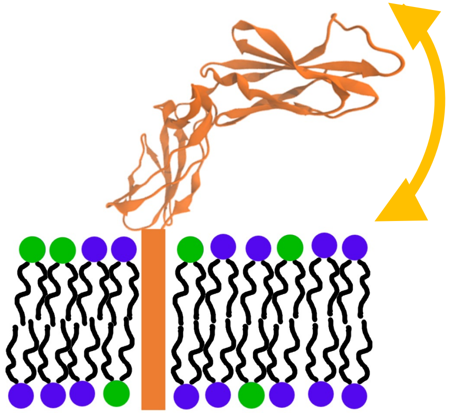

- Analysis done by model fitting
- Isotopic substitution and multiple contrast measurements used to improve resolution

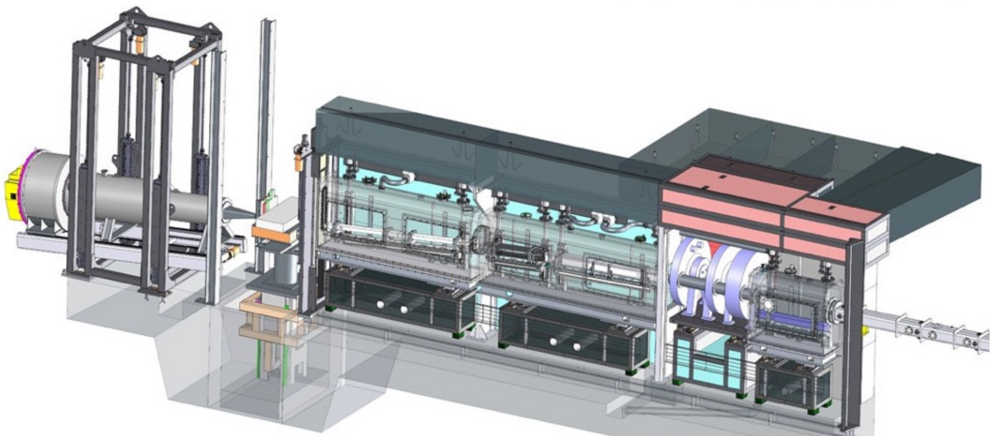

Specular reflectivity measurements

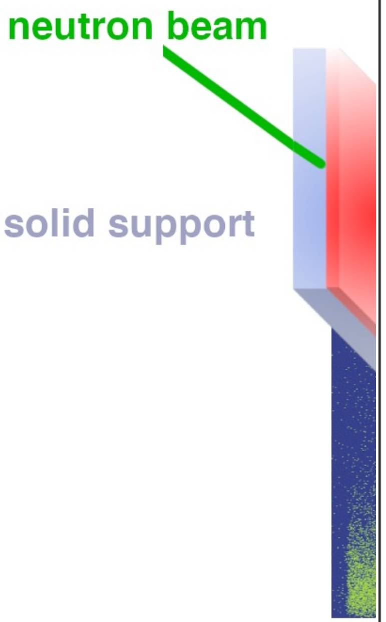

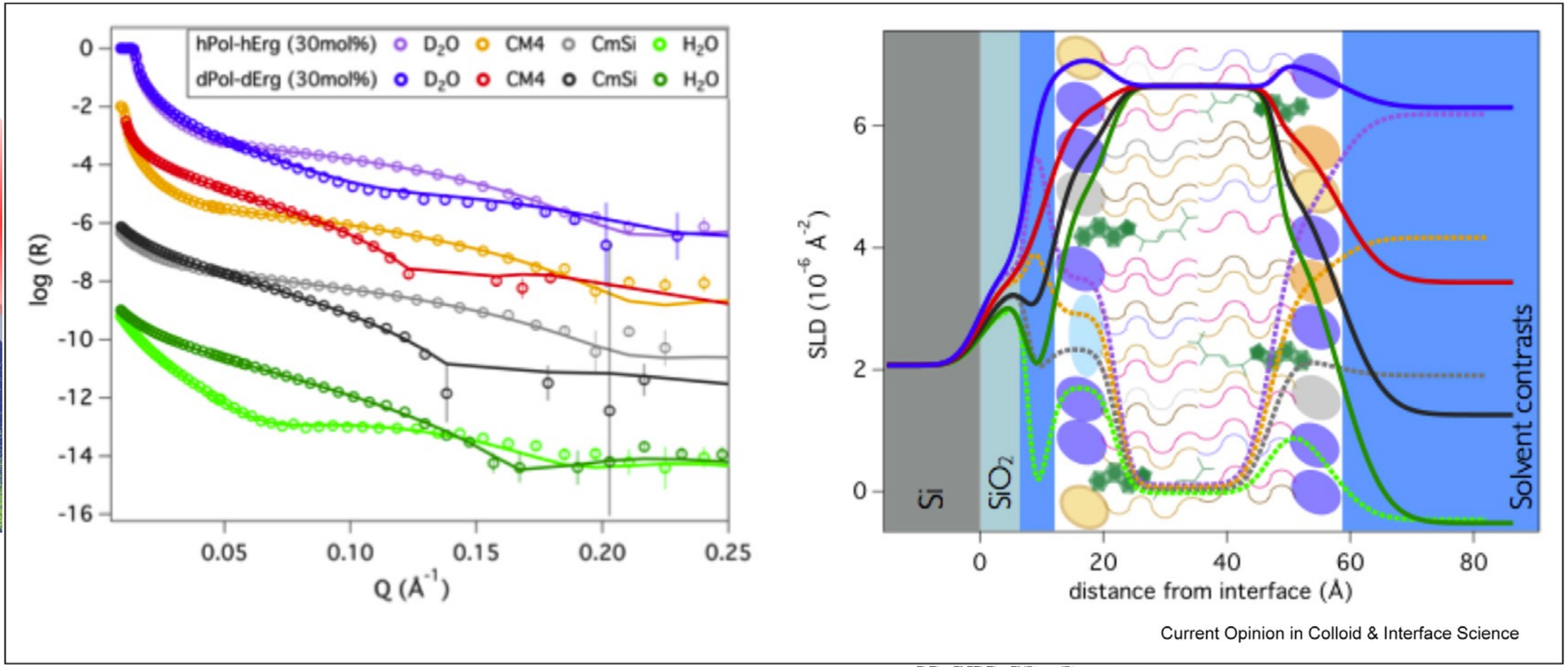

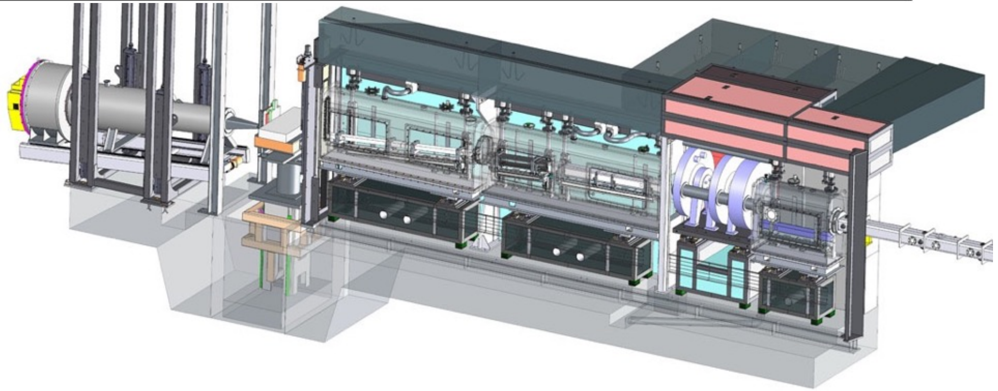

- Isotopic substitution and multiple contrast measurements used to improve resolution

Mechanisms at cell membranes

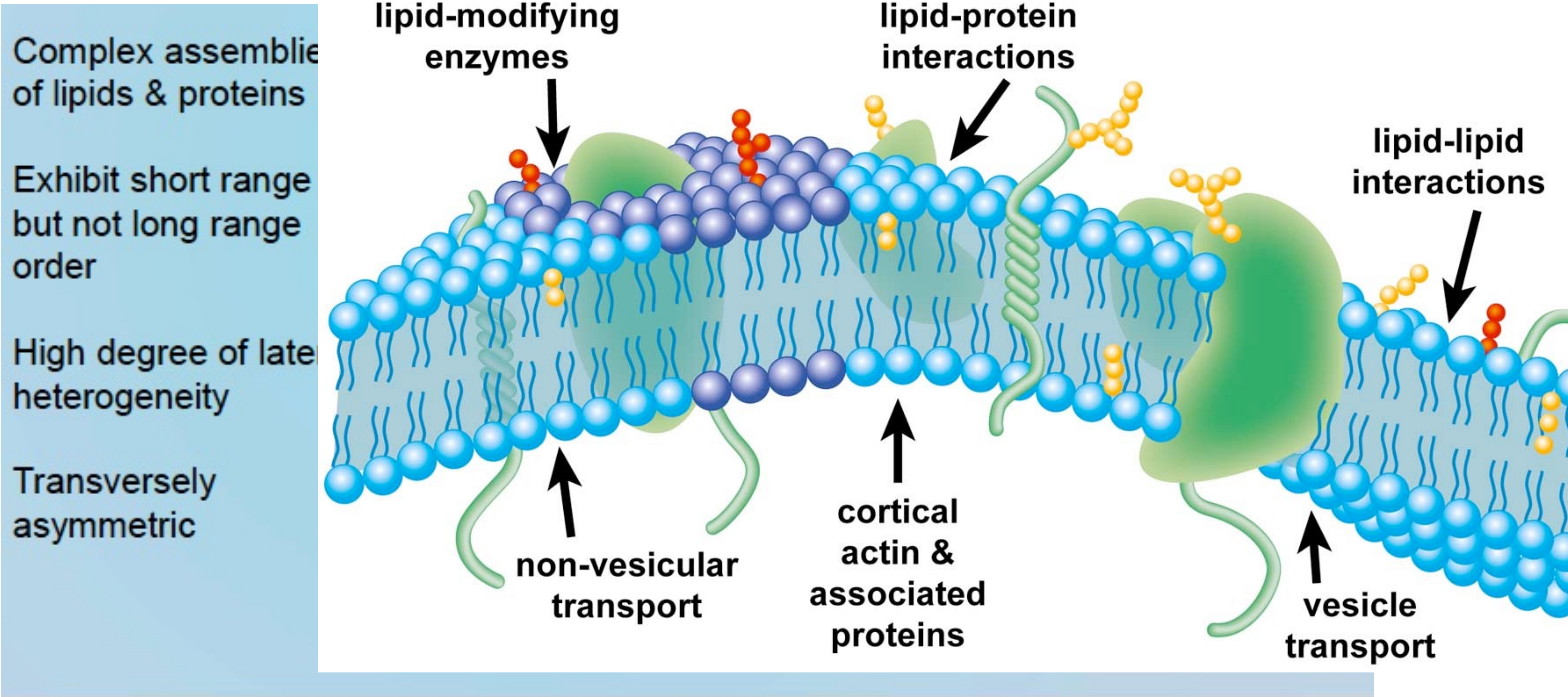

Lipid scaffold composed by a large variety of lipid species and levels of chain unsaturation, often difficult to synthesise chemically. Because of the complexity model membrane systems are used for fundamental studies.

PARTNERSHIP FOR SOFT CONDENSED MATTER

developing model membrane systems since 1997…

Total surface of membranes covers an area of 30,000 m² in our body

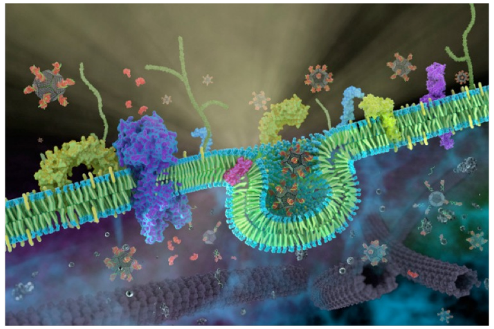

Function of membrane proteins : dependent on membrane composition, lipid-protein interaction, lipid mediated protein-protein interaction

Pharmacological interest : Drug transport through membranes (dependent on physico-chemical membrane properties), anti-microbial peptides

Membranes may play a *direct* role in **signal transduction**

Diseases associated with changes in lipid composition (diabetes, schizophrenia, Tay-Sachs syndrome, Alzheimer, Parkinson)

Cell adhesion

Nano-biotechnology applications (biosensors, bio-coatings)

and …. **fascinating chemistry and physics!**

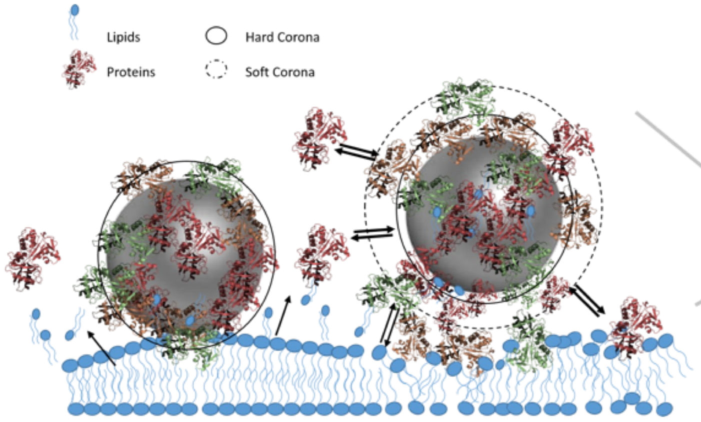

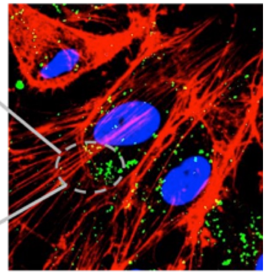

JCIS 2017

Model membranes and scattering techniques

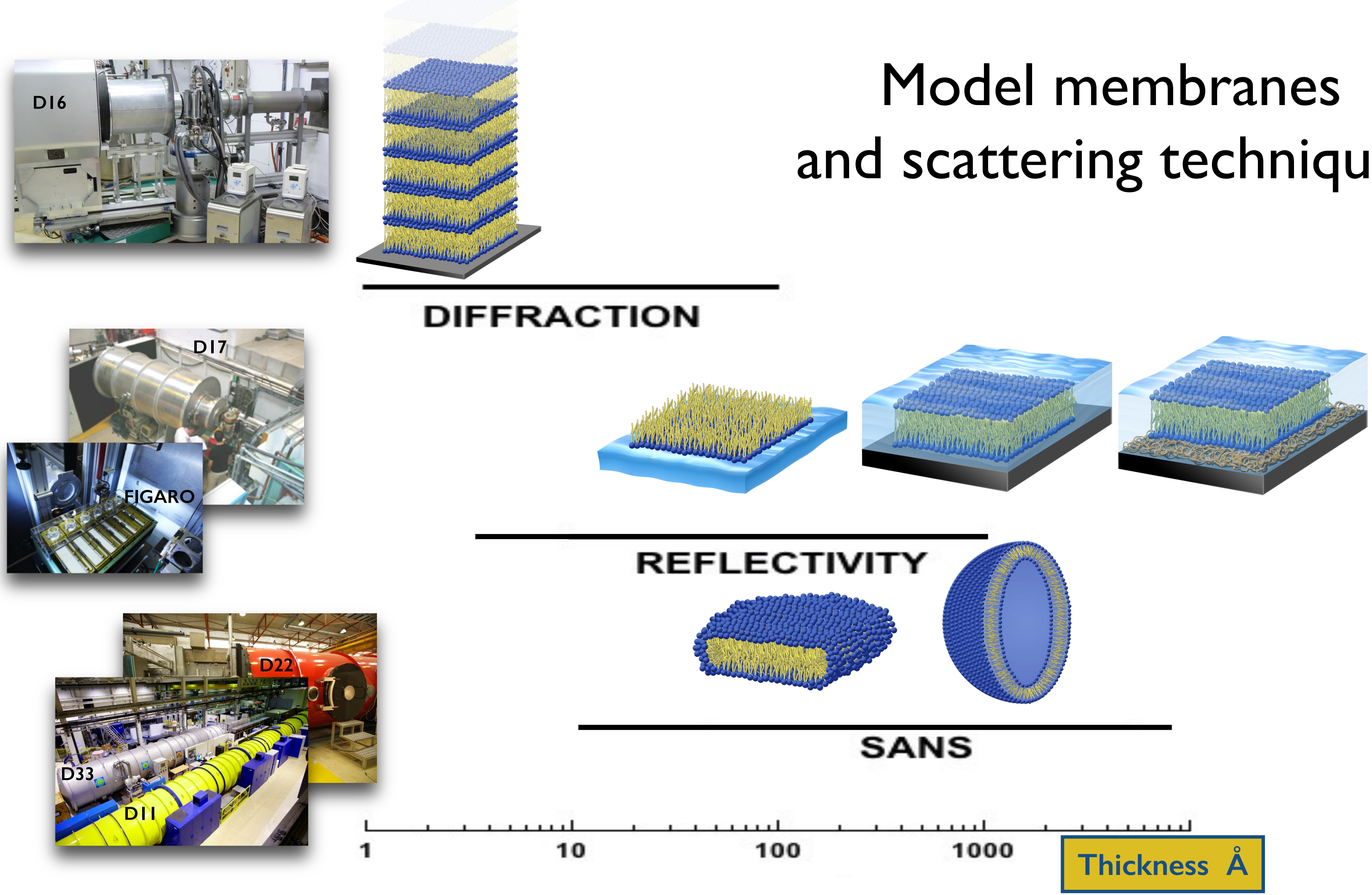

Floating bilayers prepared by Langmuir-Blodgett Langmuir-Schaefer techniques

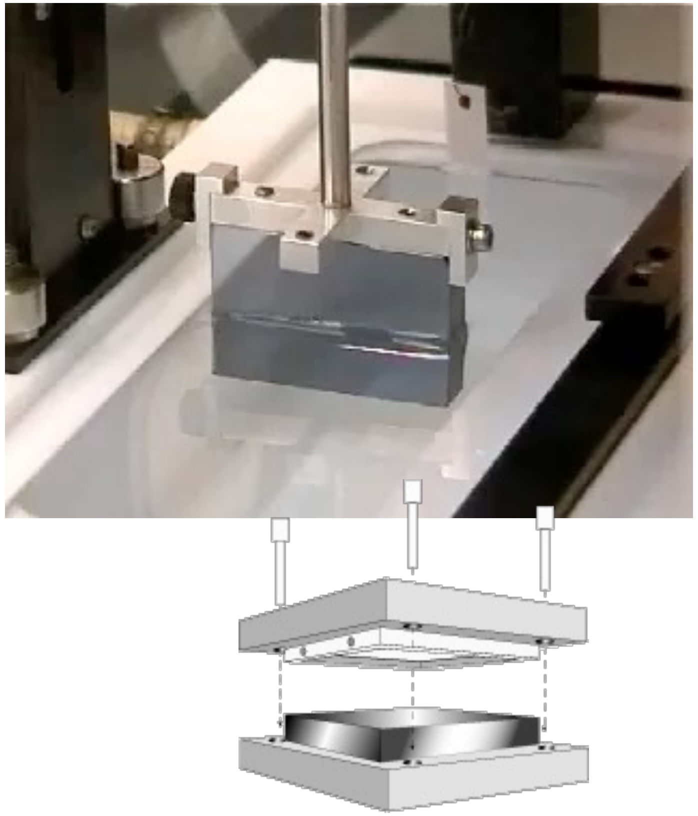

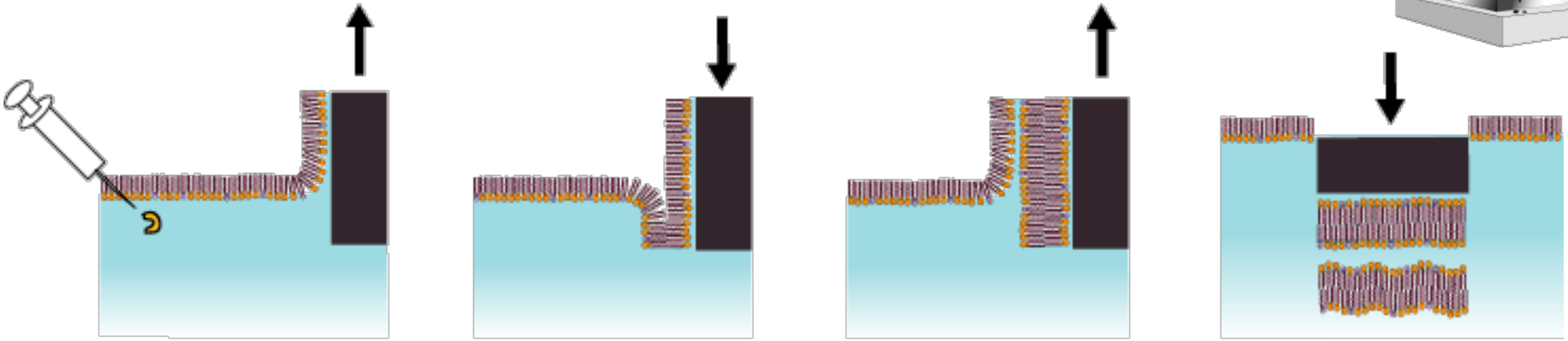

EPJB 1999

25 years of neutron and synchrotron radiation studies of structure and fluctuations of floating bilayers

- **Effect of temperature (giant swelling)**
- **Effect of charges**
- **Effect of AC current**
- **Interaction with gene delivery complexes**
- **Effect of domain forming molecules/asymmetry**
- **Lipid flip-flop**
- **Interaction with nano particles**
- **Transmembrane insertion**

EPJB 1999
EPL 2001
Langmuir 2001
Langmuir 2003
Langmuir 2005
Langmuir 2005
PNAS 2005
EPJE 2006
Soft Matter 2007
Langmuir 2009
BBA 2012
PNAS 2012
Langmuir 2012
EPJE 2013
Soft Matter 2015
PRL 2016
BBA 2018
Small 2019
J Chem Phys Lett 2019
J. Coll. Int. Sci. 2021

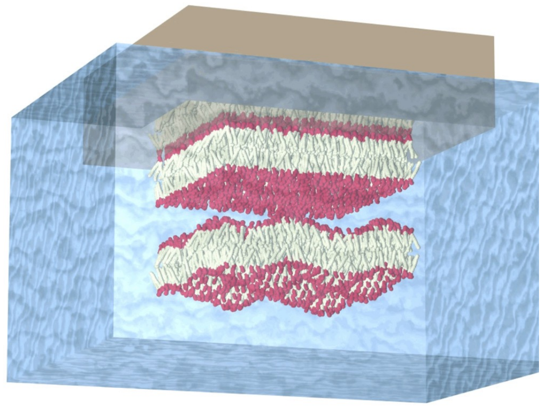

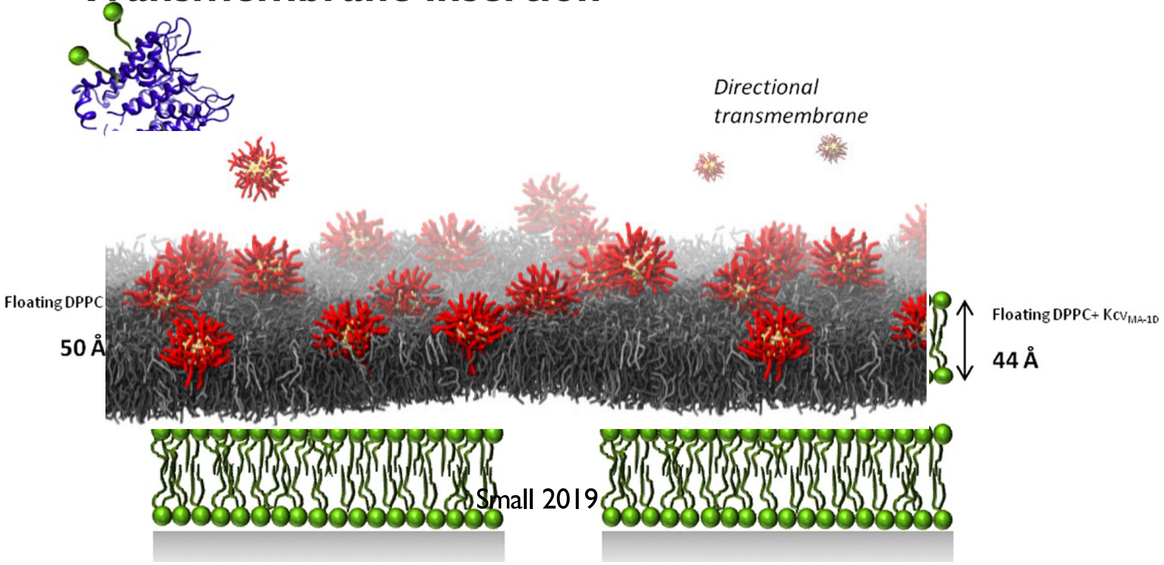

Mukhina et al., J Chem Phys Lett. 2019
Rondelli et al. BBA 2018

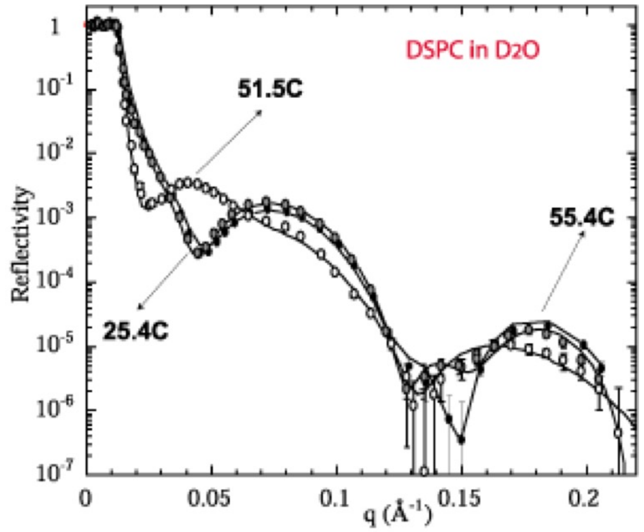

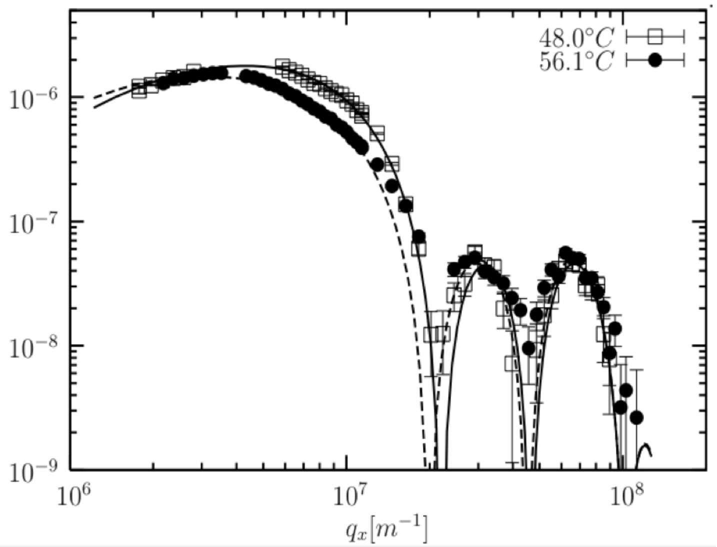

$$\left\langle z(q_\parallel)z(q_\parallel)\right\rangle = \frac{k_B T}{A+\gamma q_\parallel^2+\kappa q_\parallel^4}$$

25 years of neutron and synchrotron radiation studies of structure and fluctuations of floating bilayers

- **Effect of temperature (giant swelling)**
- **Effect of charges**
- **Effect of AC current**
- **Interaction with gene delivery complexes**
- **Effect of domain forming molecules/asymmetry**
- **Lipid flip-flop**
- **Interaction with nano particles**
- **Transmembrane insertion and induced fluctuations**

EPJB 1999
EPL 2001
Langmuir 2001
Langmuir 2003
Langmuir 2005
Langmuir 2005
PNAS 2005
EPJE 2006
Soft Matter 2007
Langmuir 2009
BBA 2012
PNAS 2012
Langmuir 2012
EPJE 2013
Soft Matter 2015
PRL 2016
BBA 2018
Small 2019
J Chem Phys Lett 2019
J. Coll. Int. Sci. 2021

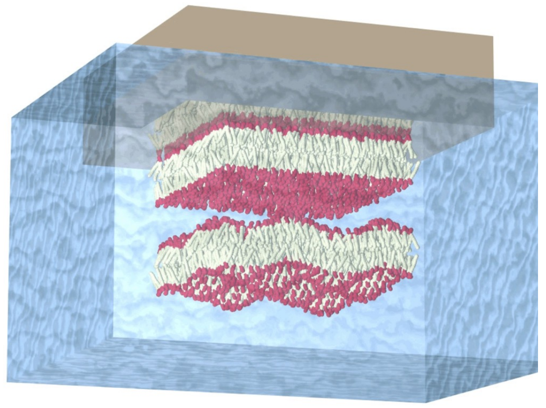

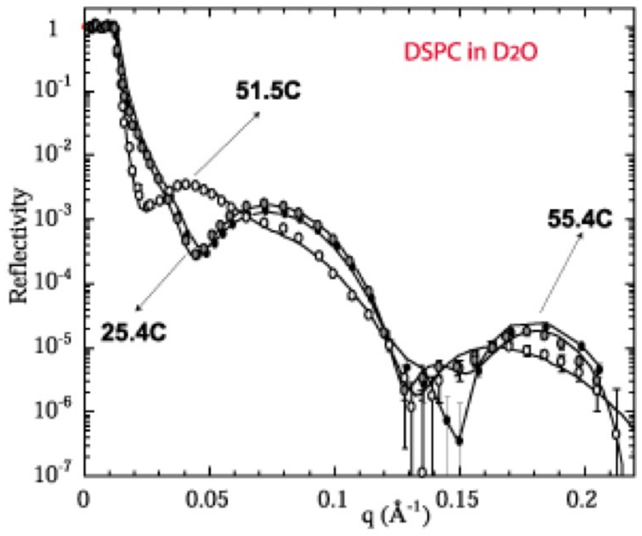

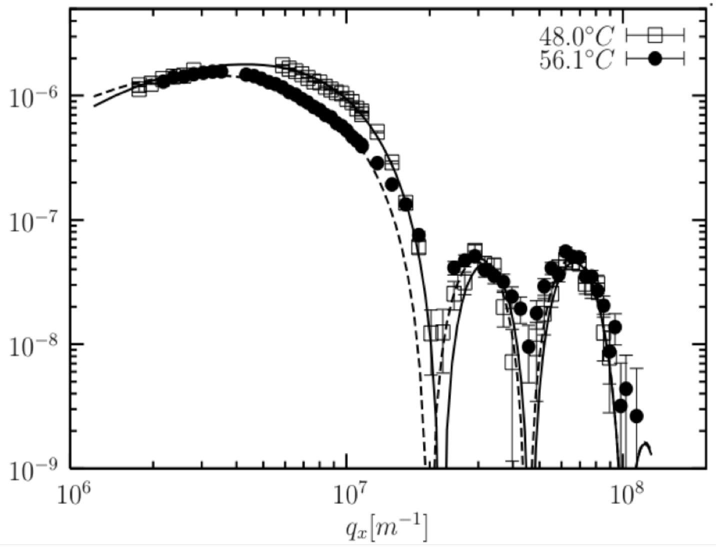

$$\left\langle z(q_\parallel)z(q_\parallel)\right\rangle = \frac{k_B T}{A + \gamma q_\parallel^2 + \kappa q_\parallel^4}$$

Journal of Colloid and Interface Science 597 (2021) 370–382

Contents lists available at ScienceDirect

Journal of Colloid and Interface Science

journal homepage: www.elsevier.com/locate/jcis

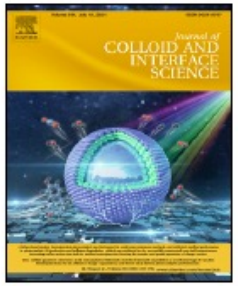

Regular Article

Insertion and activation of functional Bacteriorhodopsin in a floating bilayer

Tetiana Mukhina[a,b,1], Yuri Gerelli[a,c,*], Arnaud Hemmerle[d], Alexandros Koutsioubas[e], Kirill Kovalev[f,g,e,h,i,j], Jean-Marie Teulon[f], Jean-Luc Pellequer[f], Jean Daillant[d], Thierry Charitat[b,*], Giovanna Fragneto[a,*]

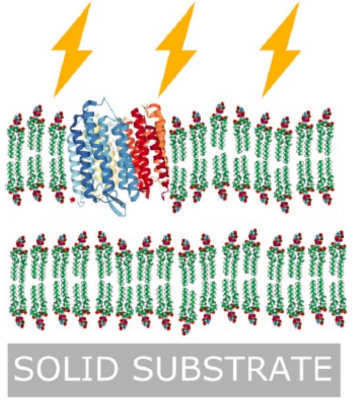

ARTICLE INFO

Article history:
Received 24 November 2020
Revised 26 March 2021
Accepted 27 March 2021
Available online 31 March 2021

ABSTRACT

The proton pump transmembrane protein bacteriorhodopsin was successfully incorporated into planar floating lipid bilayers in gel and fluid phases, by applying a detergent-mediated incorporation method. The method was optimized on single supported bilayers by using quartz crystal microbalance, atomic force and fluorescence microscopy techniques. Neutron and X-ray reflectometry were used on both single and floating bilayers with the aim of determining the structure and composition of this membrane-

Bacteriorhodopsin (BR)

26~kDa transmembrane protein that acts as a light-driven proton pump in *Halobacterium salinarum*, converting light energy into a proton gradient.

High-resolution structure of BR

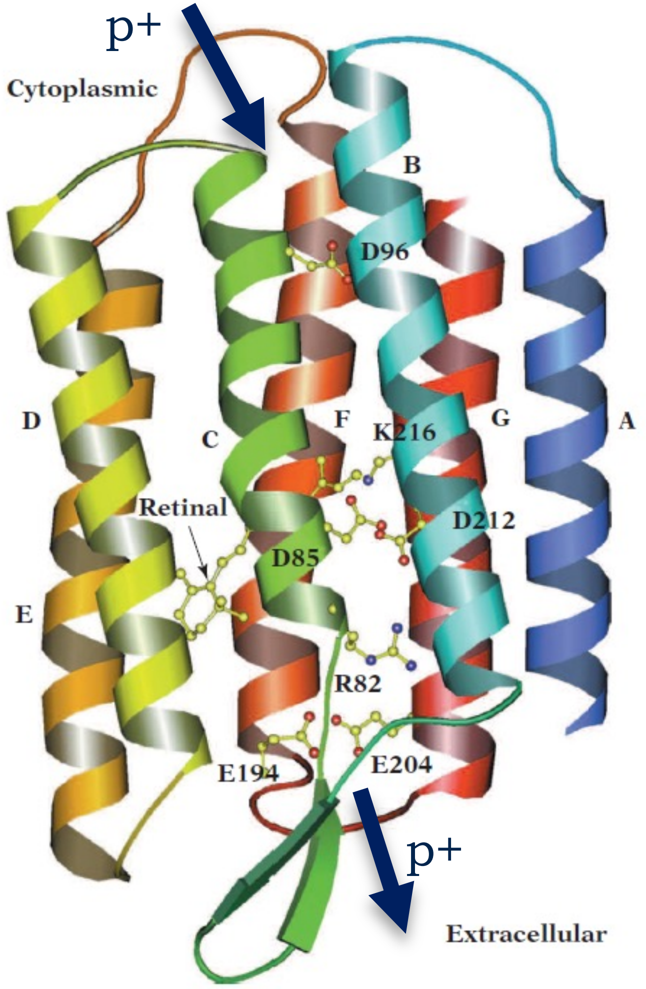

Pebay-Peyroula, E., et al., Biochim Biophys Acta. 2000, 1460:119–132.

Electron density profile of the 2D crystalline purple membrane

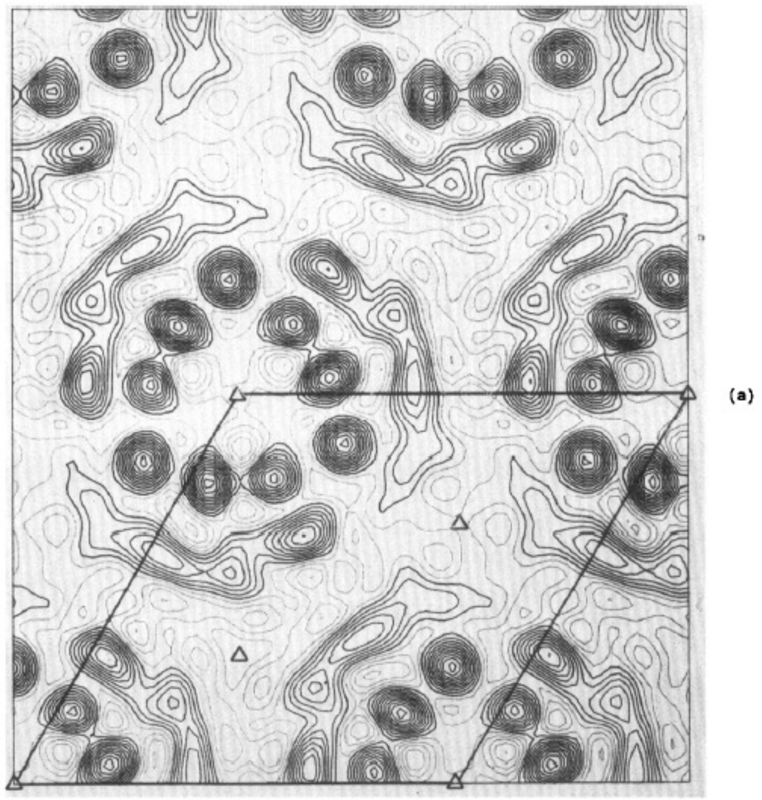

Unwin P. N. T. and R. Henderson J. Mol. Biol., 1976, 94:425 - 440

Conformational changes of BR during the photocycle

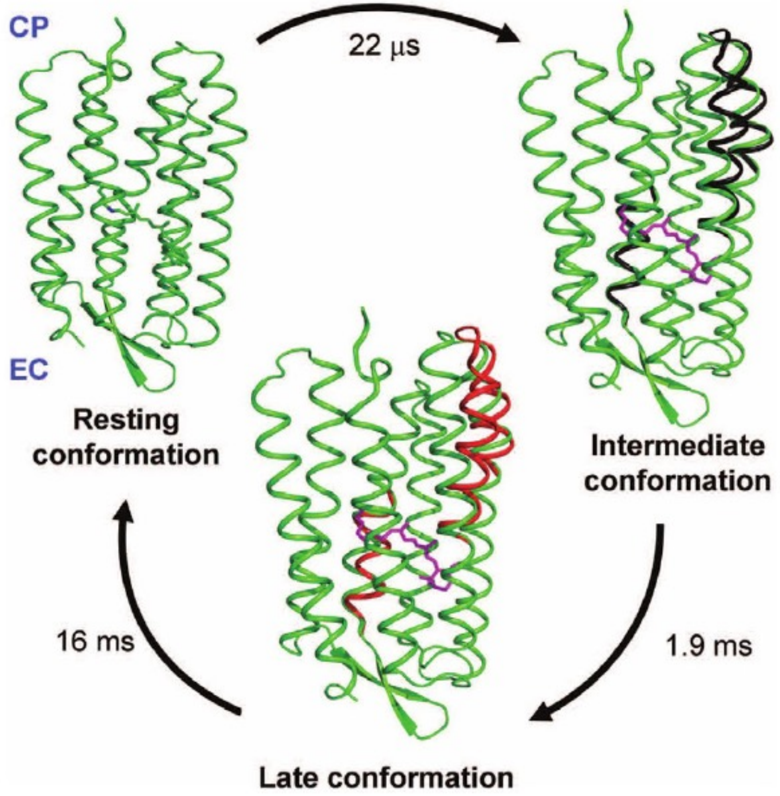

Andersson, M., et al., Structure. 2009, 17:1265–1275.

Membrane Fluctuations

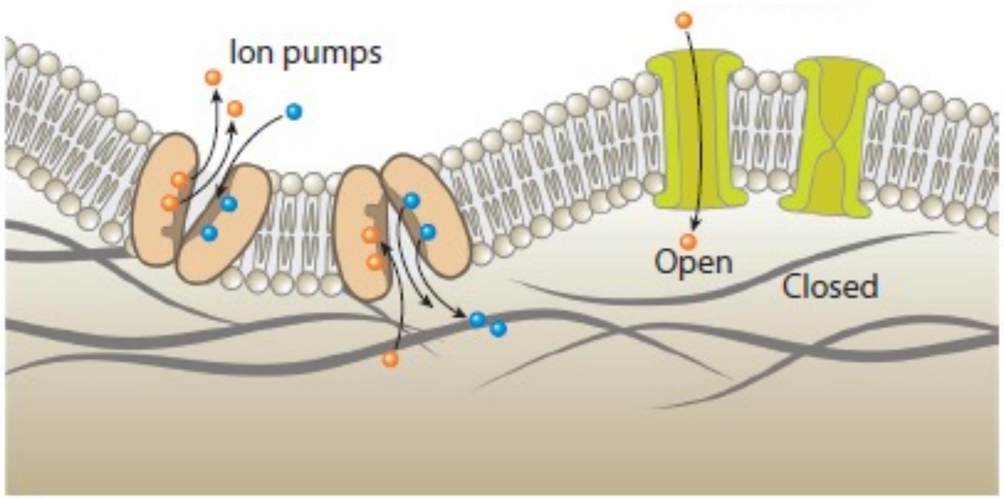

Turlier H. Annu. Rev. Condens. Matter Phys. 2019. 10:213–32

- Thermal fluctuations
- Active fluctuations - out of equilibrium system

Micropipette experiments
Videomicroscopy experiments

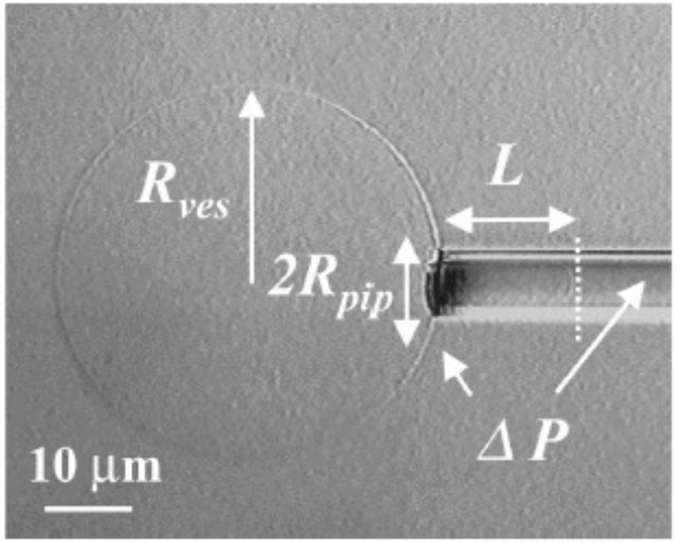

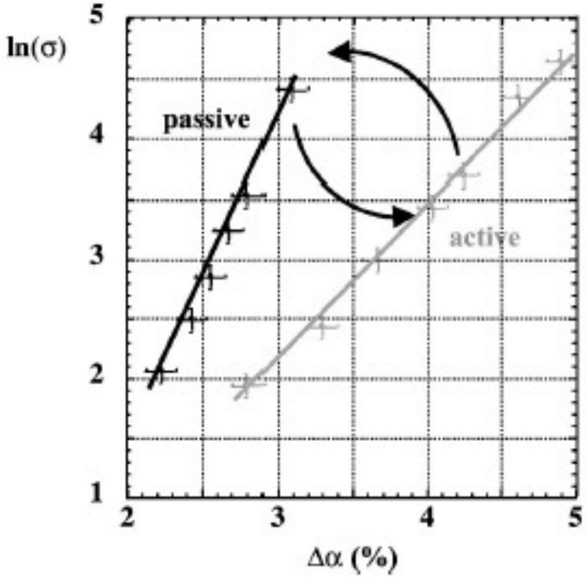

$$\Delta\alpha = \alpha_0 - \alpha = \frac{k_B T_{eff}}{8\pi\kappa}\ln\left(\frac{\sigma}{\sigma_0}\right)$$

$$1.7 \le \frac{T_{eff}}{T} \le 2.7$$

A larger excess area could be pulled out by micropipette aspiration when BR was active, indicating that its ***proton pumping activity induces an amplification of the membrane shape fluctuations*** *and a strong decrease in the effective bending modulus of the membrane.* ***Information only at the micrometer scale.***

Manneville J.-B. , Ramaswamy S., Bassereau P., Prost J. . PRL E **64** 021908

Out-of-equilibrium fluctuations of phospholipid membranes induced by active transmembrane proteins

X-ray and synchrotron radiation Specular and Off- Specular

- Structure with Å resolution
- Fluctuation spectrum
- Lateral inhomogeneities and defects
- Physical properties of the system

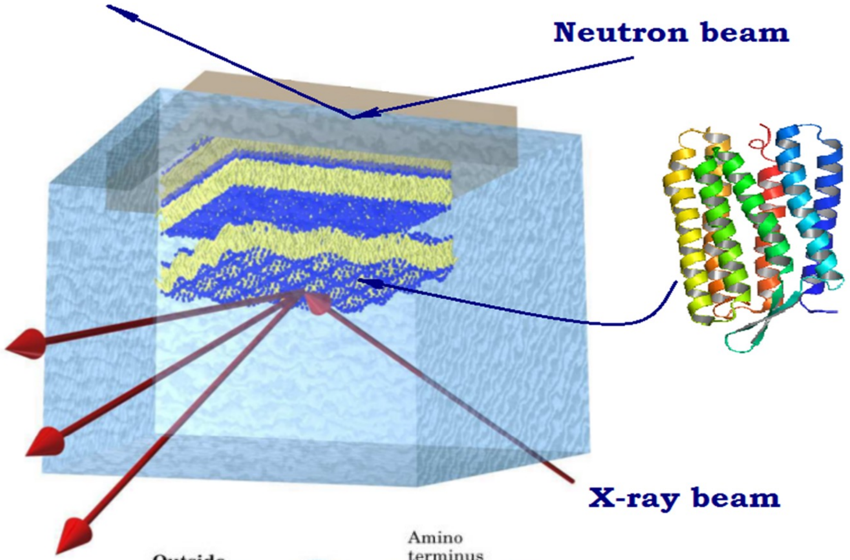

Neutron reflectometry

- Structure with Å resolution
- Atomic composition
- Interface roughness
- Solvent content

Fluorescence microscopy

- Lateral features of the system with **µm** resolution
- Sample fluorescence/bleaching

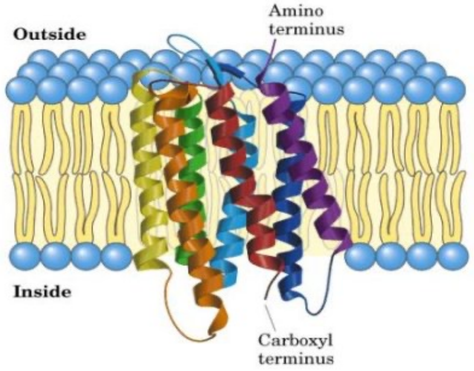

Atomic Force Microscopy AFM

- Lateral and transversal features of the system with **nm** resolution
- Mechanical properties of the sample
- Force measurements

Detergent-mediated protein incorporation

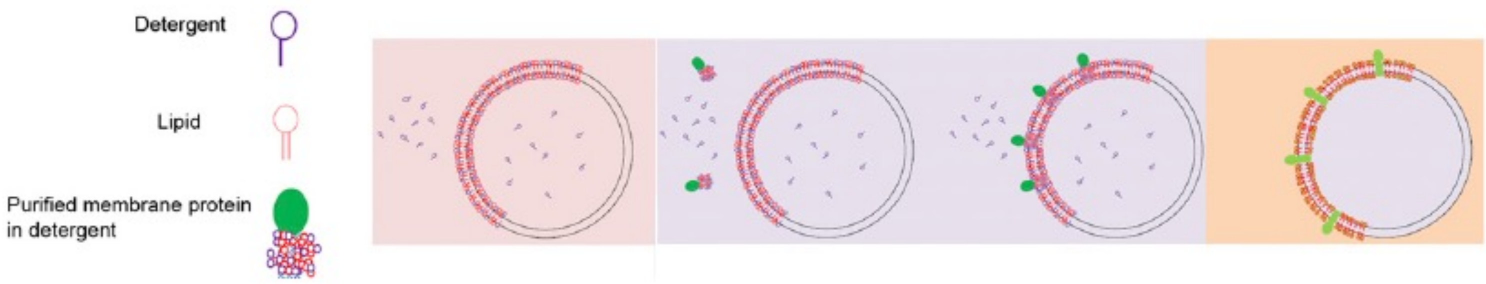

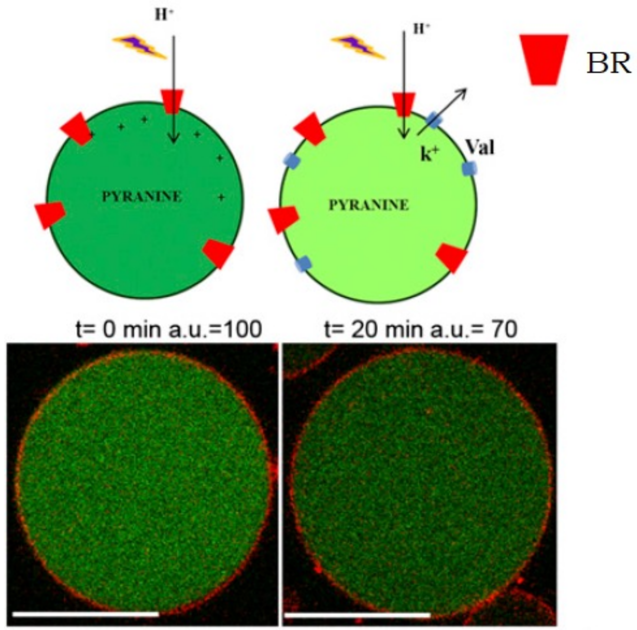

GUV with incorporated BR.

Dezi et al. PNAS , 2013, 110 (18) 7276-7281

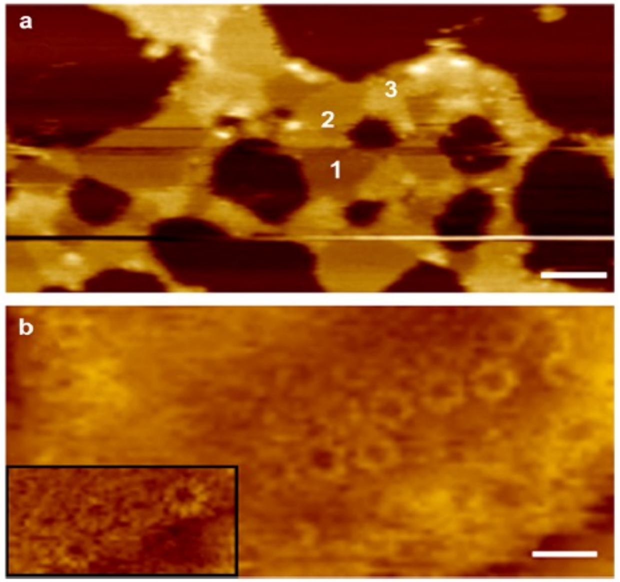

AFM imaging of LH2 protein incorporated into SLB.

Milhiet et al., Biophys. J. , 2016, 91(9) 3268–3275

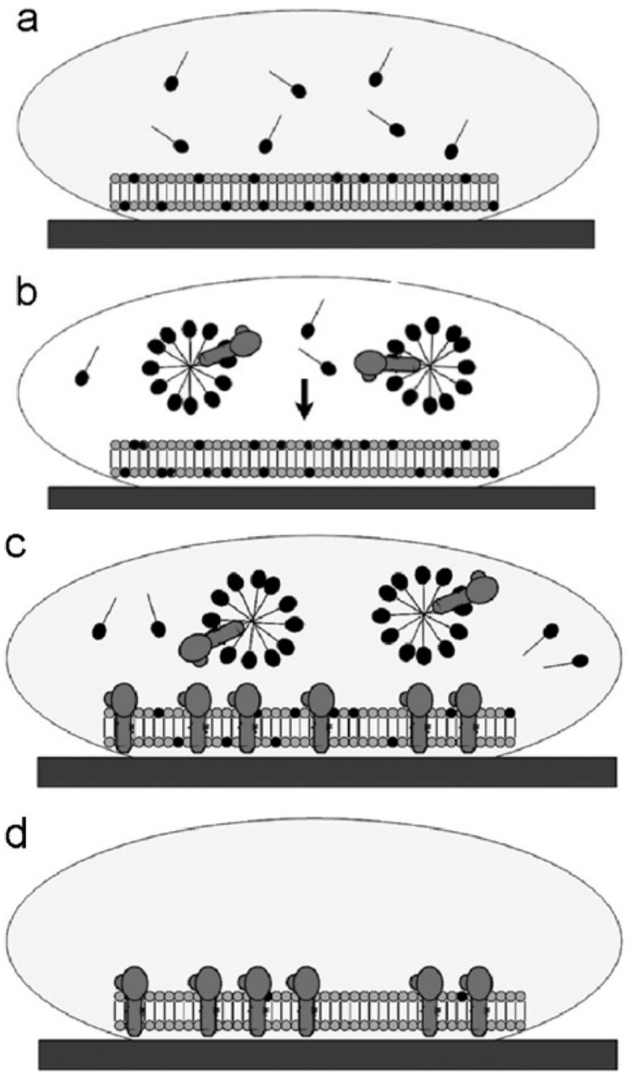

Berquand A. et al. Ultramicroscopy, 2007, 107(10-11), 928–933

Atomic force microscopy

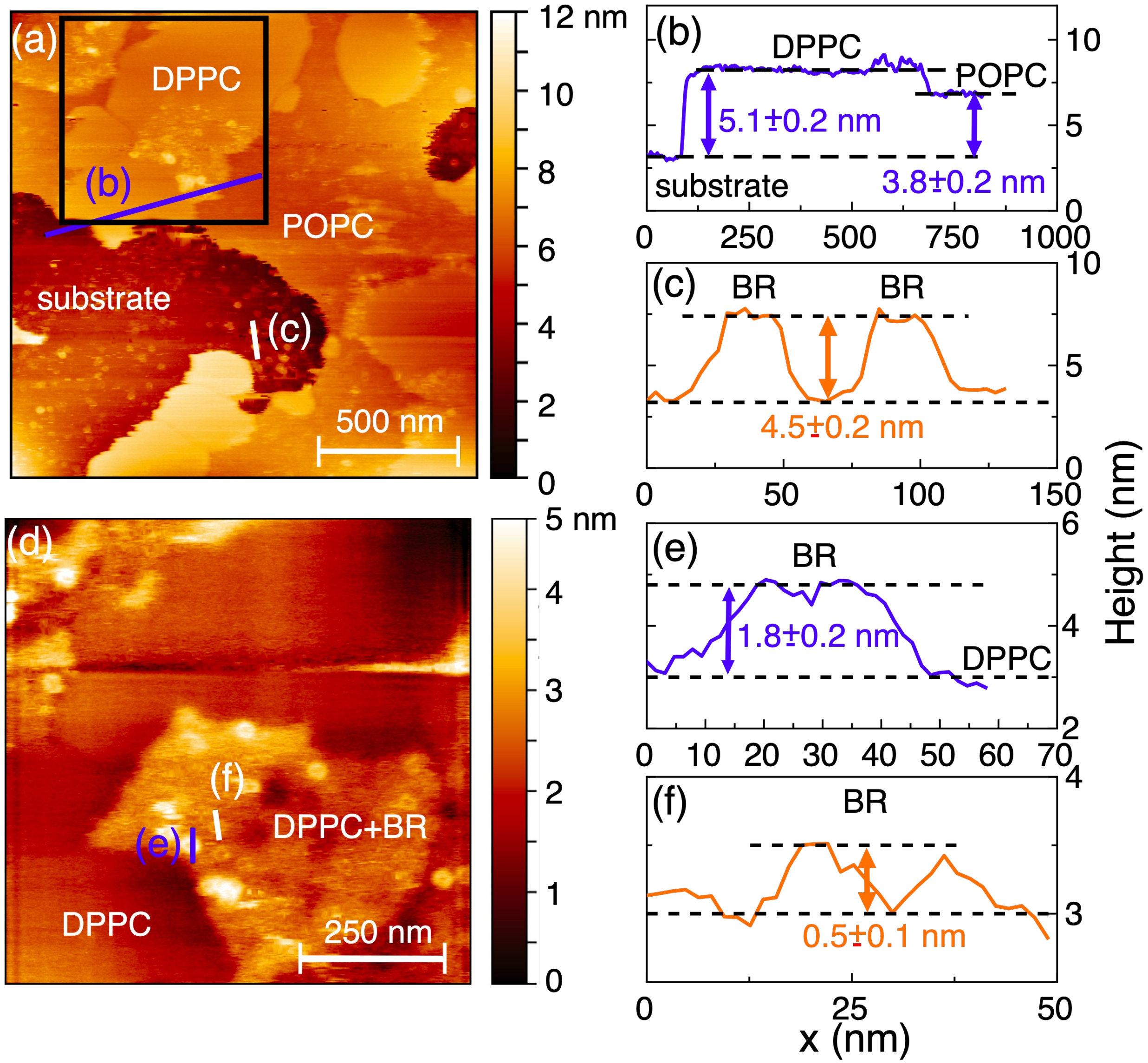

Phase separated gel-fluid
single bilayer + BR,
IBS, Grenoble

Fluorescence microscopy

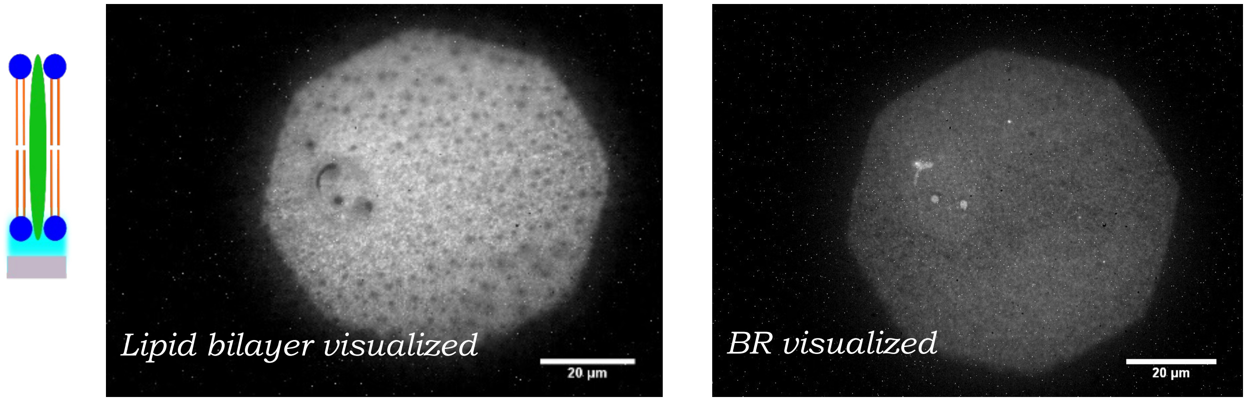

Gel **single bilayer + BR**

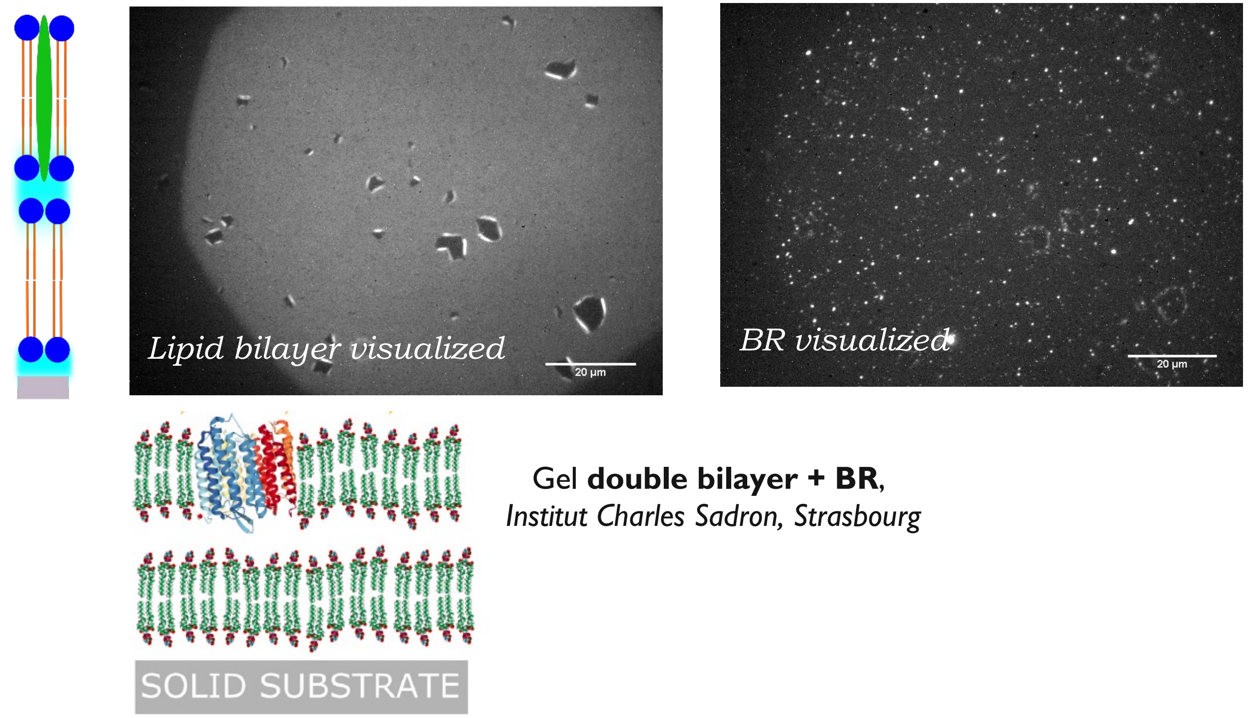

Gel **double bilayer + BR**,
Institut Charles Sadron, Strasbourg

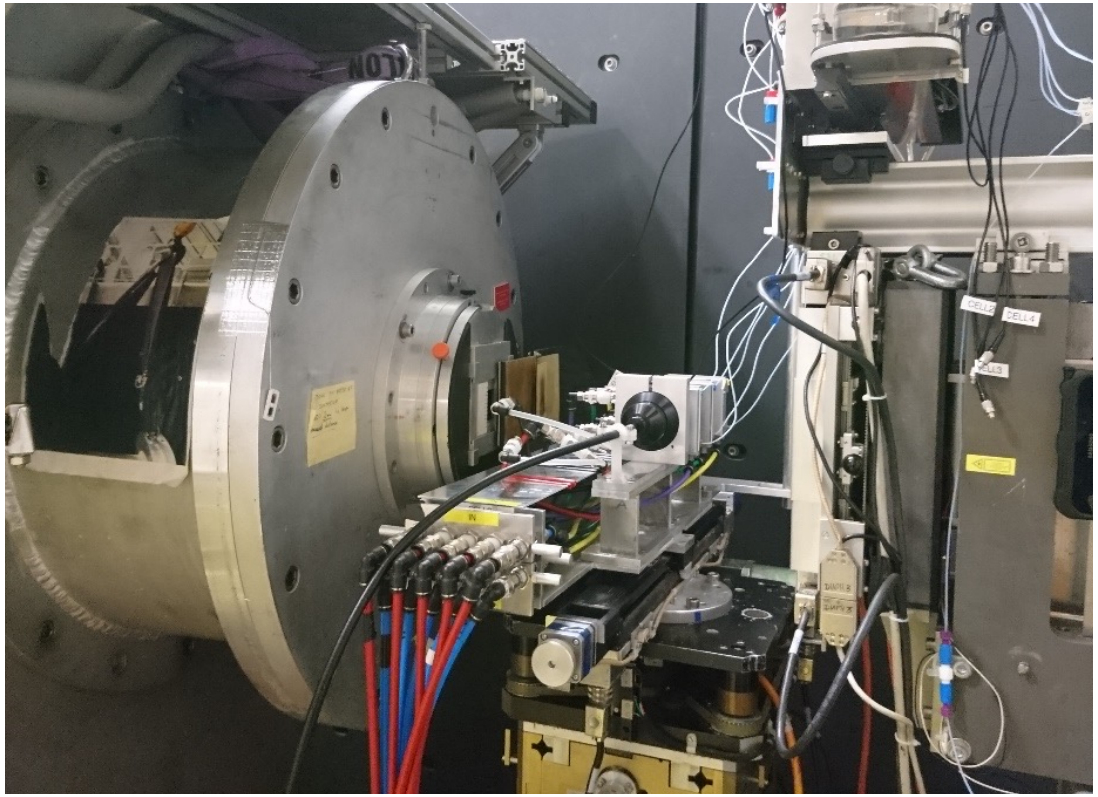

D17 reflectometer (ILL, Grenoble, France).

Time-of-flight mode

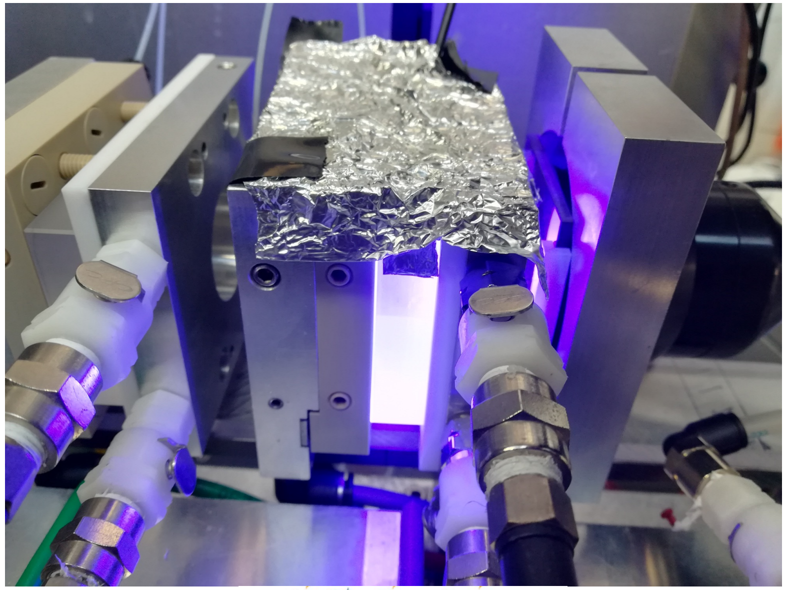

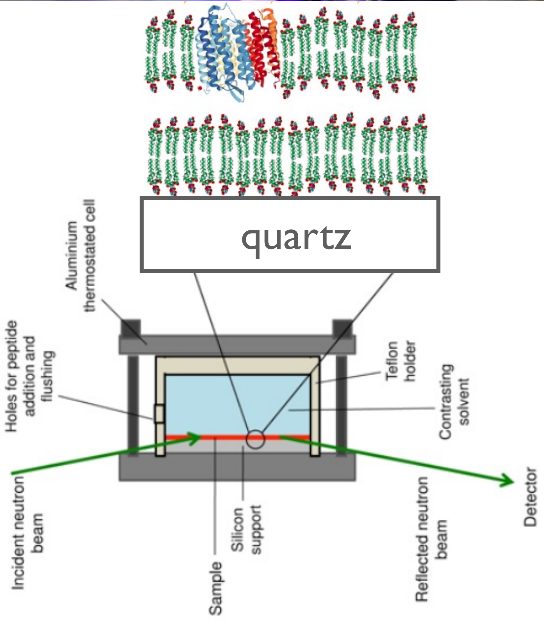

Neutron Reflectometry

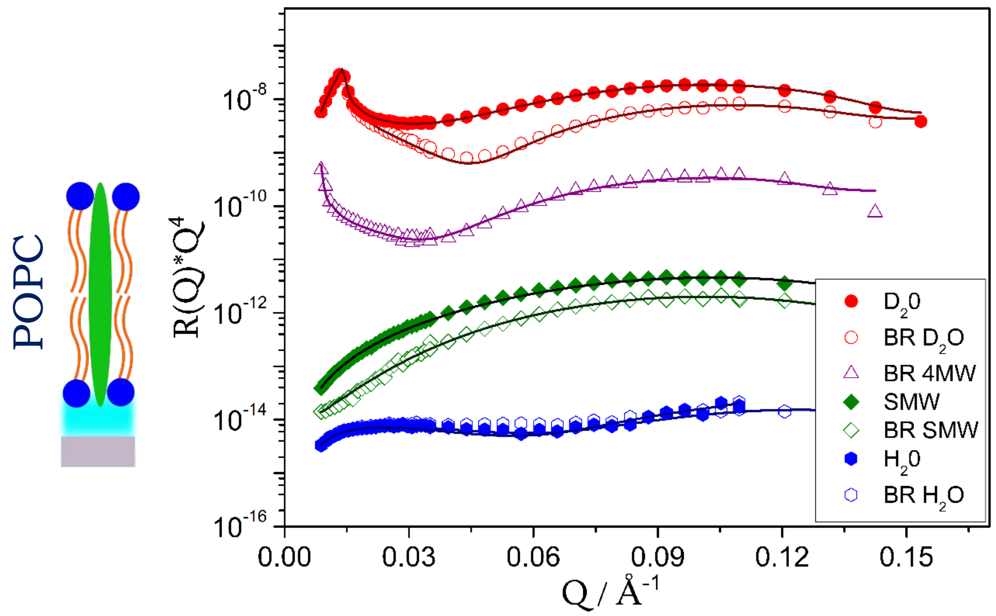

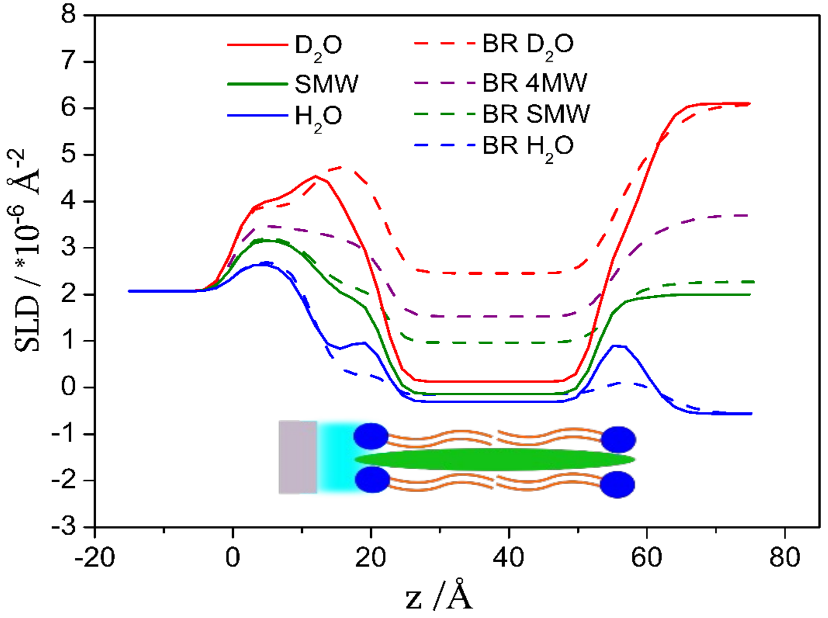

Fluid single bilayer + BR
MARIA reflectometer
JCNS, Germany

18 % by volume of BR

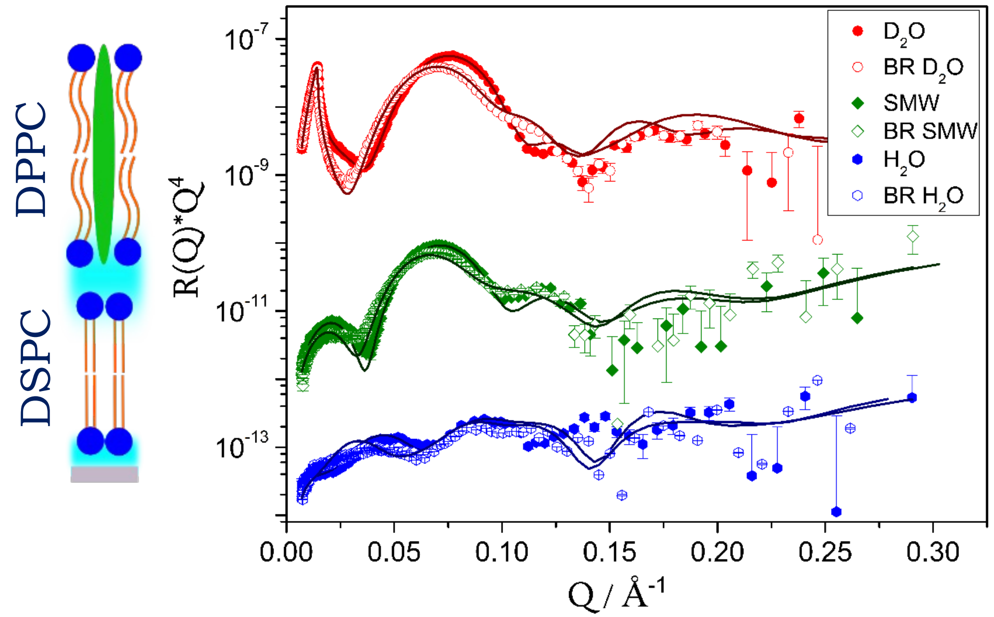

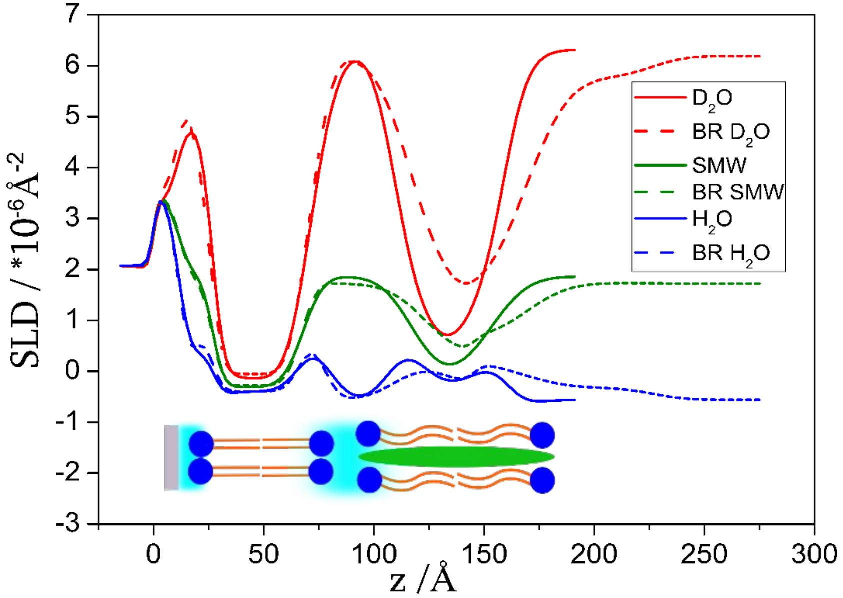

Fluid **floating bilayer + BR**
D17 reflectometer

BR insertion into the floating bilayer
+ BR layer on top

Sample environment for X-ray reflectivity experiment

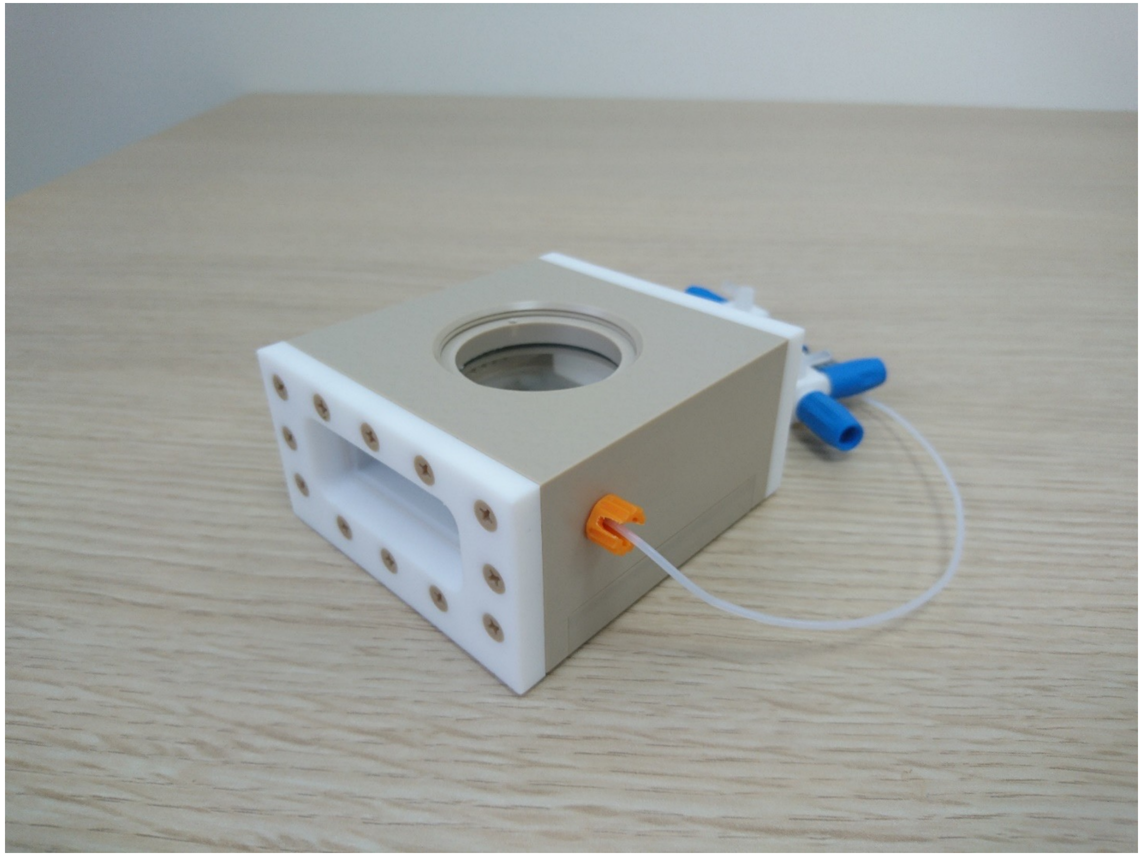

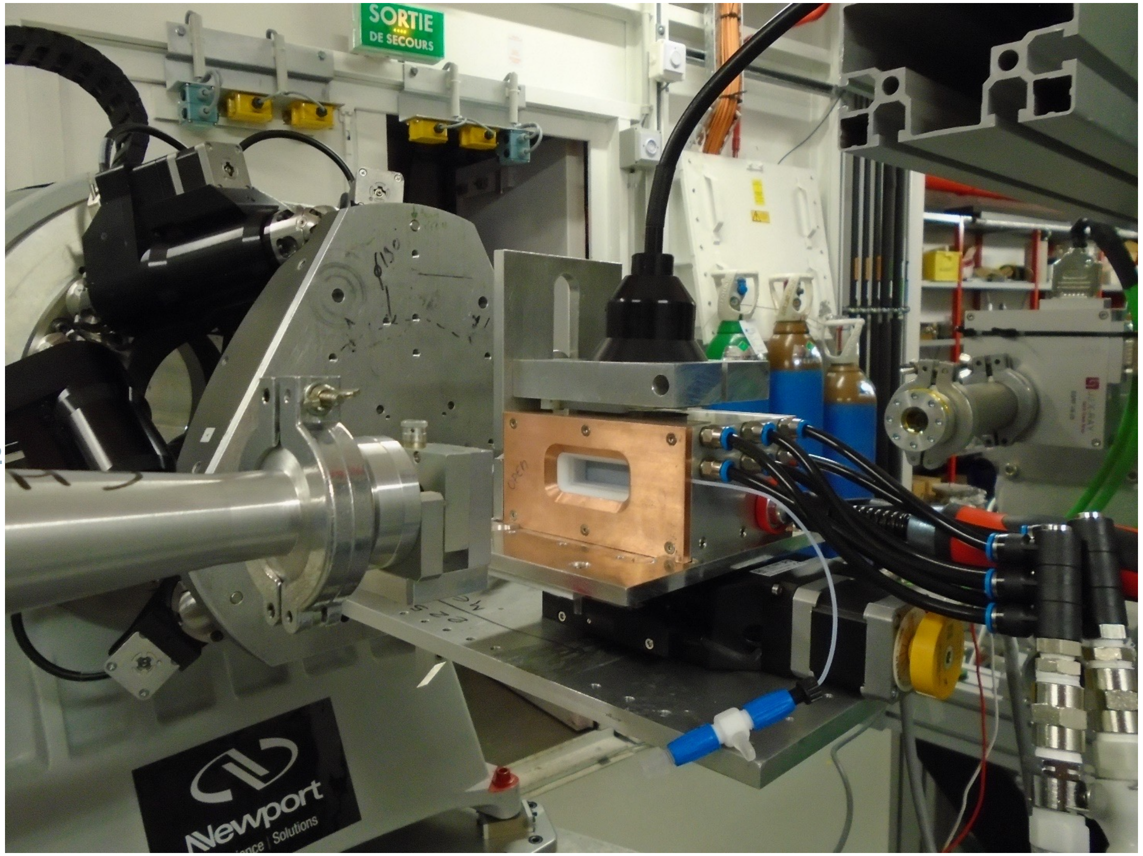

SixS beamline
SOLEIL synchrotron, France

Specular SR Reflectometry

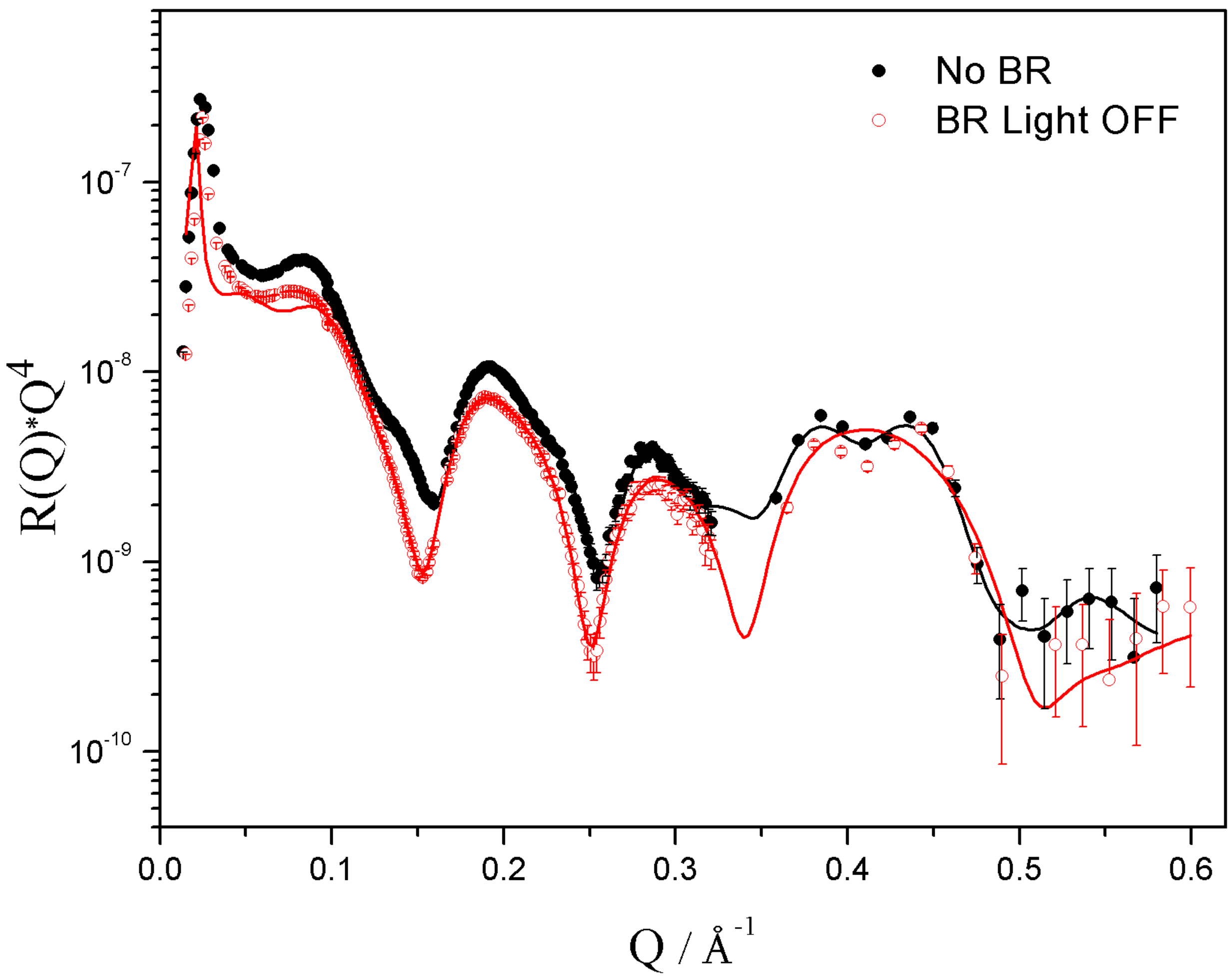

*DSPC **double bilayer** at 25°C before and after protein BR incorporation.*

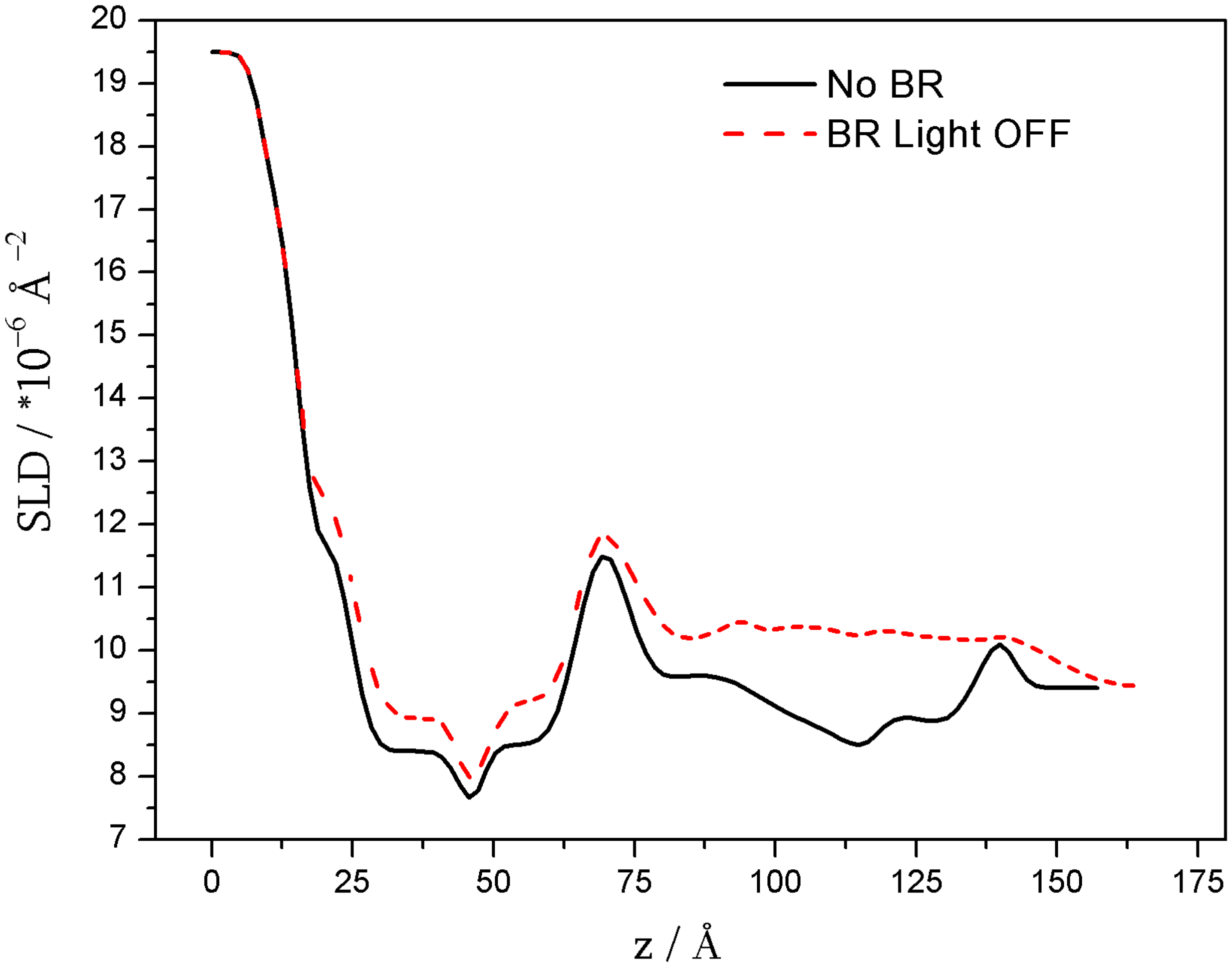

SLD profiles corresponding to the fits.

SixS beamline (SOLEIL synchrotron, France).

Specular SR Reflectometry

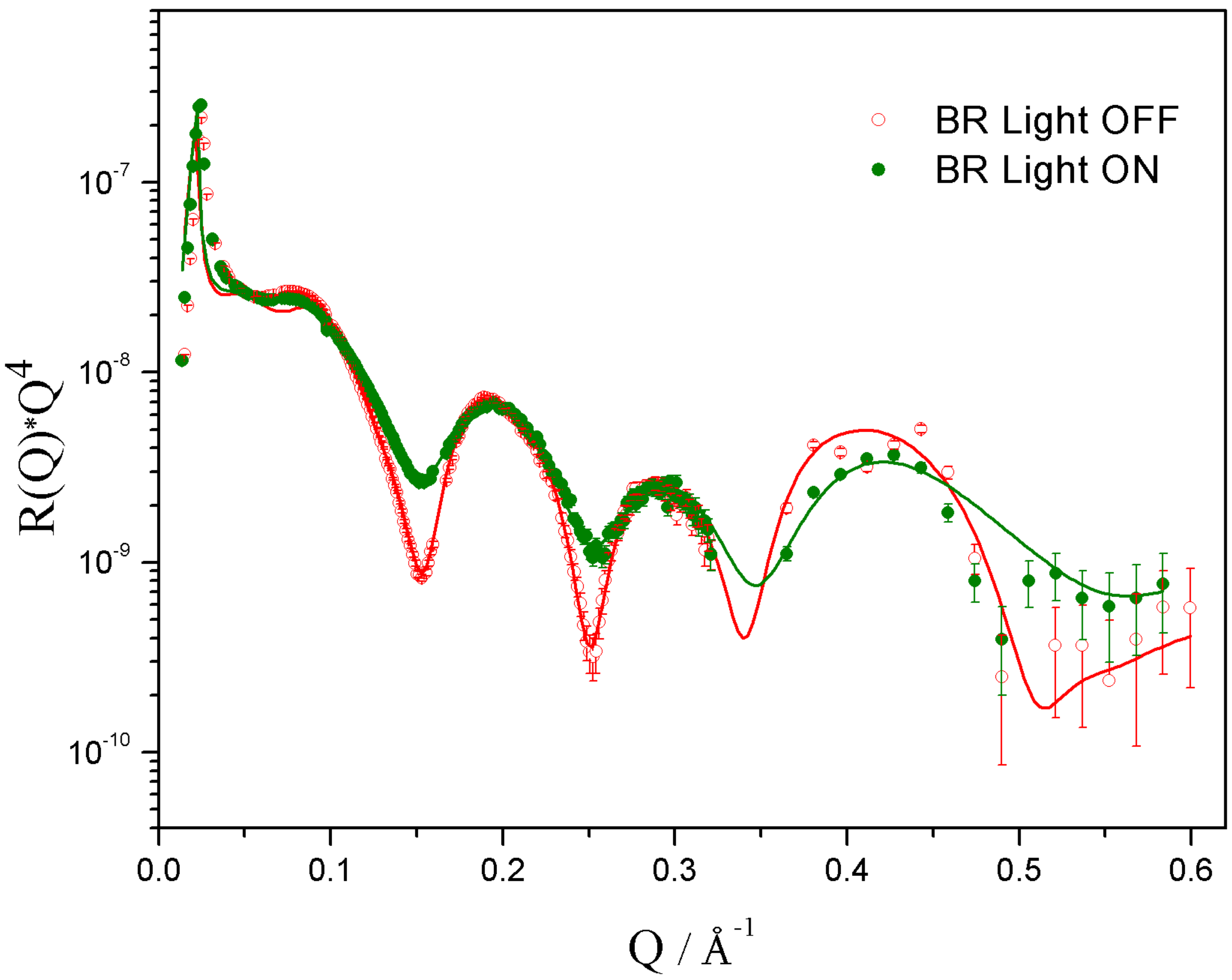

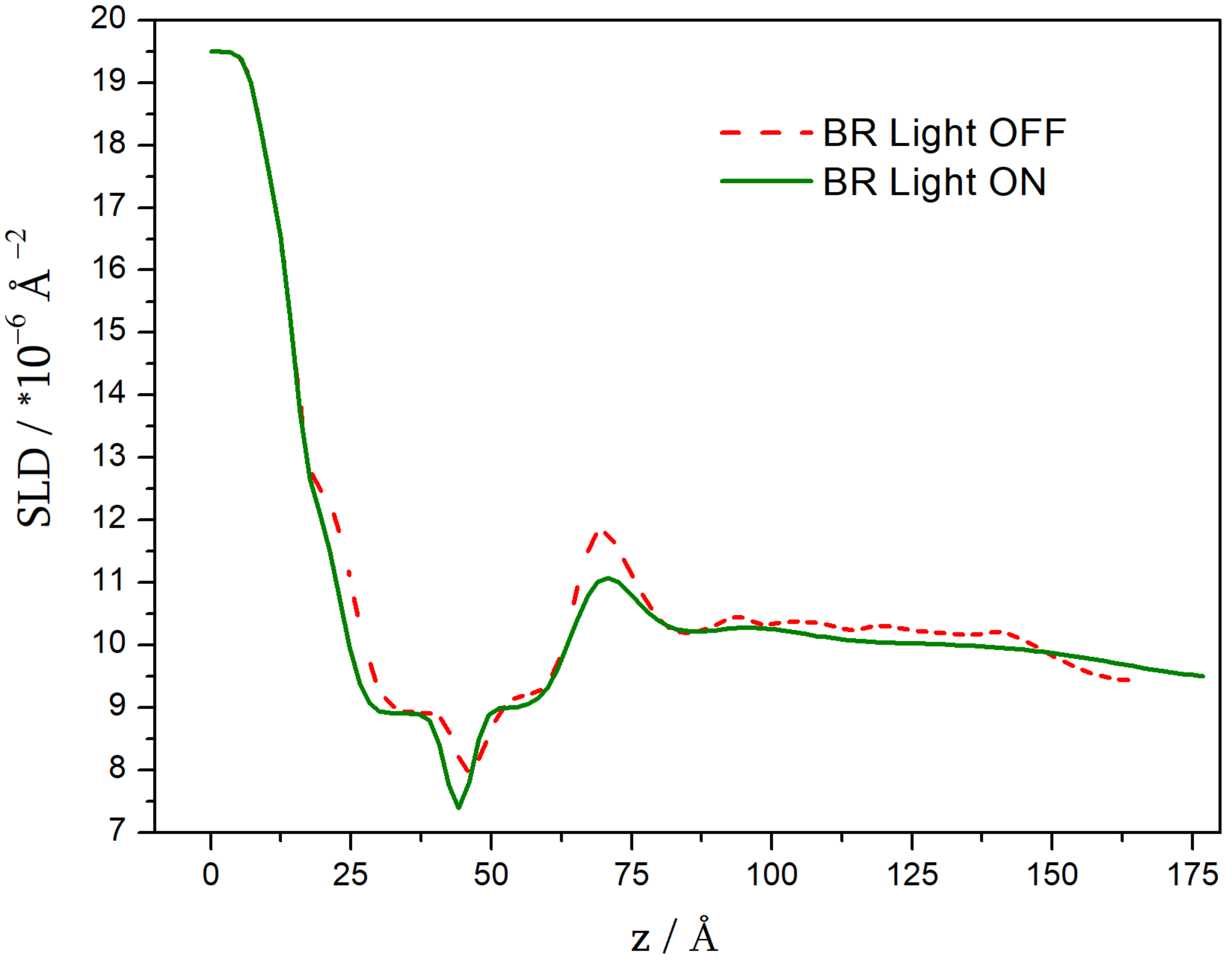

*DSPC **double bilayer** at 25°C after protein BR incorporation, with and without illumination.*

SLD profiles corresponding to the fits.

SixS beamline (SOLEIL synchrotron, France).

Specular SR Reflectometry

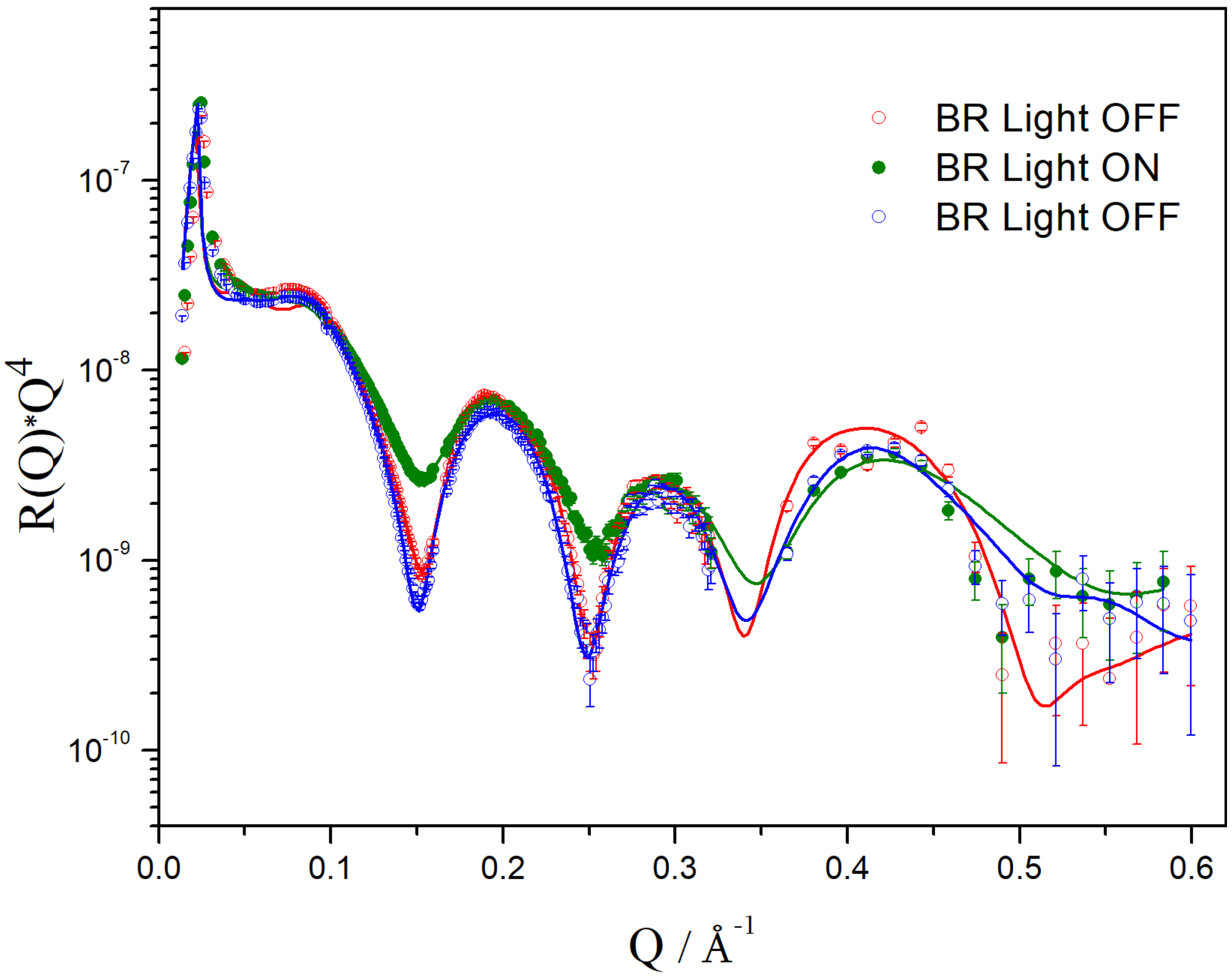

*DSPC **double bilayer** at 25°C after protein BR incorporation, with and without illumination.*

SixS beamline (SOLEIL synchrotron, France).

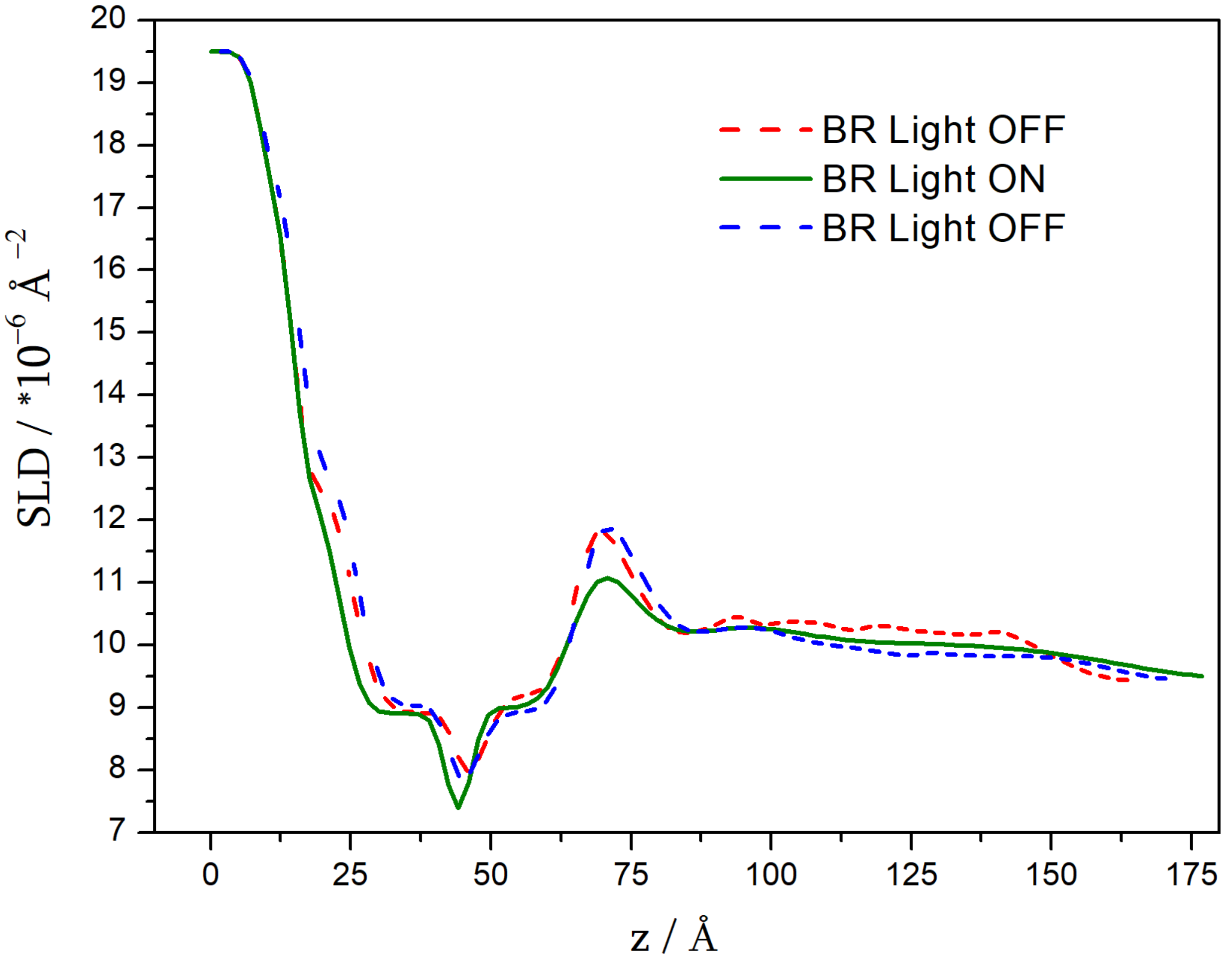

SLD profiles corresponding to the fits.

The reversible effect of light illumination is shown.

Specular SR Reflectometry

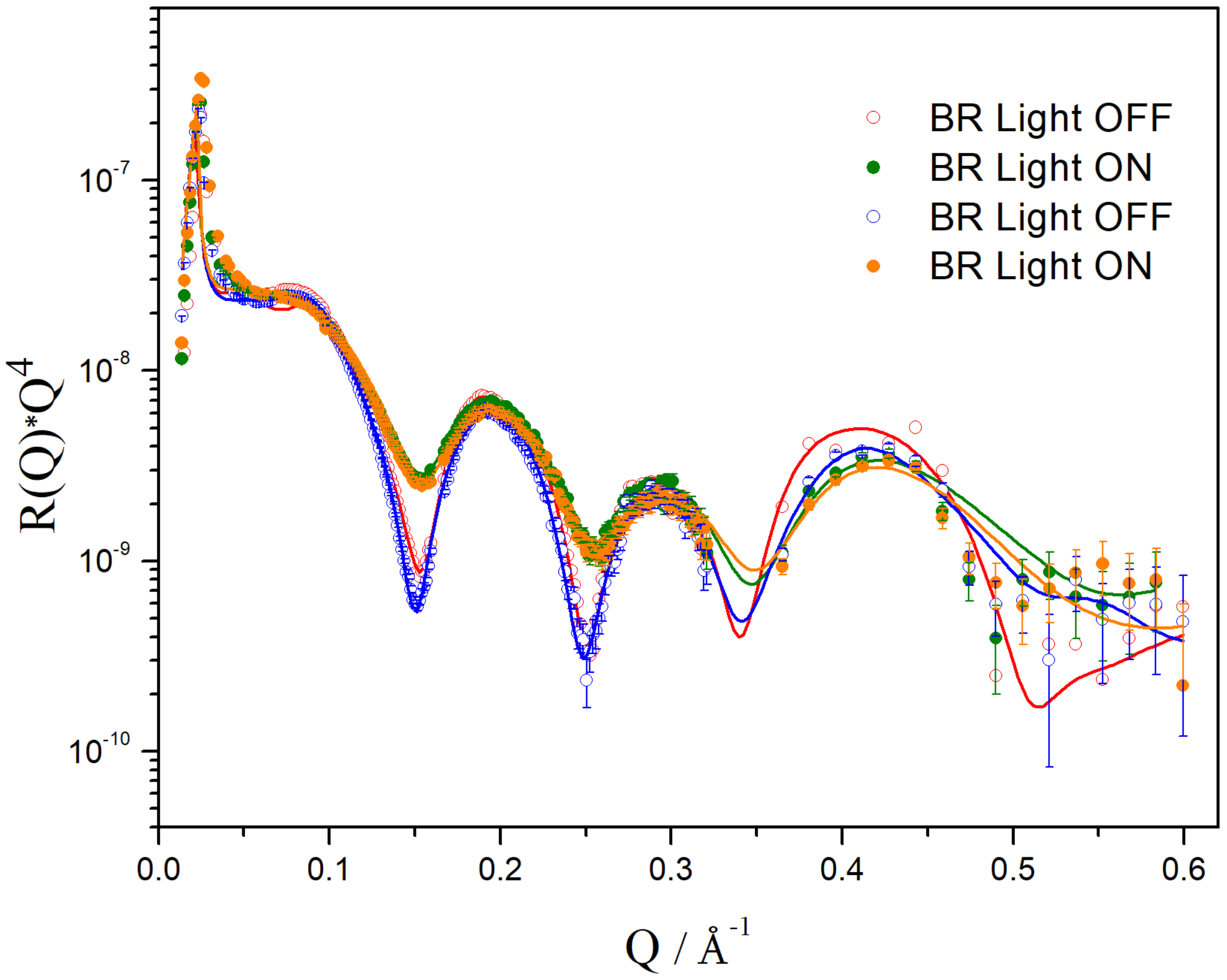

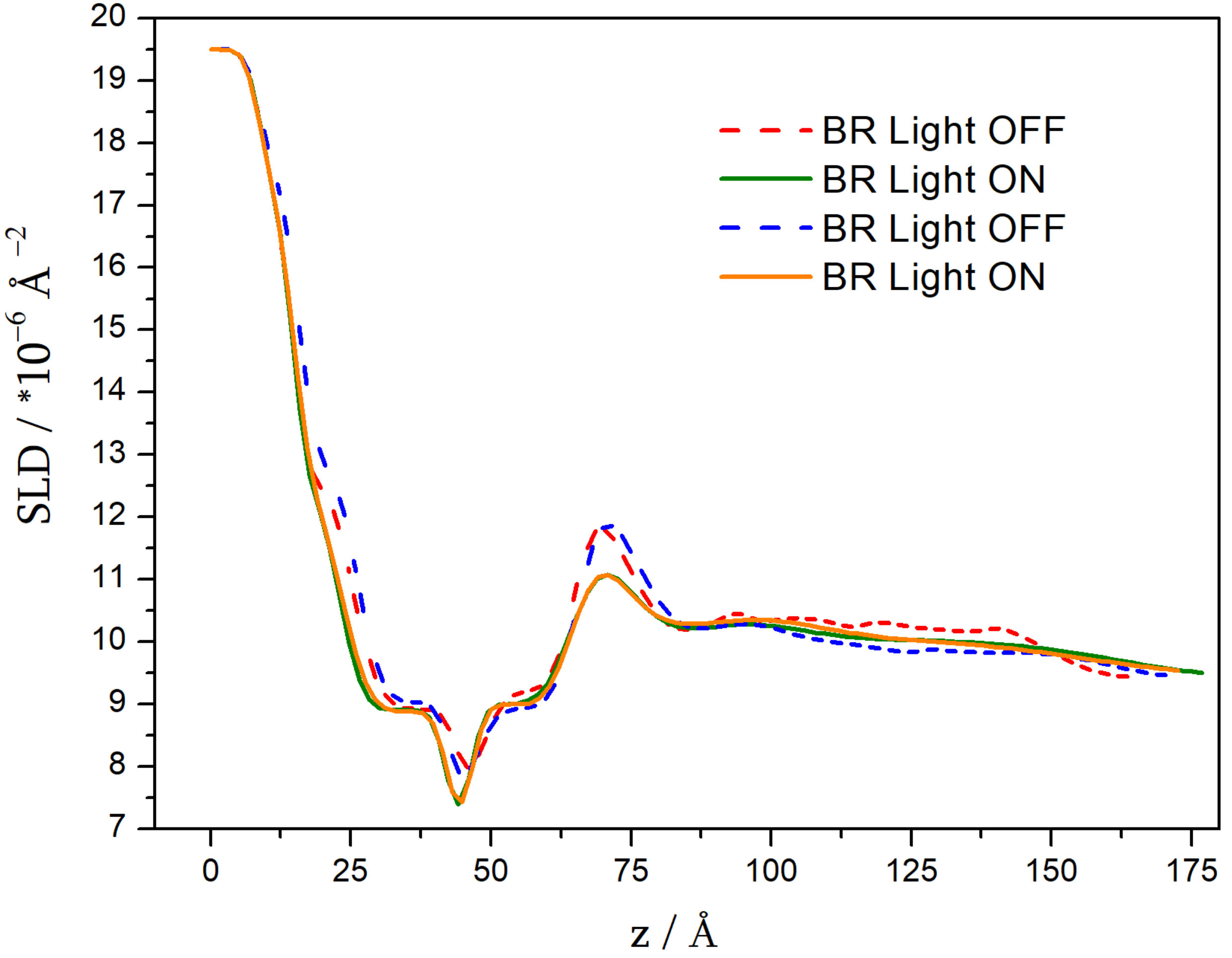

*DSPC **double bilayer** at 25°C after protein BR incorporation, with and without illumination.*

SixS beamline (SOLEIL synchrotron, France).

SLD profiles corresponding to the fits.

The reversible effect of light illumination is shown.

Specular SR Reflectometry

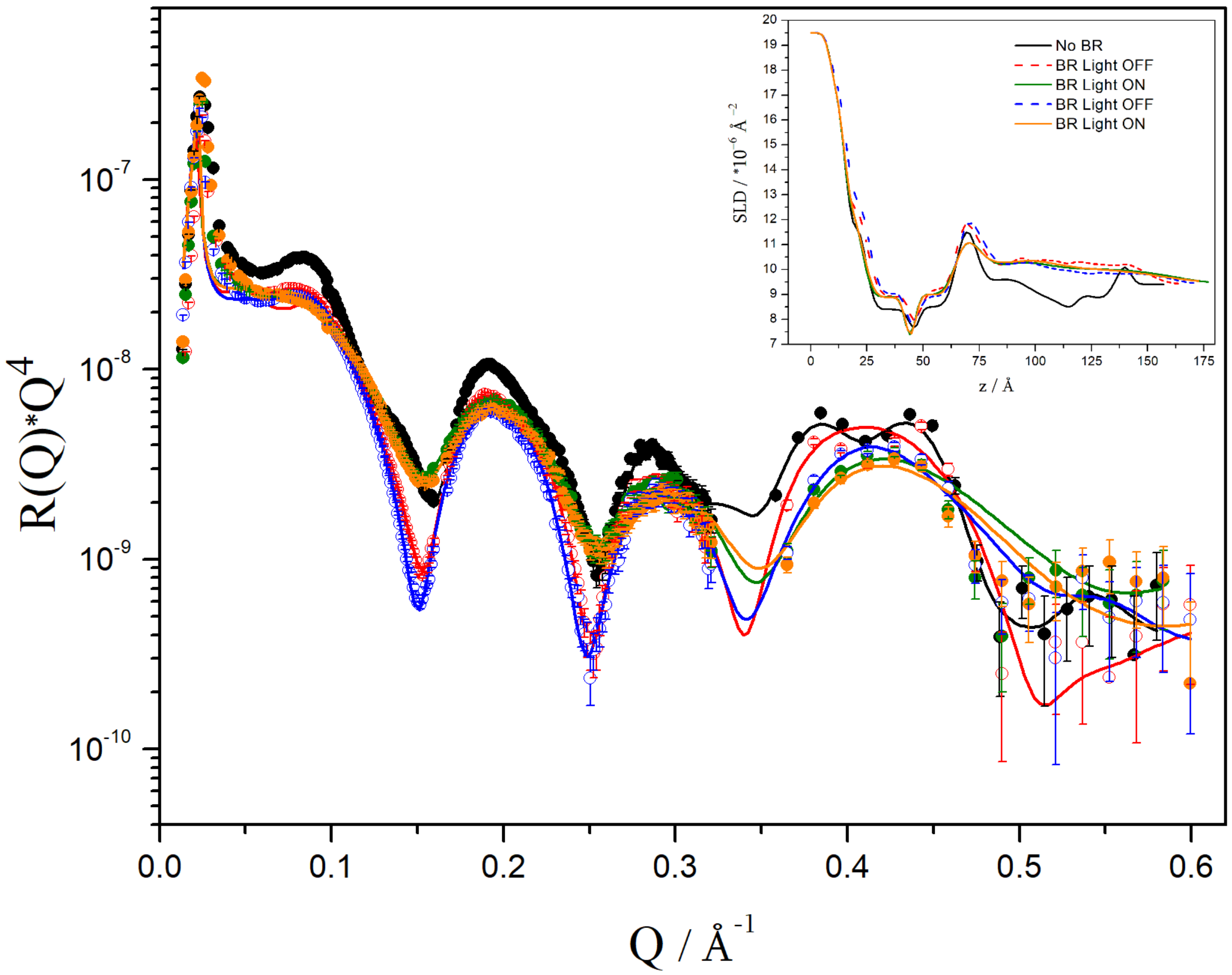

*DSPC **double bilayer** at 25°C with and without BR, with and without illumination. **Inset:** SLD profiles.*

SixS beamline (SOLEIL synchrotron, France).

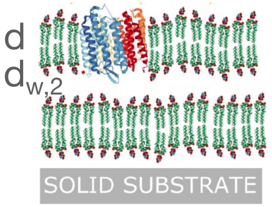

BR incorporation:

	No BR	**BR**
SLD*ch21* [10^{-4} nm^2]	8.85 ± 0.05	10.5 ± 0.05
d [nm]	5.4 ± 0.3	6.1 ± 0.3
$d_{w,2}$ [nm]	1.5 ± 0.2	1.3 ± 0.2
σ_{spec} [nm]	0.2 ± 0.1	0.8 ± 0.2

Light OFF ↔ Light ON:

	Light OFF	**Light ON**
d [nm]	6.1 ± 0.5	7.2 ± 0.5
$d_{w,2}$ [nm]	1.3 ± 0.2	1.8 ± 0.2
σ_{spec} [nm]	0.8 ± 0.2	1.5 ± 0.2

Off-specular reflection with and without illumination

$\langle \delta\rho(r)\delta\rho(r')\rangle$ ~ *static* roughness, defects, fluctuations …

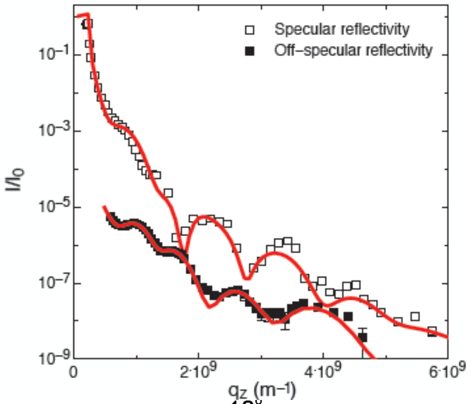

Fitting with models of correlation functions:

➡**structure**,

➡**elastic parameters** (bending modulus, surface tension),

➡ **interaction** potentials.

Malaquin et al., EPJE (2010), Hemmerle et al., PNAS (2012)

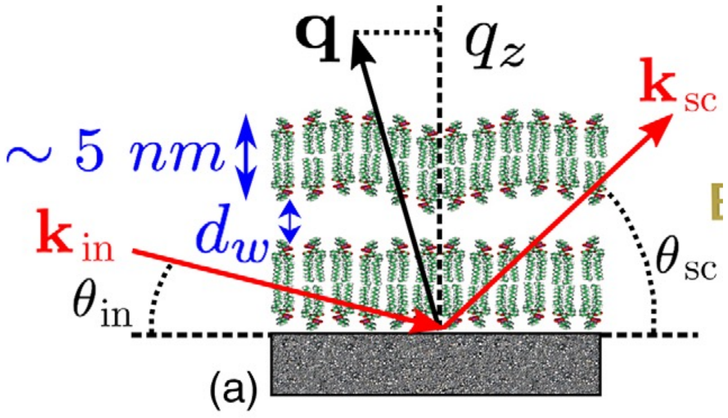

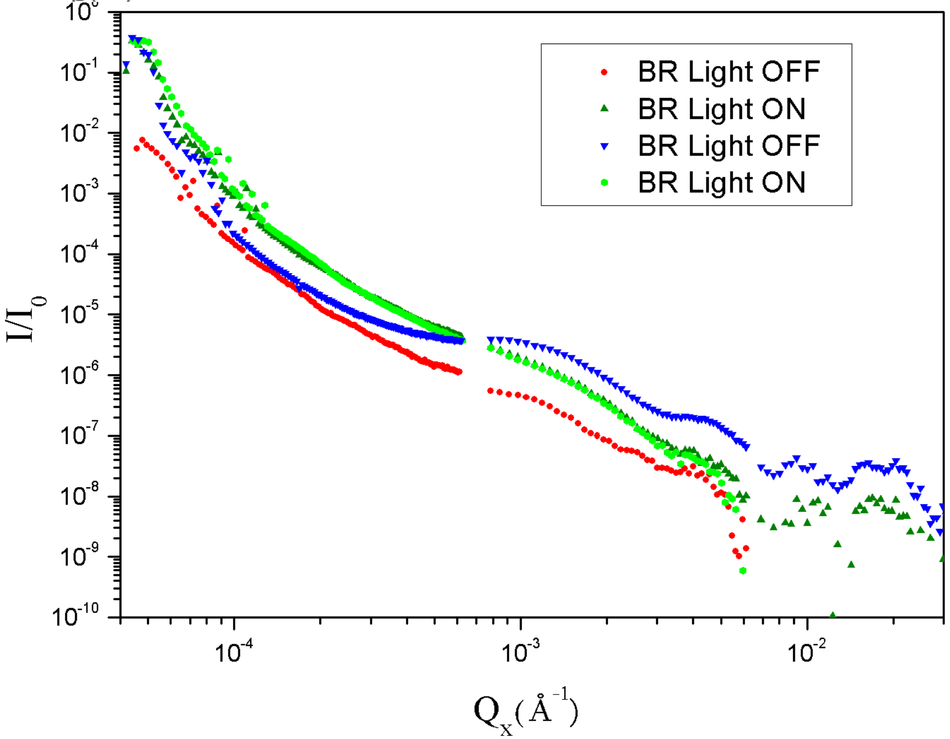

$$\left\langle z(q_\parallel)z(q_\parallel)\right\rangle = \frac{k_B T}{A+\gamma q_\parallel^2+\kappa q_\parallel^4}$$

… *Analysis in progress*

Off -specular X-ray Reflectometry

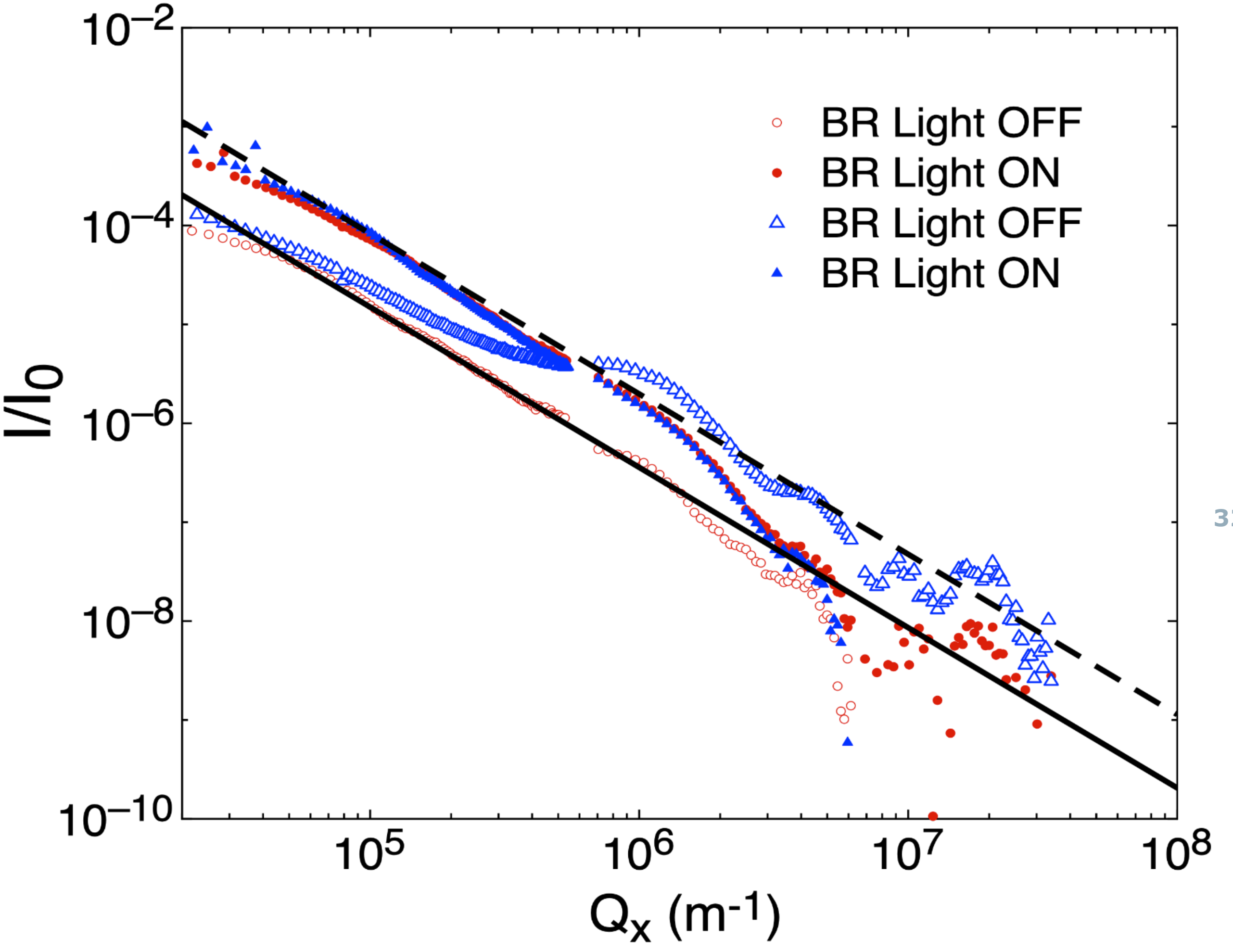

Off-specular XRR for the same DSPC double bilayer.

Reversible effect of light illumination.

$$\frac{(I/I_0)_{\mathrm{ON,off-spec},\,Q_x\to 0}}{(I/I_0)_{\mathrm{OFF,off-spec},\,Q_x\to 0}} = \frac{\sigma^2_{\mathrm{ON,off-spec}}}{\sigma^2_{\mathrm{OFF,off-spec}}} = 4.1 \pm 0.8$$

Effective temperature:

$$\left(\frac{T_{eff}}{T}\right)_{\mathrm{spec}} = \frac{\sigma^2_{\mathrm{ON,\,spec}}}{\sigma^2_{\mathrm{OFF,spec}}} = 3.5 \pm 2.5$$

$$\left(\frac{T_{eff}}{T}\right)_{\mathrm{off-spec}} = \frac{\sigma^2_{\mathrm{ON,off-spec}}}{\sigma^2_{\mathrm{OFF,off-spec}}} = 4.1 \pm 0.8$$

Micropipette aspiration experiments by J.-B. Manneville et al.:

$$1.7 \leq \frac{T_{eff}}{T} \leq 2.7$$

SUMMARY

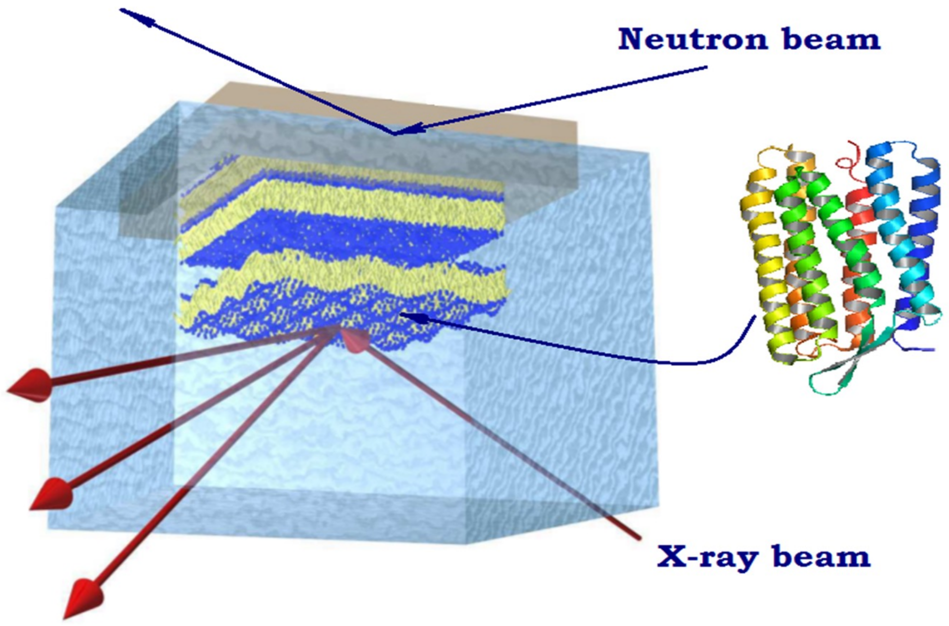

- Successful BR incorporation into membrane-mimic systems
- Reversible effect of light-induced protein activity on membrane structure and fluctuations
- Magnification of membrane fluctuations

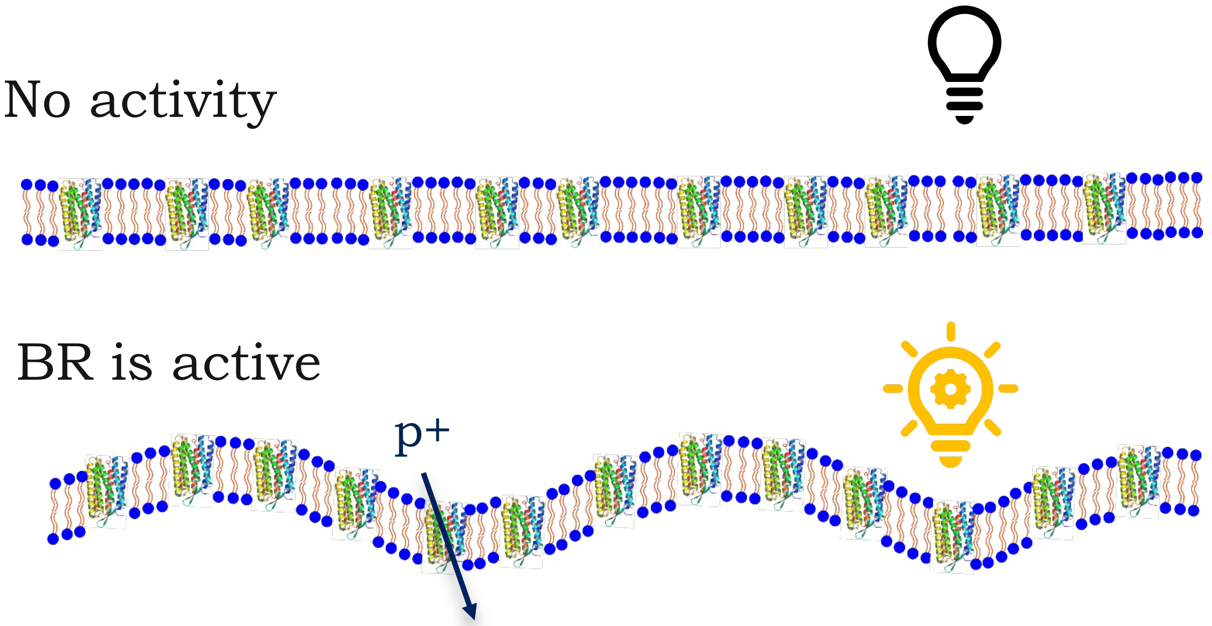

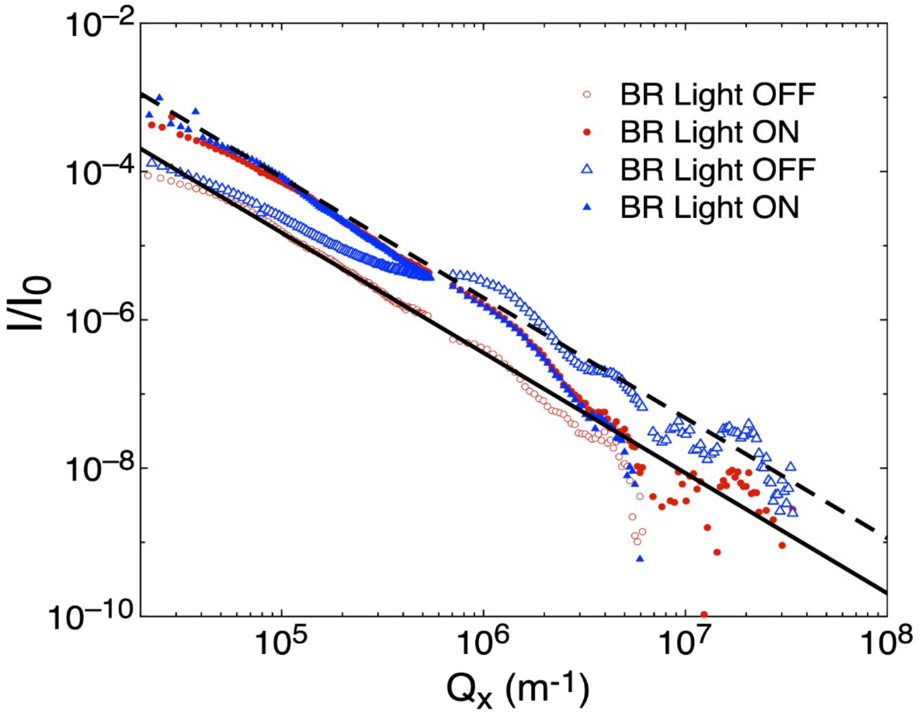

ELSEVIER

Current Opinion in Colloid & Interface Science

Volume 38, November 2018, Pages 108-121

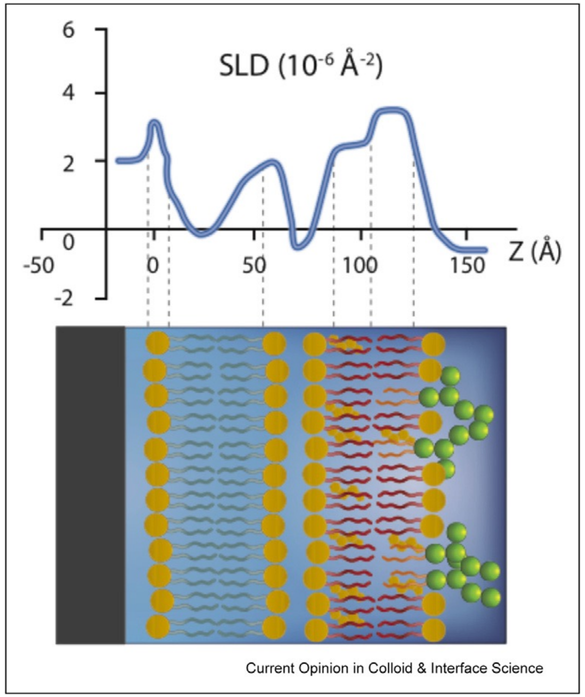

Neutrons and model membranes: Moving towards complexity

Giovanna Fragneto [1], Robin Delhom [2], Loïc Joly [1 3], Ernesto Scoppola [4]

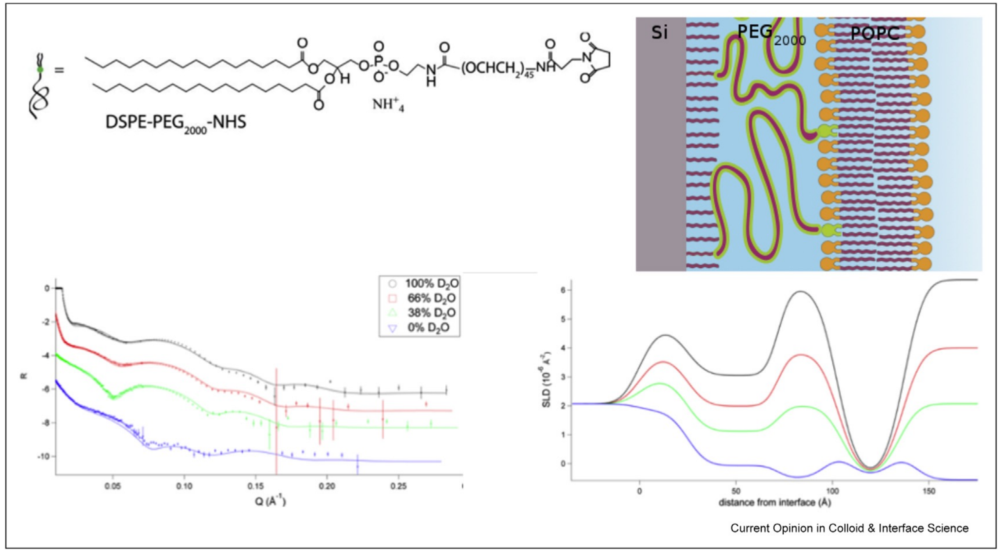

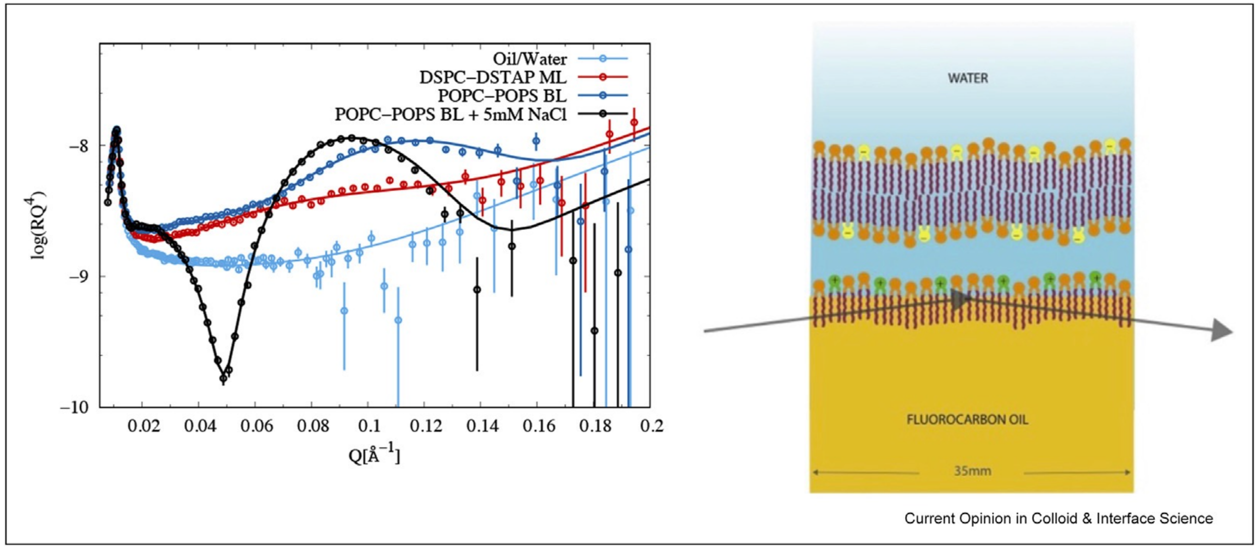

Moving towards complexity:

deuterated (and non) lipid extraction and purification

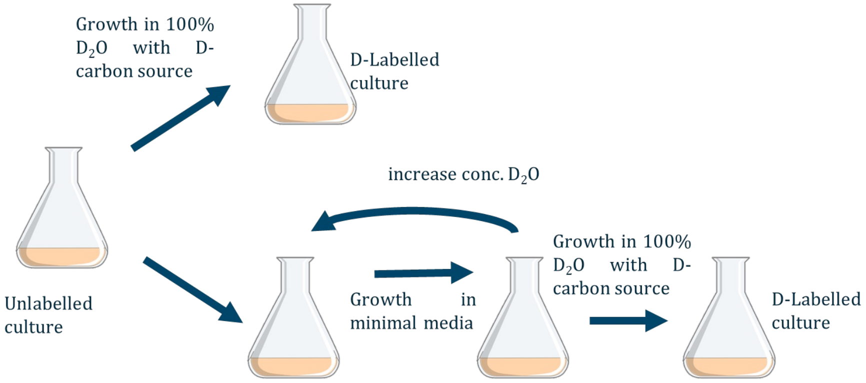

www.ill.eu/L-Lab

PARTNERSHIP FOR SOFT CONDENSED MATTER

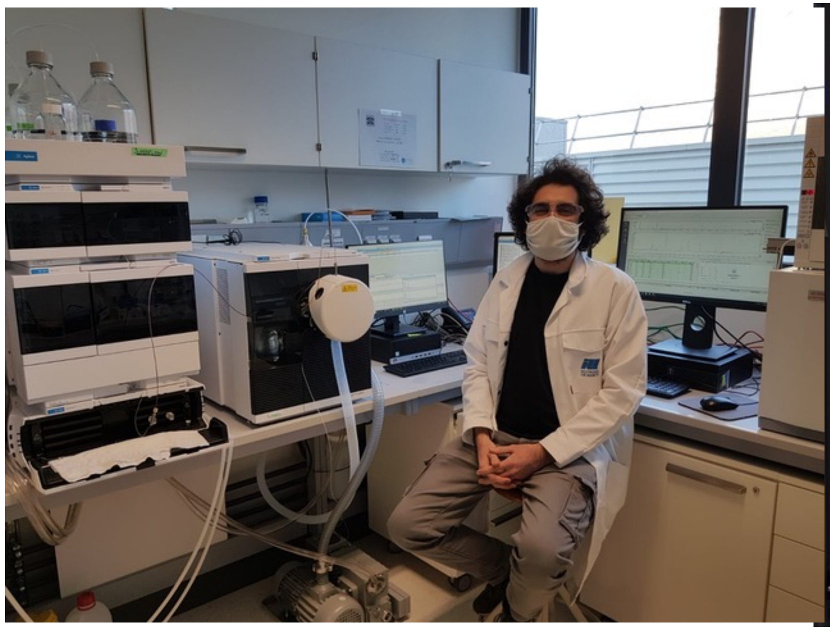

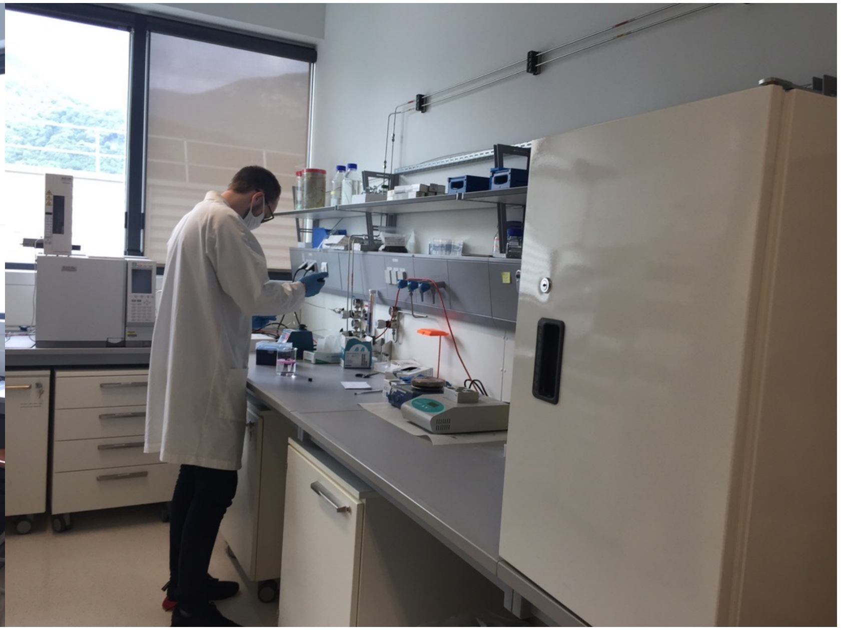

Yeast lipid production at DEMAX

The Deuteration and Macromolecular Crystallisation (DEMAX) platform supports life science and soft matter research users of neutron instruments.

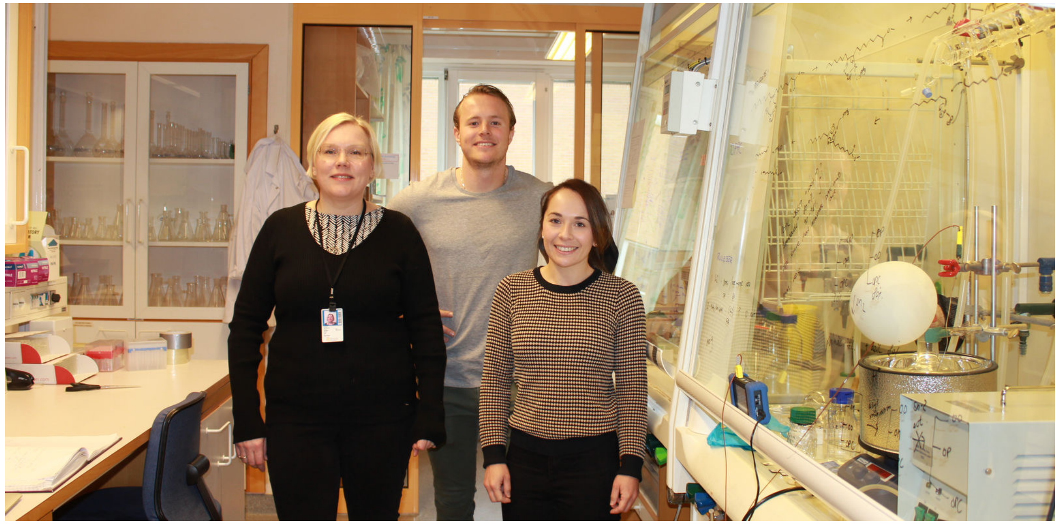

https://europeanspallationsource.se/science-support-systems/demax

Workflow for purification

From cell culture to phospholipid extracts ~ 4 PW

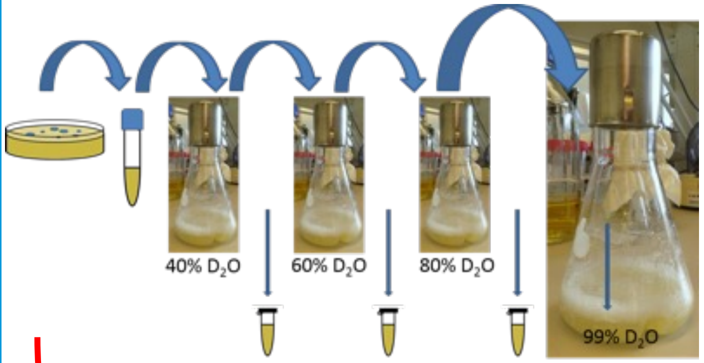

Adaptation to D_2O

Shaker flasks (4-6L)

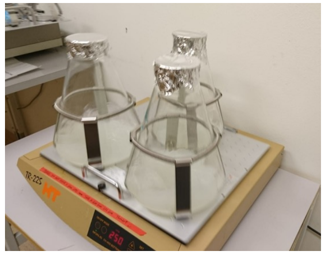

2 weeks (LP3)

Freeze-dry

~15-25g dry cell paste

Solvent Extraction (25g, 2L)

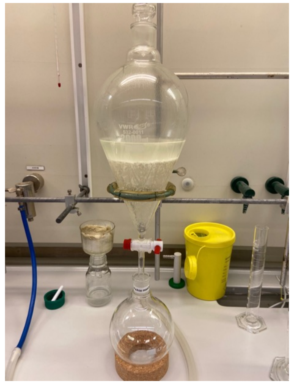

total lipid extract 600-800mg

Flash chromatography

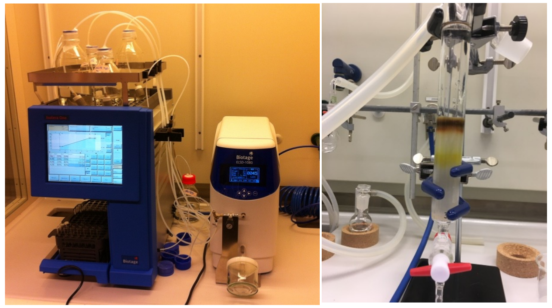

phospholipid extract ~250mg

preparative HPLC or LC

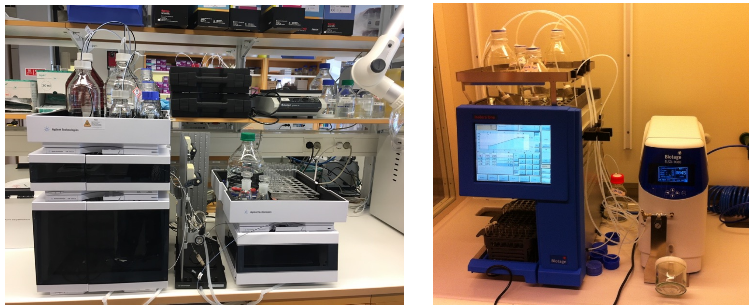

phospholipid classes (10-100mg each)
PC, PE, PS, PI, CL, PG

De Ghellinck *et al.* *PlosONE 2014*

Workflow for lipid analysis

Lipid composition ~1 PW per TLC plate/ batch

% deuteration:
FTIR check internal (1 day)
GC/LC-MS external (availability)

Preparative TLC

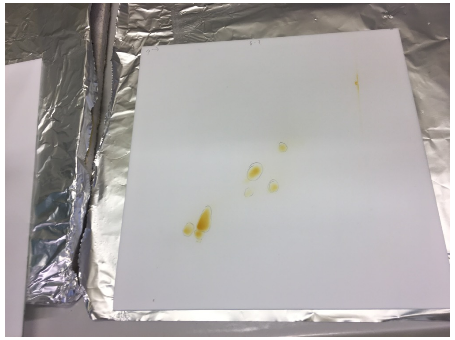

Automated GC sample preparation

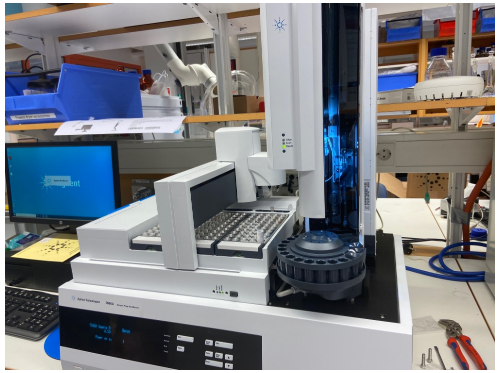

GC-FID

- total PL extract
- each PL class

analysis in triplicate for errors in composition

reusability good after neutrons:

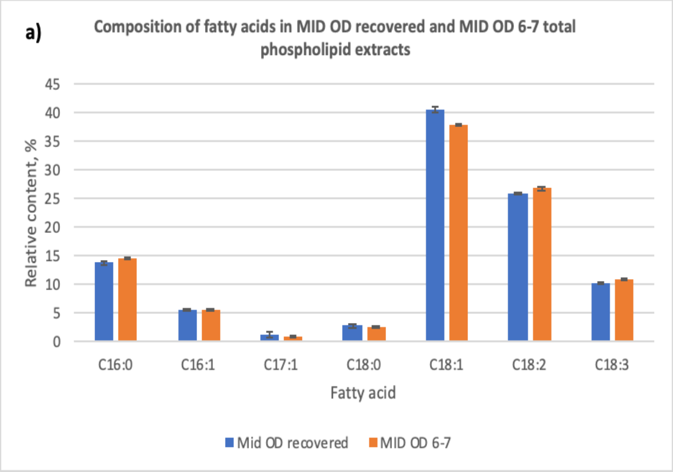

Phospholipid composition

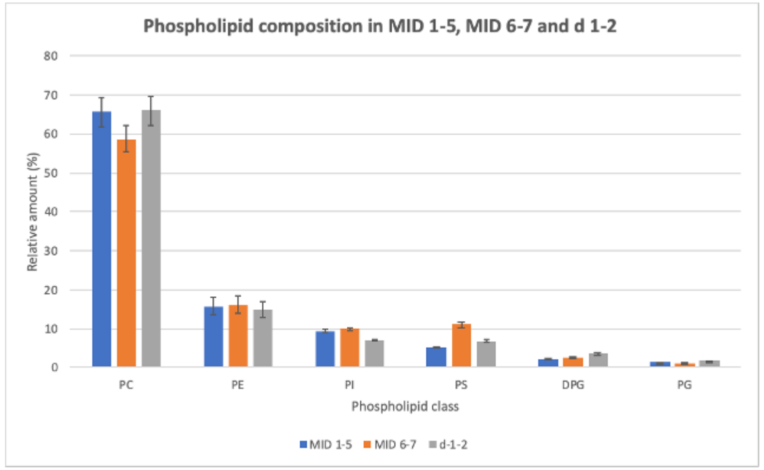

Lipid chain composition in each PL class

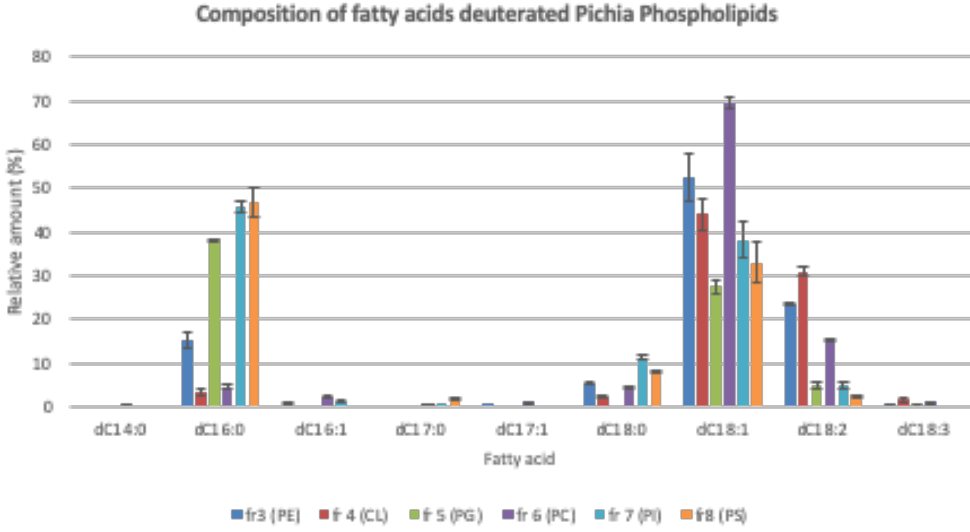

Separation of the phospholipid classes by Normal phase-HPLC

Successful separation of phospholipids classes from *P.pastoris* and *E.coli* total lipid extracts.

TOTAL YIELD

PC = ~51 mg
PE = ~24 mg
PI = ~13 mg
PS = ~18 mg

A total of ~106 mg GPL mixture from 5 g/yeast biomass

A total of ~89 mg GPL mixture from 5 g/E.coli biomass

PE = ~54 mg
PG = ~23 mg
CL = ~13 mg

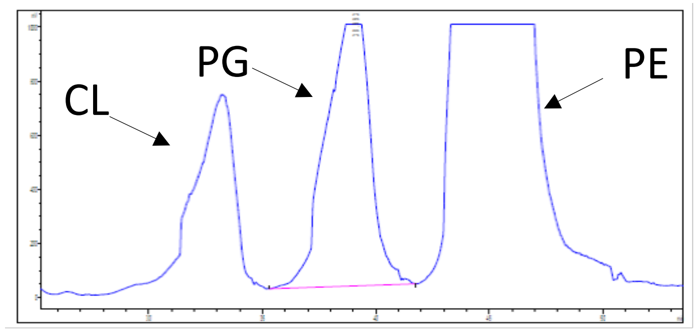

E.Coli lipids chromatogram

PL	RT
CL	30 m
PG	35 m
PE	40 m

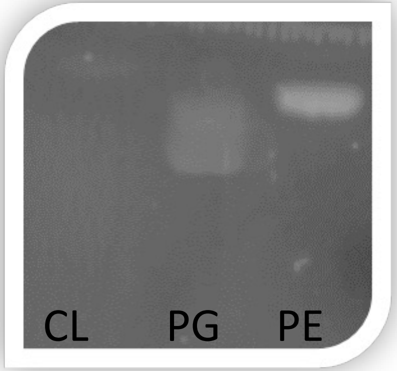

Pichia pastoris lipids chromatogram

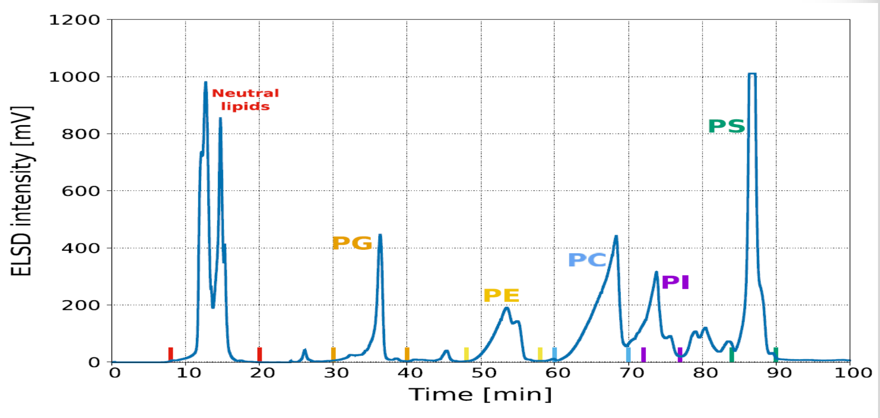

PL	RT
CL	30 m
PG	35 m
PE	43 m
PC	59 m
PI	72 m
PS	83 m

The implementation of an additional purification step by High Performance Liquid Chromatography-Evaporative Light Scattering Detector (HPLC-ELSD) enabled a better separation of the GPL mixtures from the neutral lipid fraction that includes sterols, and also allowed for the GPLs to be purified according to their different polar headgroups.

Fatty acyl chain composition – *Pichia pastoris*

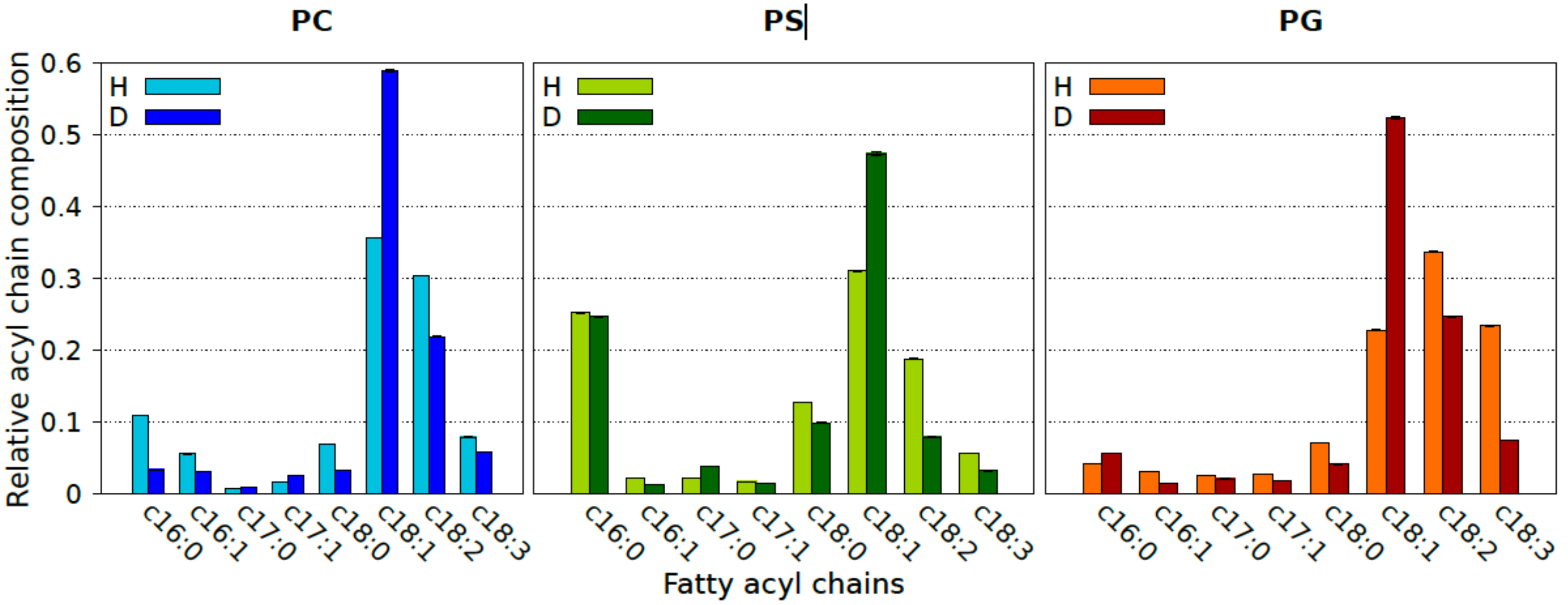

Figure 2: GC-FID analysis of the fatty acid distribution for the investigated GPL classes. Data are mean ± S.D. of three technical repeats. A complete table with all the values can be found in *Supplementary Material* **Table S1.**

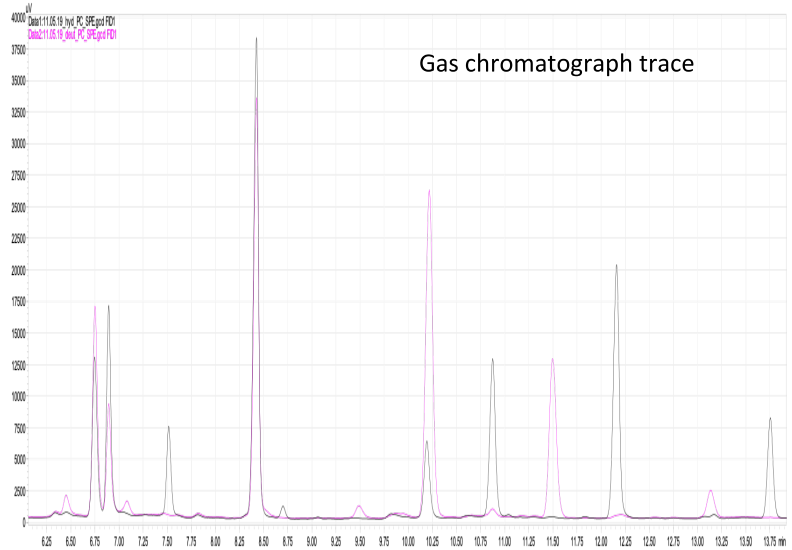

FAMEs analyses revealed that deuteration triggered a significant increase in the oleic acid content = reflected across classes

Decrease in the polyunsaturated FA content.

Decreased palmitic acid levels across the classes while an increase in the stearic acid is noticed in the acidic phospholipids

Corucci et al. JCIS 2023

Structural Characterization of the Purified Lipid Mixtures

- The structure of membrane mono/bilayers has been characterized by techniques (DSC, QCM) that are available within the PSCM.
- Neutron characterization of membrane mimics from the purified lipid mixtures has been carried out within the LSS and SMSS groups including:

1.) SANS from liposomes, nanodiscs, vesicles.

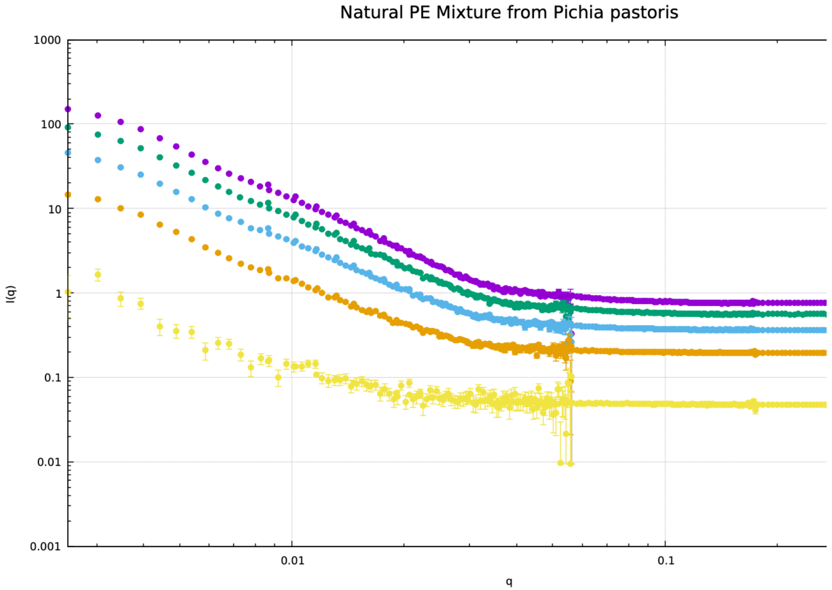

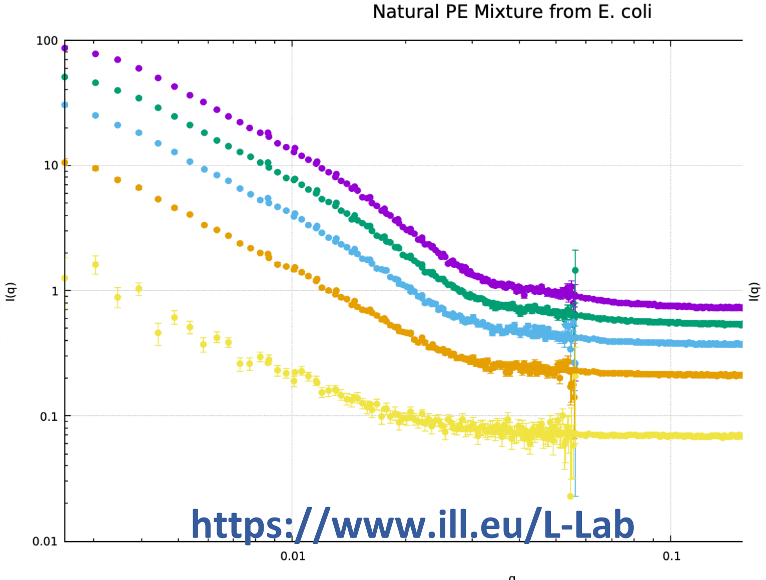

https://www.ill.eu/L-Lab

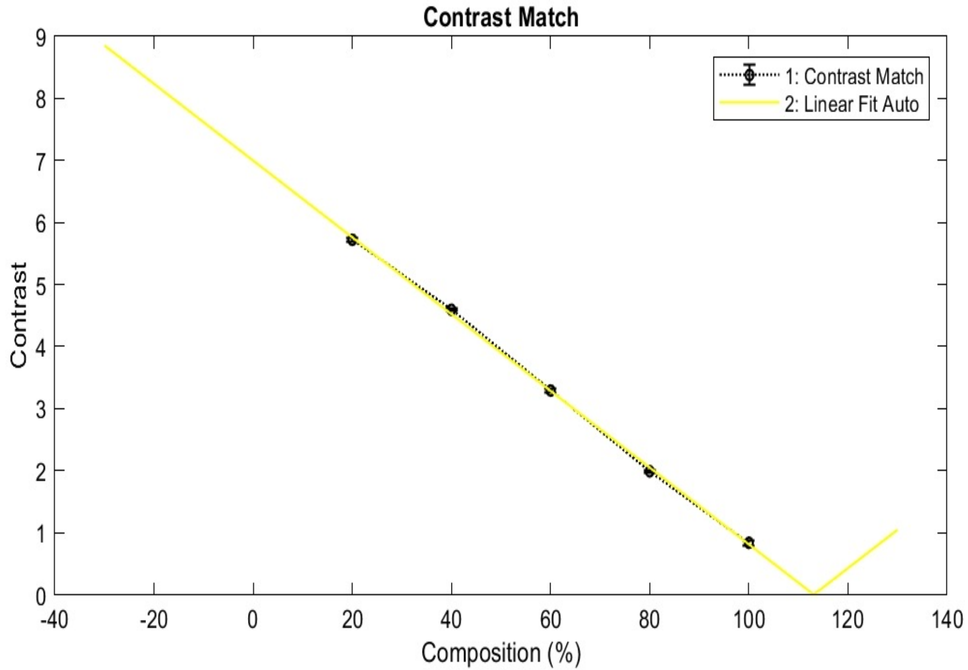

Structural Cha … Lipid Mixtures

- The structure of membran … ized by techniques (DSC, QCM) that are available with
- Neutron characterization c … ed lipid mixtures has been carried out at the ILL w … ding:

1.) SANS from liposomes anc

2.) Diffraction from stacked l … umidity),

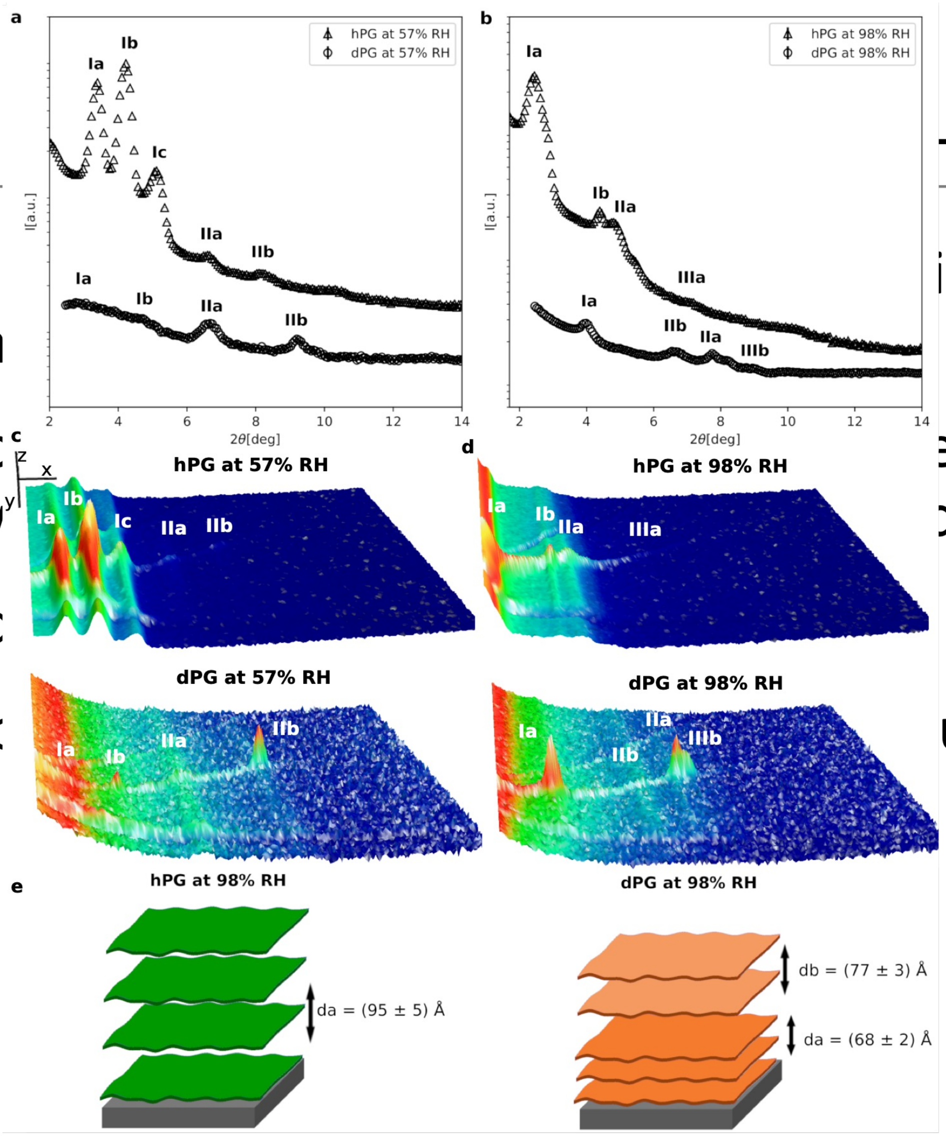

frontiers in Chemistry
ORIGINAL RESEARCH
published: 18 March 2021
doi: 10.3389/fchem.2021.628186

Structural Characterization of Natural Yeast Phosphatidylcholine and Bacterial Phosphatidylglycerol Lipid Multilayers by Neutron Diffraction

Alessandra Luchini[1], Giacomo Corucci[2,3], Krishna Chaithanya Batchu[2], Valerie Laux[2], Michael Haertlein[2], Viviana Cristiglio[2] and Giovanna Fragneto[2,3]*

Contents lists available at ScienceDirect
Colloids and Surfaces B: Biointerfaces
journal homepage: www.elsevier.com/locate/colsurfb

The impact of deuteration on natural and synthetic lipids: A neutron diffraction study

Alessandra Luchini[a,b], Robin Delhom[a], Bruno Demé[a], Valérie Laux[a], Martine Moulin[a], Michael Haertlein[a], Harald Pichler[c,d], Gernot A. Strohmeier[c,e], Hanna Wacklin[f,g], Giovanna Fragneto[a,*]

https://www.ill.eu/L-Lab

Structural Characterization of the Purified Lipid Mixtures

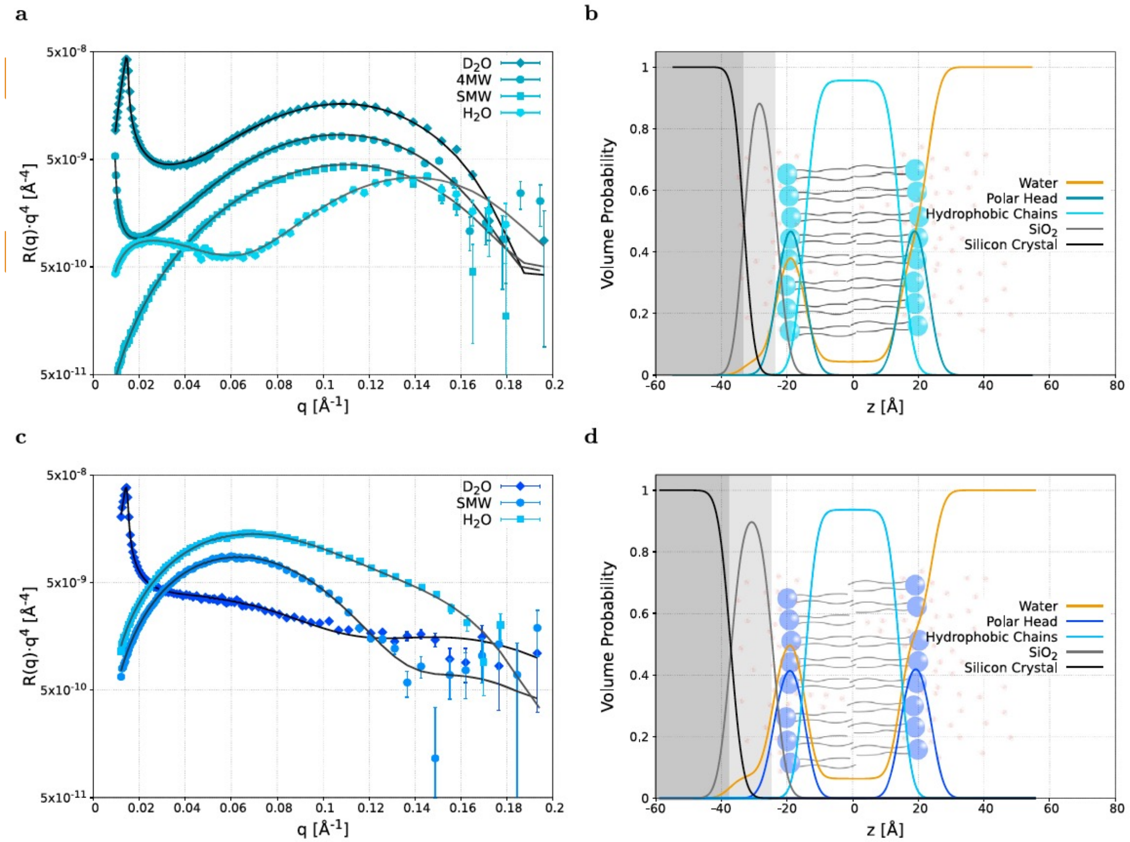

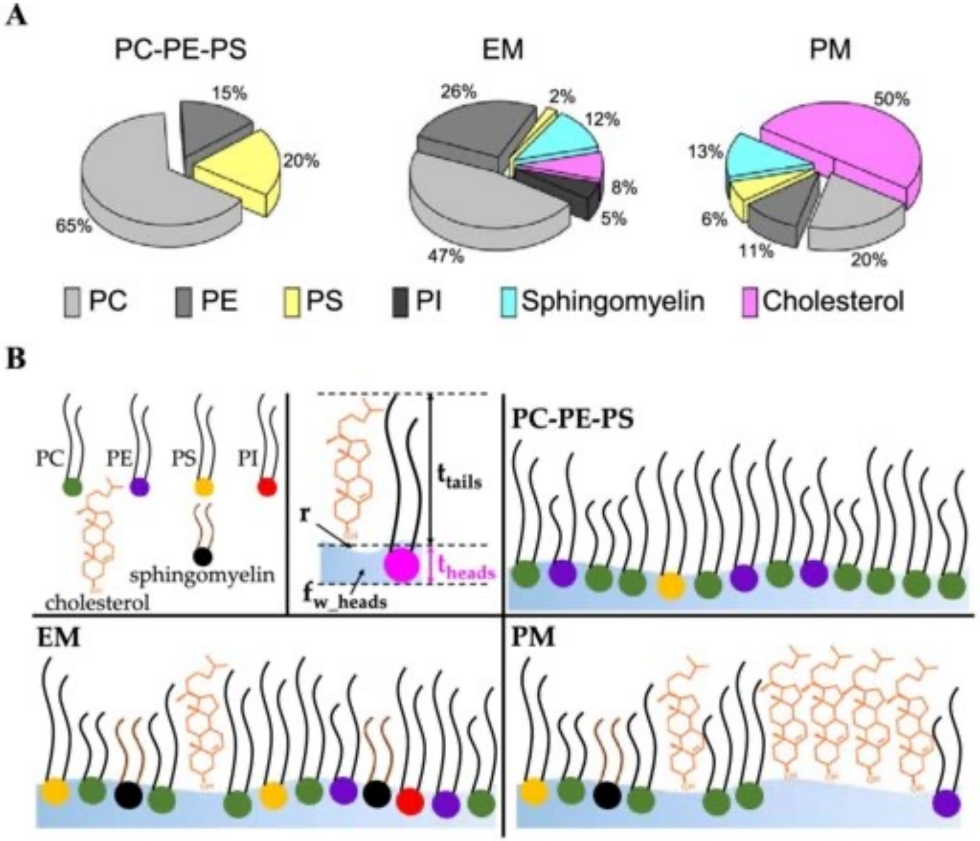

Santamaria, JCIS 2023

https://www.ill.eu/L-Lab

PC/PS

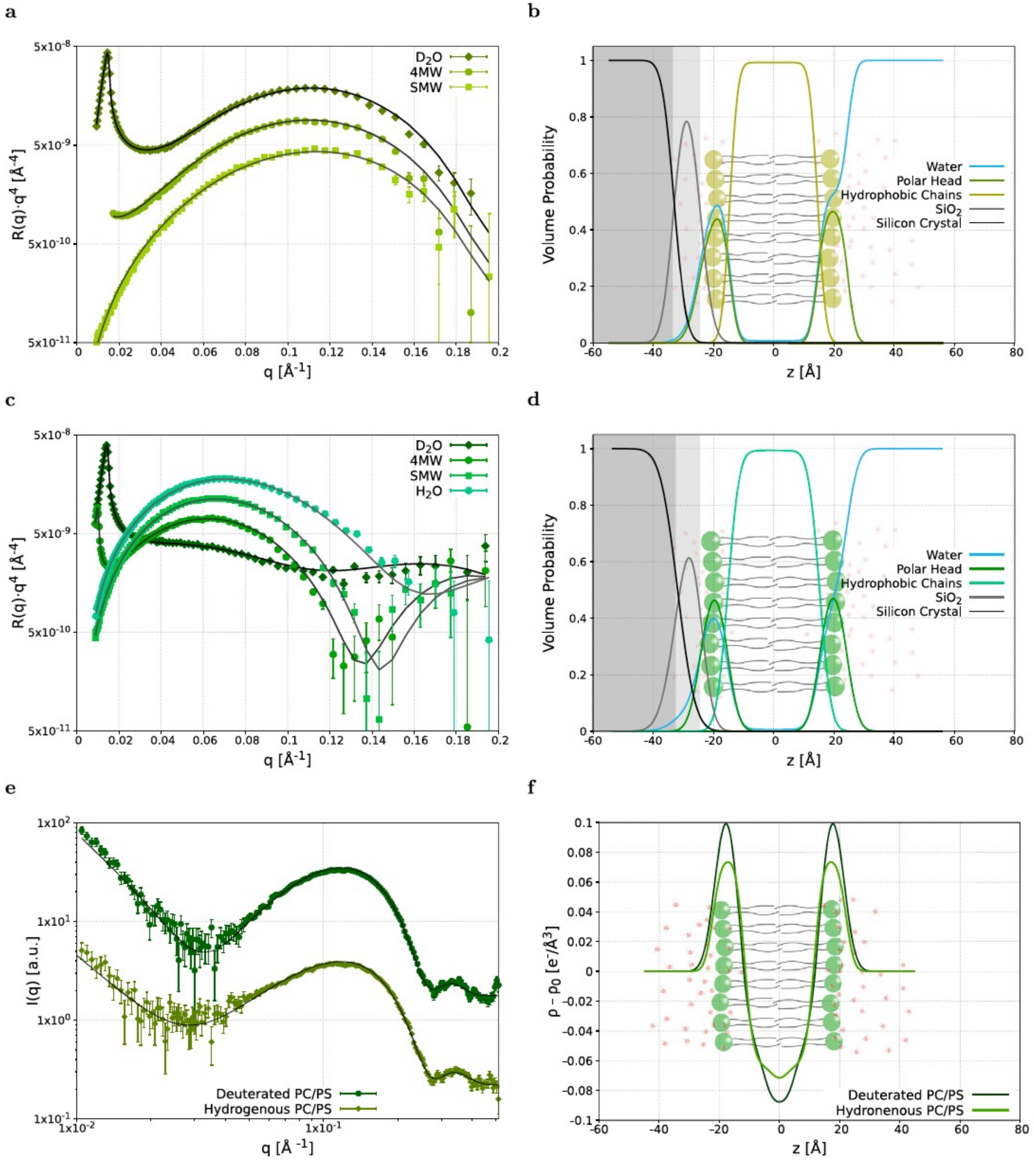

PC/PG

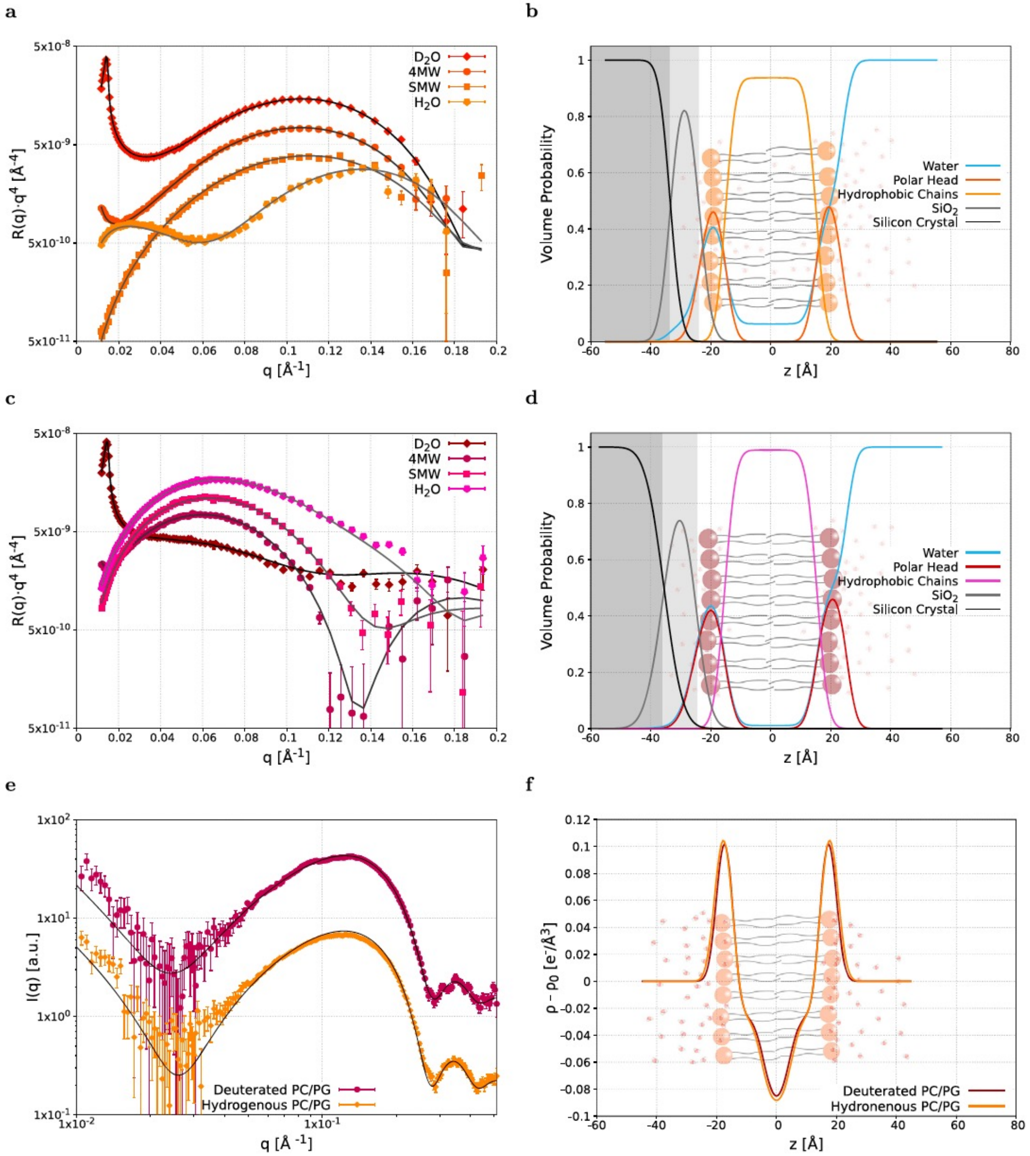

All bilayers from natural extracts show the same structure at the interface (within errors)

Corucci et al. JCIS 2023

scientific reports

OPEN

Check for updates

Lipid bilayer degradation induced by SARS-CoV-2 spike protein as revealed by neutron reflectometry

Alessandra Luchini[1,5], Samantha Micciulla[2,5], Giacomo Corucci[2], Krishna Chaithanya Batchu[2], Andreas Santamaria[2], Valerie Laux[2], Tamim Darwish[3], Robert A. Russell[3], Michel Thepaut[4], Isabelle Bally[4], Franck Fieschi[4] & Giovanna Fragneto[2]✉

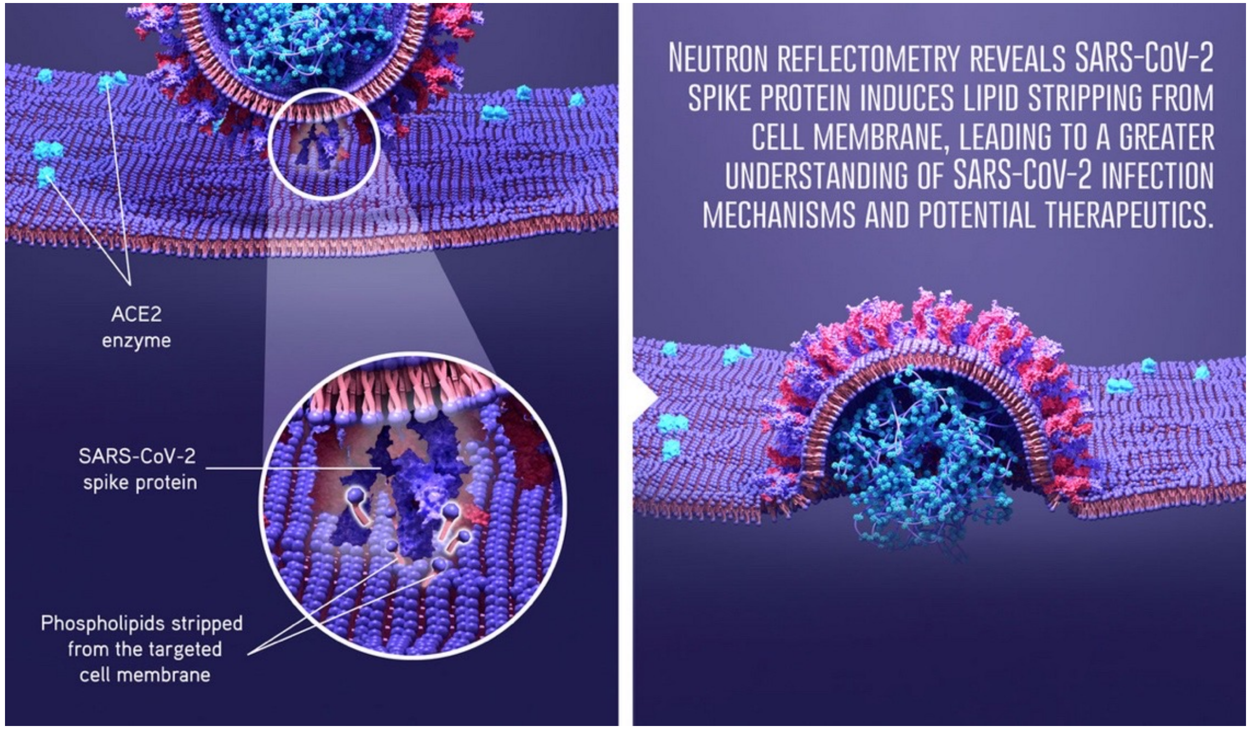

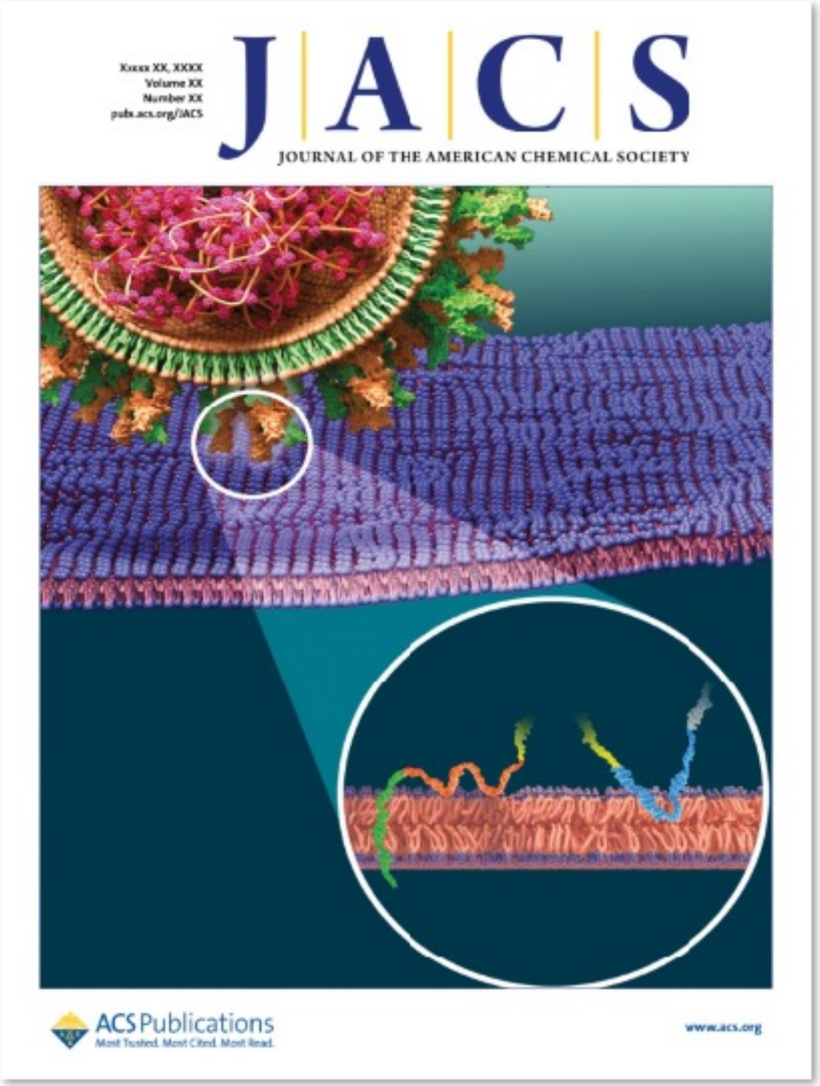

Perspectives:

✤Antibiotic resistance

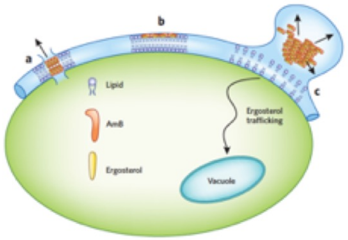

✤Amyloid interactions with membranes

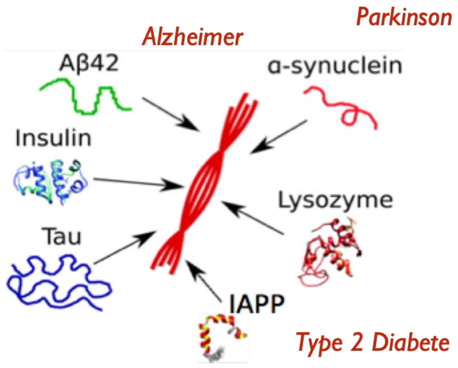

✤Viral entry

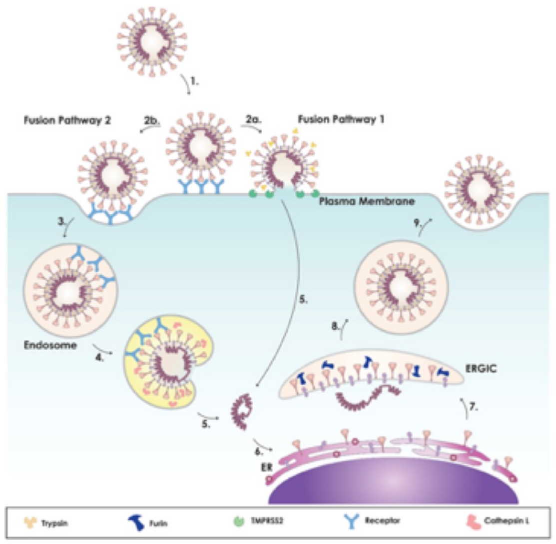

✤Protein/peptide/drug/… membrane interactions

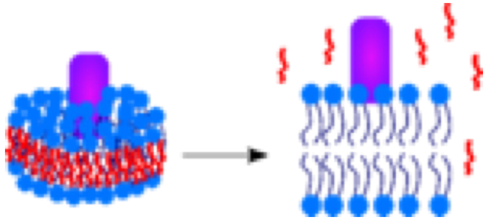

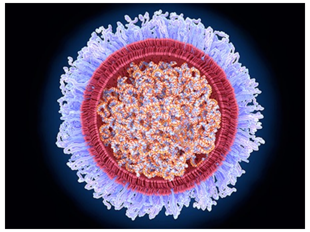

ACS Nano 2021

✤Matched nano discs: low resolution protein structures

✤Transmembrane protein reconstitution

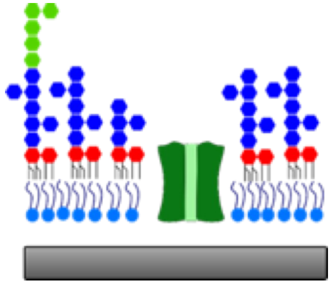

✤Effects of deuteration on membrane composition

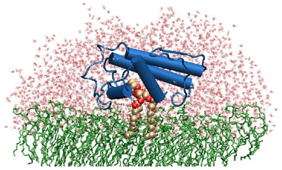

✤Enzyme mechanisms at membrane surface

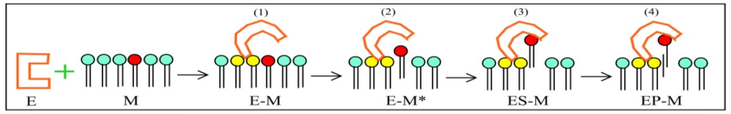

The ILL Reactor

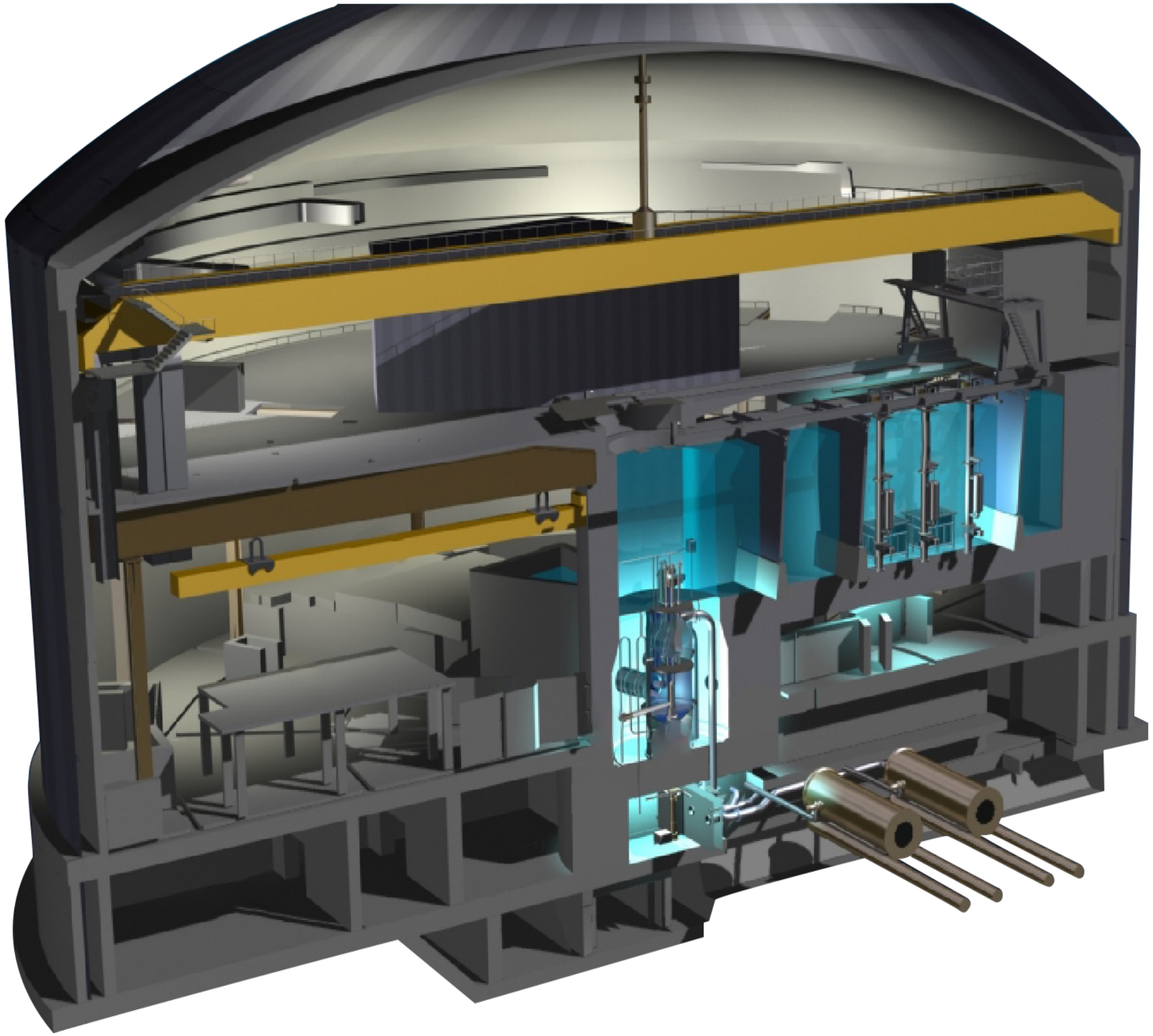

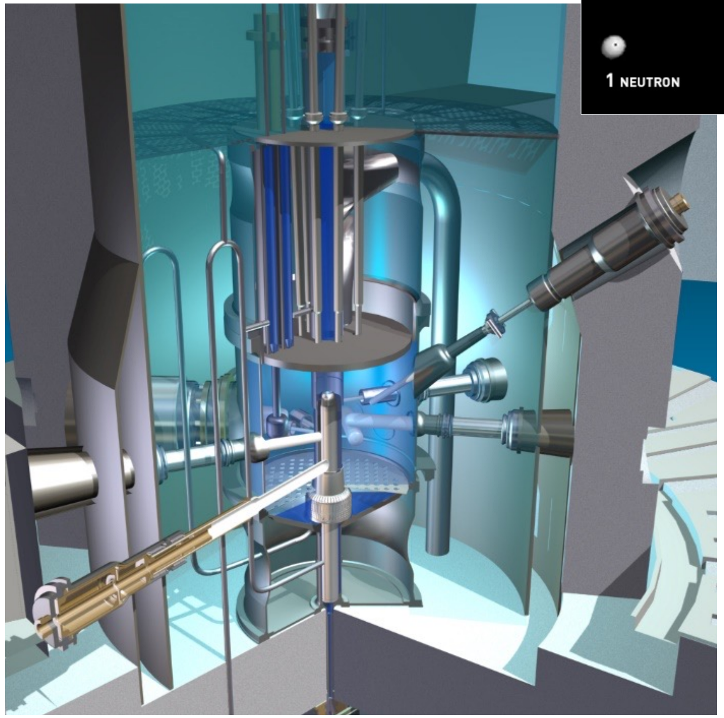

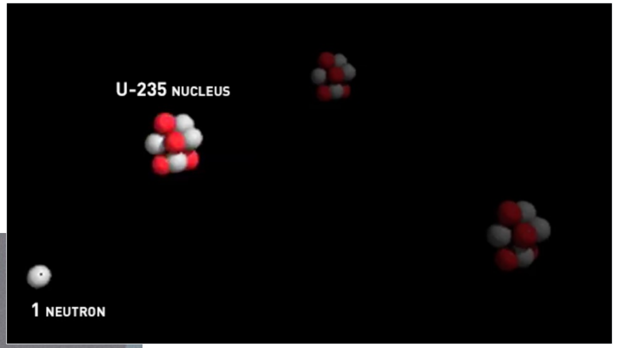

A neutron source generating

5 x 10^{18} fast neutrons/sec

at a max power of 58 MW

Neutron Source Brightness

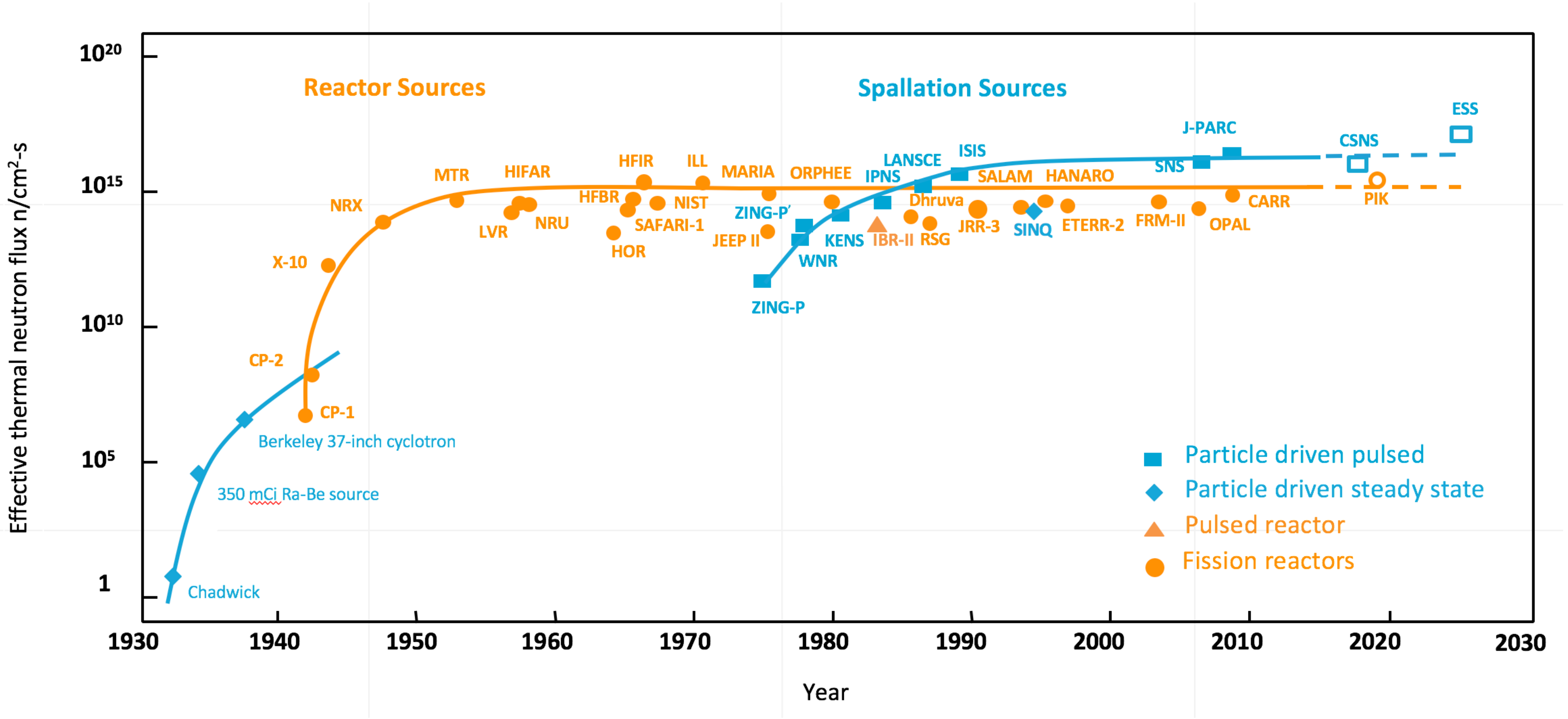

(Updated from *Neutron Scattering*, K. Skold and D. L. Price, eds., Academic Press, 1986)

European Spallation Source

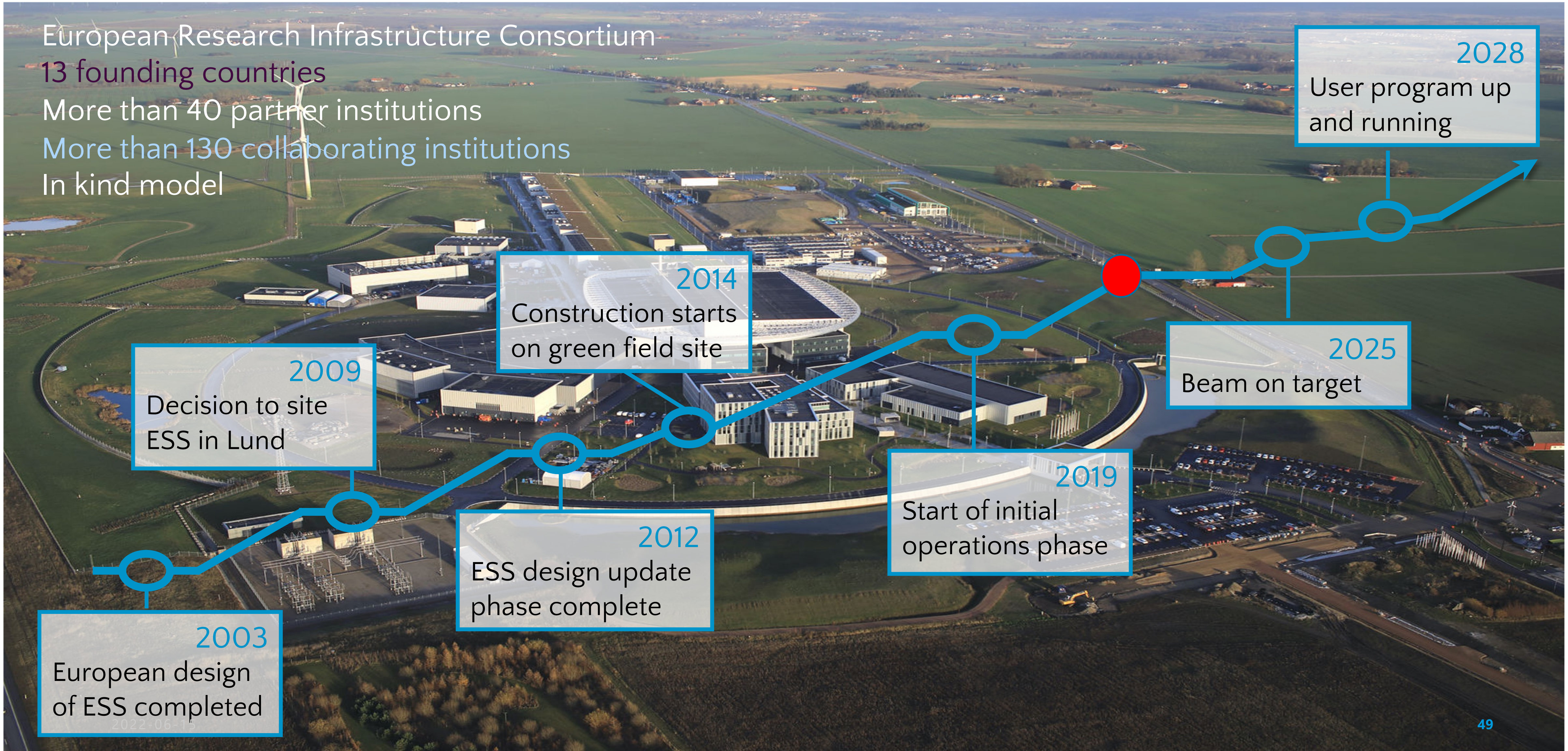

How it works

The technology

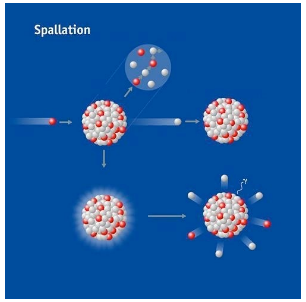

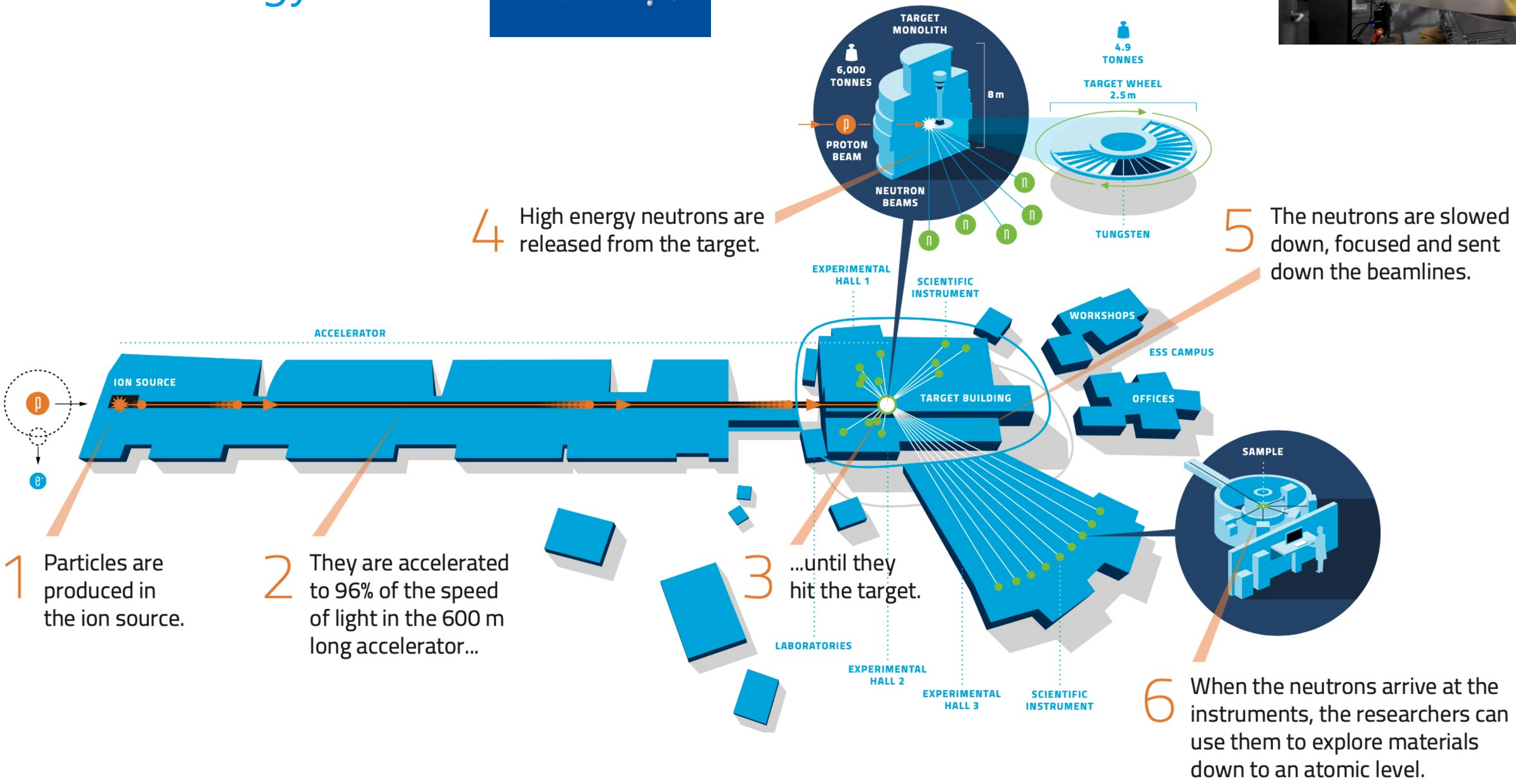

Long-pulse Performance and Flexibility

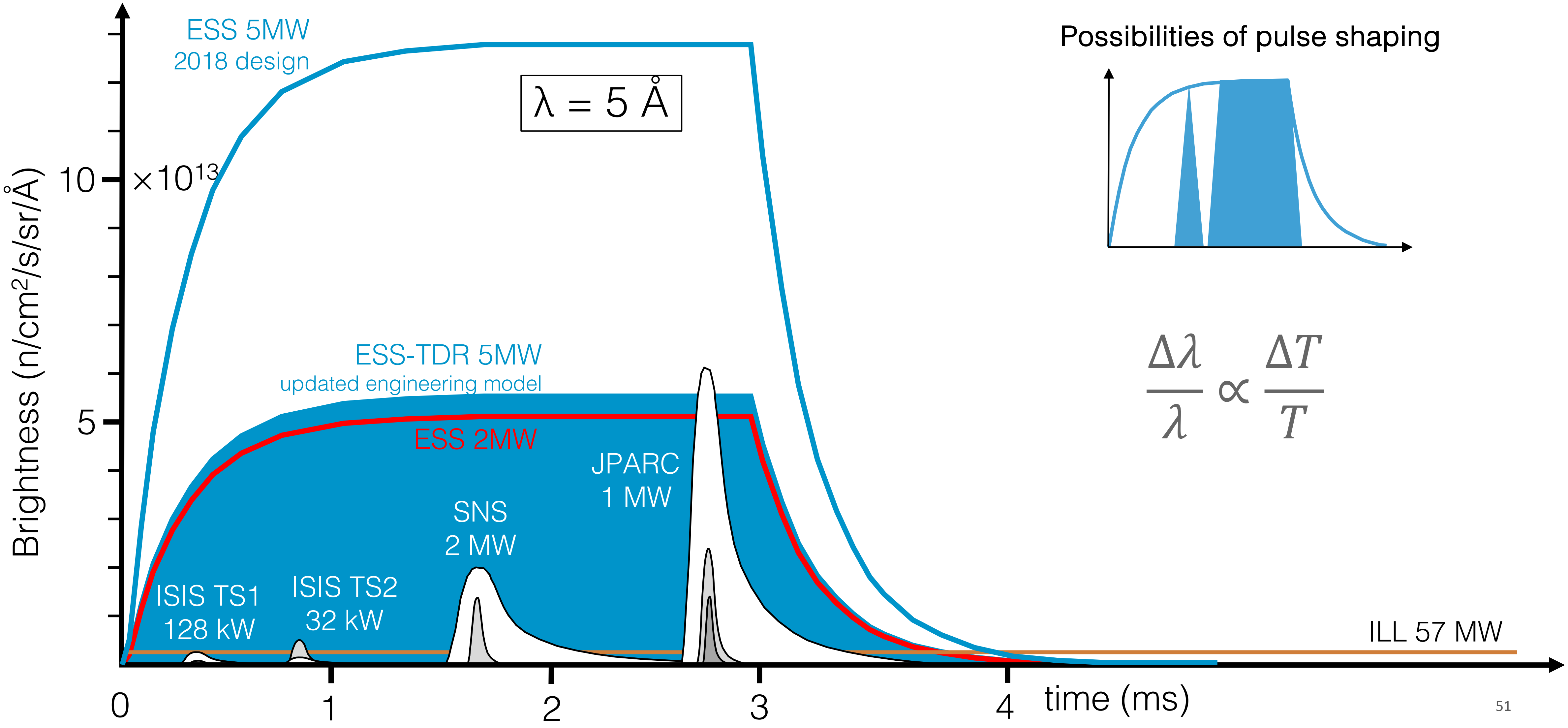

Possibilities of pulse shaping

$$\frac{\Delta\lambda}{\lambda} \propto \frac{\Delta T}{T}$$

Neutron Scattering Techniques

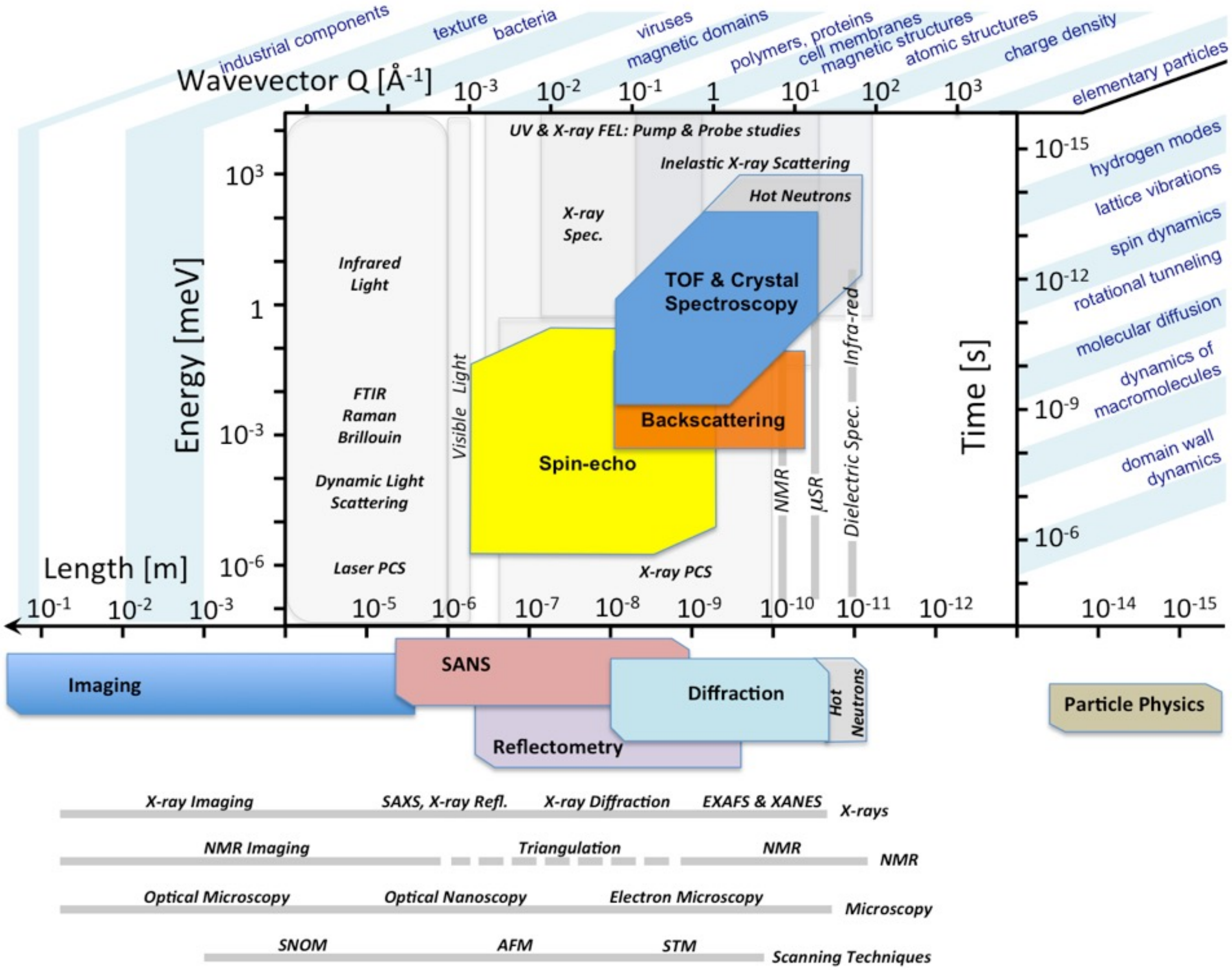

Neutron Instruments

Andersen, K. H.; Argyriou, D. N.; Jackson, A. J. et al. The Instrument Suite of the European Spallation Source. *Nuclear Instruments and Methods in Physics Research Section A:* **2020**, *957*, 163402. https://doi.org/10.1016/j.nima.2020.163402.

15 instruments + Test Beamline

Diffractometers (DREAM, MAGiC, HEIMDAL)
SANS (LoKI, SKADI)
Reflectometers (Estia, FREIA)
Imaging (ODIN)
Engineering Diffraction (BEER)
Macromolecular Crystallography (NMX)
Spectrometers (CSPEC, T-REX, BIFROST, MIRACLES, VESPA)

Novel detector technologies and geometries
Complex pulse-shaping

Shared neutron bunker – common space for components
Common timing system for facility
Single controls infrastructure (EPICS)
Control and data recording running remotely from instrument

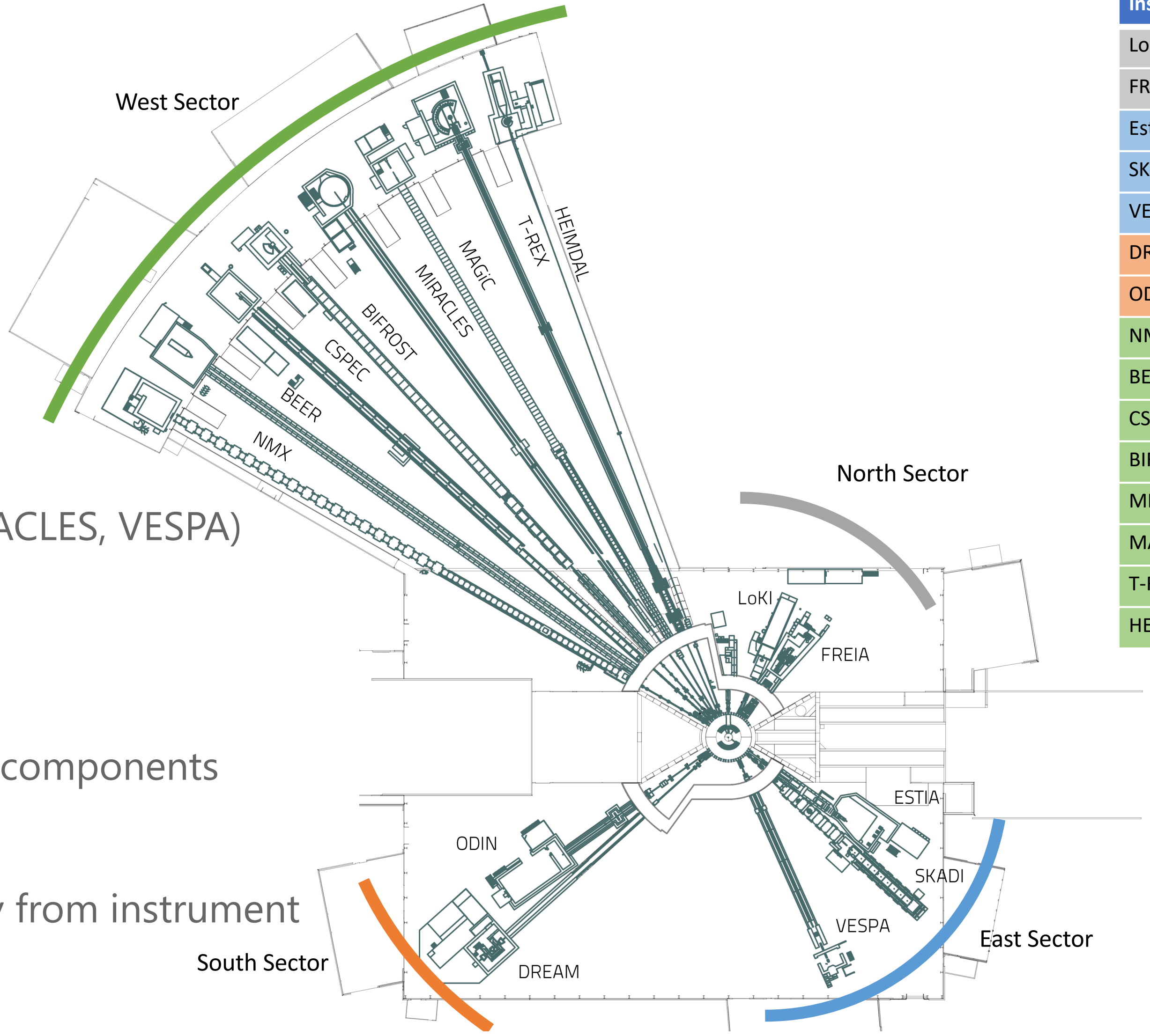

Instrument	Beamport
LoKI	N7
FREIA	N5
Estia	E2
SKADI	E3
VESPA	E7
DREAM	S3
ODIN	S2
NMX	W1
BEER	W2
CSPEC	W3
BIFROST	W4
MIRACLES	W5
MAGiC	W6
T-REX	W7
HEIMDAL	W8

Estia

Focussing Polarised Reflectometer for Tiny Samples

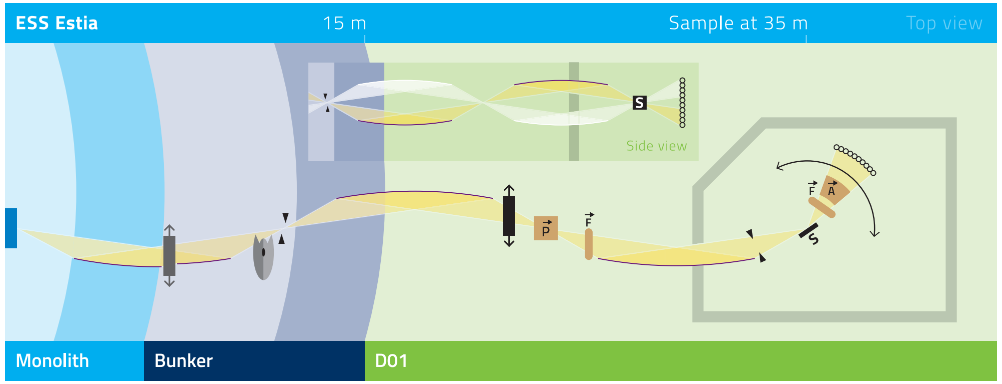

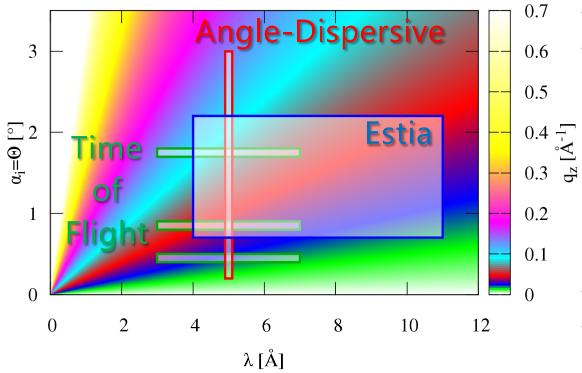

Estia Quick Facts.

Estia Quick Facts	
Instrument Class	Reflectometry
Moderator	Cold
Primary Flightpath	35 m
Secondary Flightpath	4 m
Wavelength Range	3.75–28 Å
Polarised Incident Beam	Optional
Polarisation Analysis	Optional
Sample Orientation	Vertical
Total Q-Range	0.001 to 3.15 Å^{-1}/−0.001 to −0.3 Å^{-1}
Standard Mode (14 Hz)	
Bandwidth	7 Å
Flux at Sample at 2 MW[a]	6×10^8 n s^{-1} cm^{-2}
Relative Q-Range	$Q_{max} = 2.85 \times Q_{min}$
Q-Resolution ΔQ/Q	7.8%–3.0% over Q-range
2-Pulse Skipping Mode (4.7 Hz)	
Bandwidth	21 Å
Flux at Sample at 2 MW[a]	2×10^8 n s^{-1} cm^{-2}
Relative Q-Range	$Q_{max} = 6.6 \times Q_{min}$
Q-Resolution ΔQ/Q	7.8%–1.3% over Q-range

[a]Full-divergence beam averaged over 5(H) × 10(V) mm².

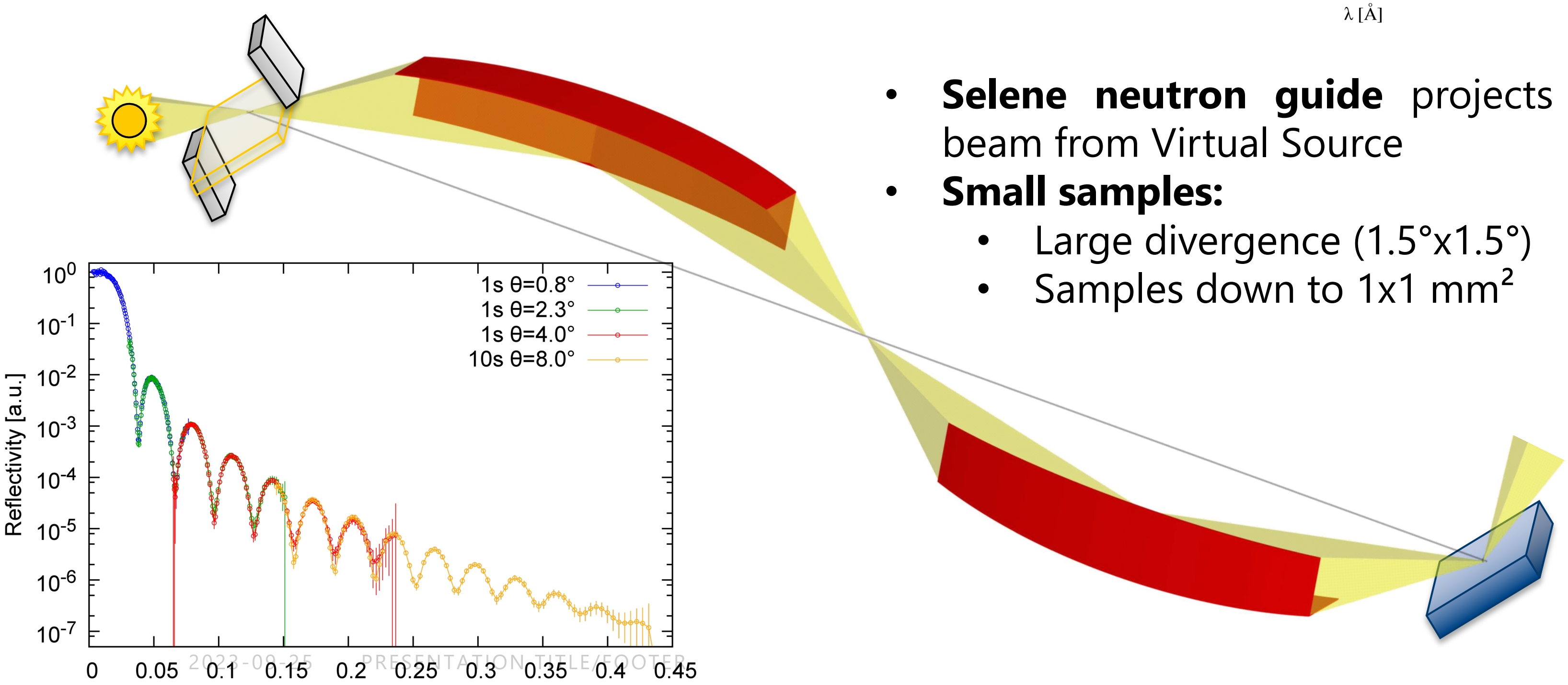

- **Selene neutron guide** projects tiny beam from Virtual Source
- **Small samples:**
  - Large divergence (1.5°x1.5°)
  - Samples down to 1x1 mm²

PAUL SCHERRER INSTITUT

For the study of surfaces and interfaces including magnetic layers

ESTIA

Science Case

ESTIA is optimised for small samples and polarisation analysis:

The investigation of the **chemical and magnetic** depth-profile near surfaces and of **lateral correlations and structures**

- functional devices: spin-valves, spintronics
- diffusion processes: Li batteries, corrosion protection
- multifunctional materials: interface-coupled electric and magnetic properties
- towards real materials: raster-scanning of bent, faceted or multi-domain surfaces

- **Small samples:**
  - Large divergence (1.5°x1.5°)
  - Samples down to 1x1 mm²
- **Polarization >99%** for curved transmission polarizer and analyser
- Simultaneous measurement of two polarization states

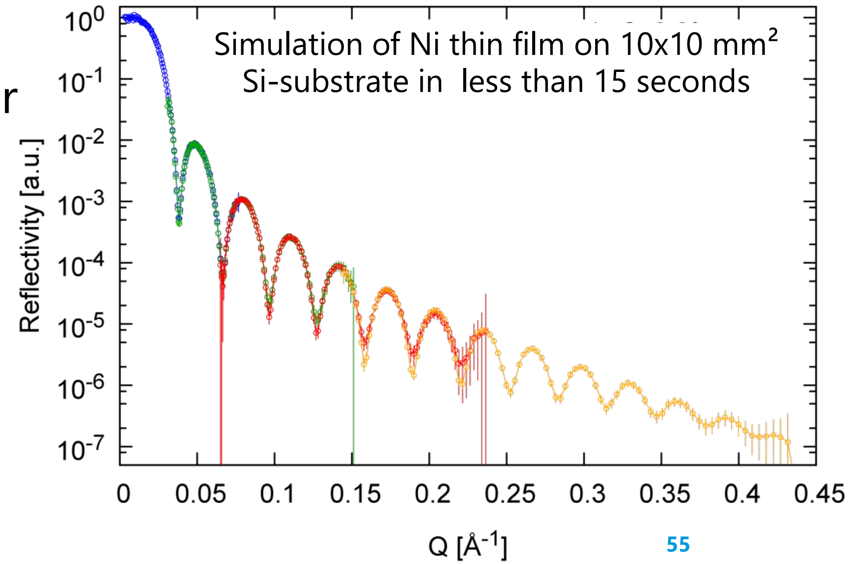

FREIA

Science Case

In-situ time-resolved reflectometry for soft condensed matter, life science and functional materials

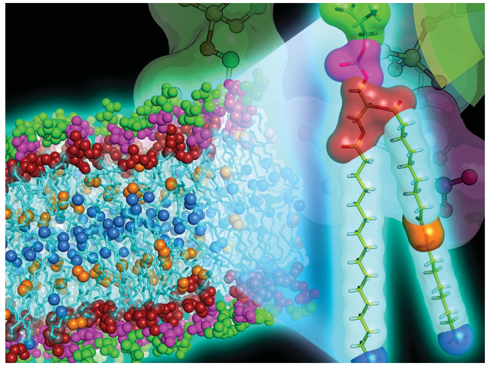

Instrument characteristics to allow very fast measurements:

- Very high flux
- Horizontal sample geometry
- Flexible collimation
- Variable resolution
- Broad simultaneous Q
- No sample movement

Dynamics

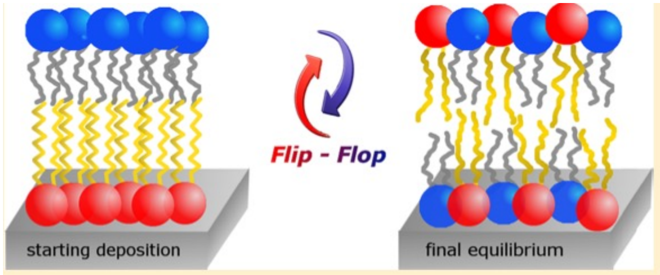

- deposition, structure and phase behavior
- adsorption, self-assembly and reactions
- gas/liquid/solid interfaces

Applications

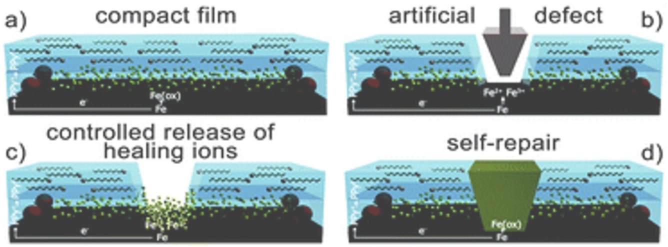

- response to external stimuli
- in situ and in operando
- complex sample environments

Design

Function

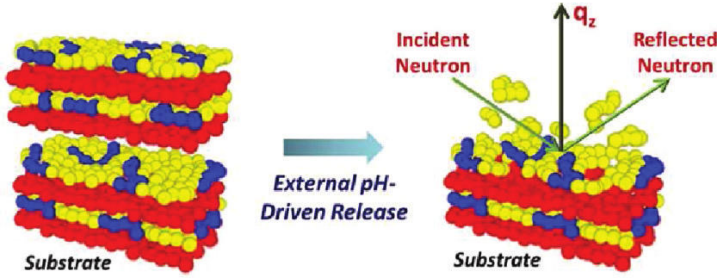

Expected perfomances of ESS reflectometers compared to ILL ones

FOM = Peak brightness* divergence (vertical & horizontal) * λmax/λmin

FREIA and ESTIA: wide divergence mode: large q-range kinetic measurements

FOM = Peak brightness* divergence (vertical & horizontal) * λmax/λmin

ESS-2MW: D17 new guide: usable flux on the sample by a factor of 2.5

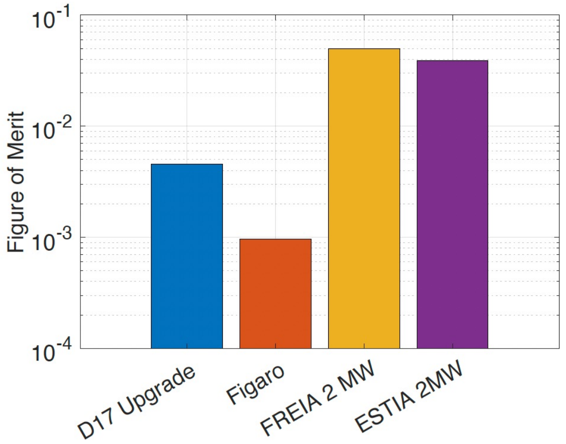

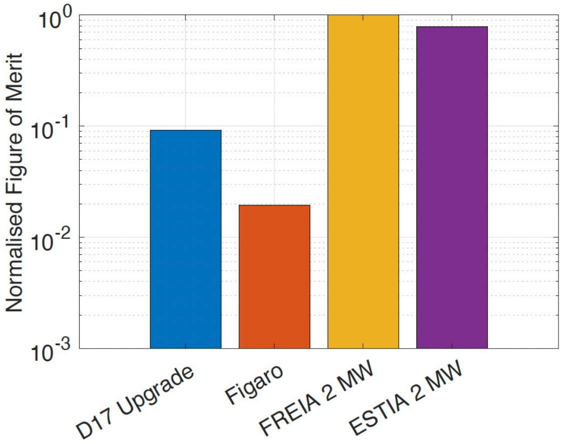

2MW

FREIA and ESTIA: wide divergence mode: large q-range kinetic measurements

FOM = Peak brightness* divergence (vertical & horizontal) * λmax/λmin

ESS-5MW: D17 new guide: usable flux on the sample by a factor of 2.5

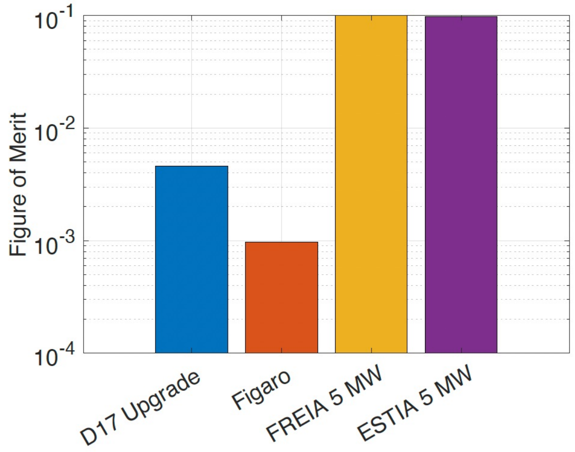

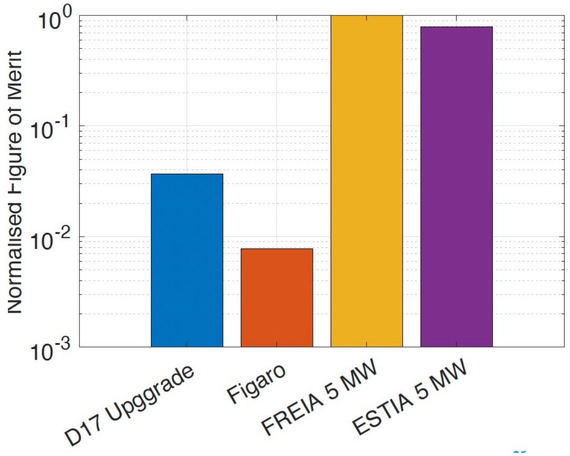

5MW

Areas that neutrons already contribute to:

Challenges for neutron science

nature > collection

Collection | 17 February 2023

Extracellular vesicles

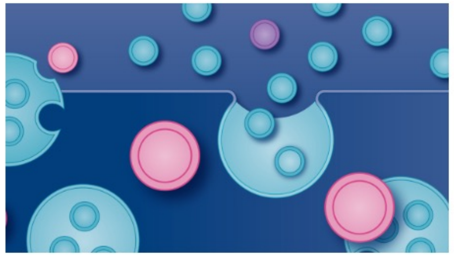

Extracellular vesicles (EVs) have emerged as important means of cell–cell communication, having the potential to transfer various cargoes – encompassing proteins, nucleic acids, metabolites or even entire organelles — between cells. By now, the importance of EV-mediated cell–cell communication has been documented in a plethora of physiological and pathological situations, across the different kingdoms. In addition, their secretion and cargo composition can change depending on the biological context, making EVs suitable biomarkers for several diseases. EVs have also been harnessed as drug delivery agents and standalone therapeutics.

nature > collection

Collection | 14 April 2023

Cancer research

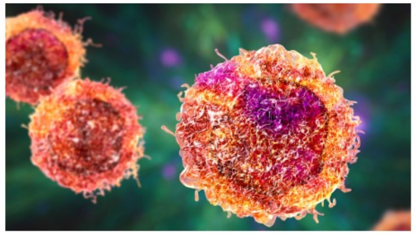

Cancer is a leading cause of death, accounting for nearly one in six deaths worldwide. Many cancers can be cured, especially if detected early and treated effectively. Nevertheless, an unmet need for the development of treatments for aggressive and often metastatic tumors remains. Preclinical and clinical research in the areas of cancer screening and detection, as well as development of new therapies are at the core of this challenge. This development is cemented by an understanding of basic cancer biology and tumor immunology and tumor profiling studies that link bench and bedside to allow for an improved understanding of therapy response and resistance. In this collection, we highlight the breadth of cancer research in these areas at the Nature Portfolio.

Article | Open Access | Published: 14 April 2023

Temporal nanofluid environments induce prebiotic condensation in water

Andrea Greiner de Herrera, Thomas Markert & Frank Trixler

Communications Chemistry 6, Article number: 69 (2023) | Cite this article

468 Accesses | 2 Altmetric | Metrics

COMMENT | 02 May 2023

Address the growing urgency of fungal disease in crops

More political and public awareness of the plight of the world's crops when it comes to fungal disease is crucial to stave off a major threat to global food security.

Bacterial cellulose comes out of the woodwork

Polymer scientists in Japan are harnessing the power of botany and bacteria to produce bioplastics that don't harm the environment.

NATURE INDEX | 14 December 2022

Three ways to combat antimicrobial resistance

With a dearth of new antibiotics coming to market, researchers are finding creative ways to keep bacteria at bay.

NEWS FEATURE | 04 April 2023

Conquering Alzheimer's: a look at the therapies of the future

Researchers are looking to drug combinations, vaccines and gene therapy as they forge the next generation of treatments for the condition.

Courtesy H. Wacklin-Knecht

E.g. what ESS could advance (with smaller samples/higher throughput/deuteration):

Challenges for neutron science

RESEARCH BRIEFINGS | 26 April 2023

New protein–protein interactions designed by a computer

Creating protein interactions through computational design is a key challenge in the fields of both basic and translational biology. An approach that uses the machine-learned fingerprints of protein-surface features was used to produce synthetic proteins that engage immunotherapeutic or viral targets with binding affinities comparable to those of naturally occurring proteins.

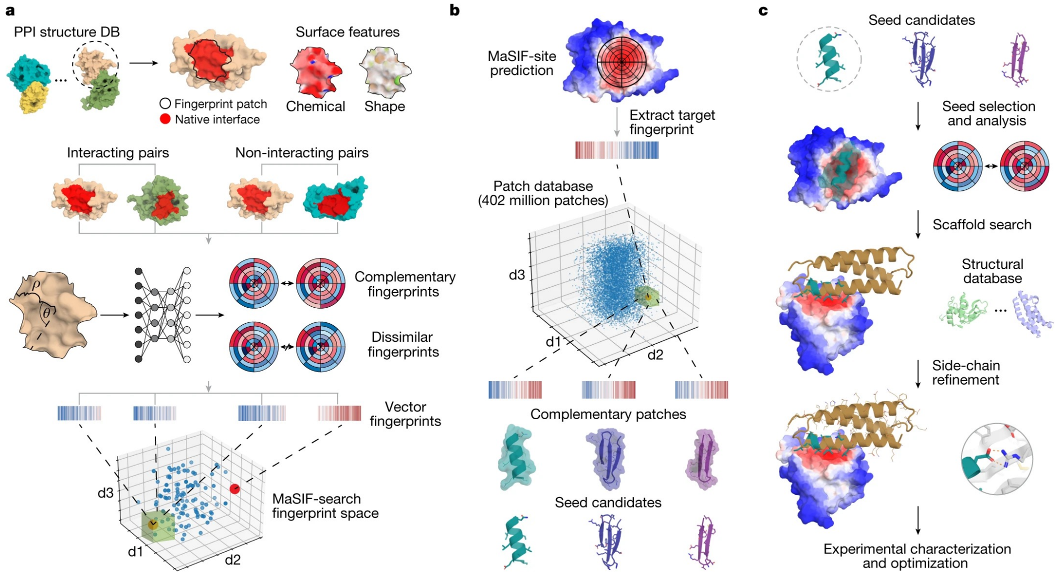

This is a summary of: Gainza, P. *et al.* De novo design of protein interactions with learned surface fingerprints. *Nature* https://doi.org/10.1038/s41586-023-05993-x (2023).

nature > articles > article

Article | Published: 05 April 2023

mRNA recognition and packaging by the human transcription–export complex

Belén Pacheco-Fiallos, Matthias K. Vorländer, Daria Riabov-Bassat, Laura Fin, Francis J. O'Reilly, Farja I. Ayala, Ulla Schellhaas, Juri Rappsilber & Clemens Plaschka

Nature **616**, 828–835 (2023) | Cite this article

RESEARCH BRIEFINGS | 26 April 2023

Step-by-step assembly of a β-barrel protein in a bacterial membrane

Gram-negative bacteria that are resistant to multiple drugs cannot survive without the cell-surface machinery that builds a β-barrel pore structure from outer membrane proteins. Snapshots of different stages in the assembly process provide insights into this crucial mechanism, and could lead to the development of new antibiotics.

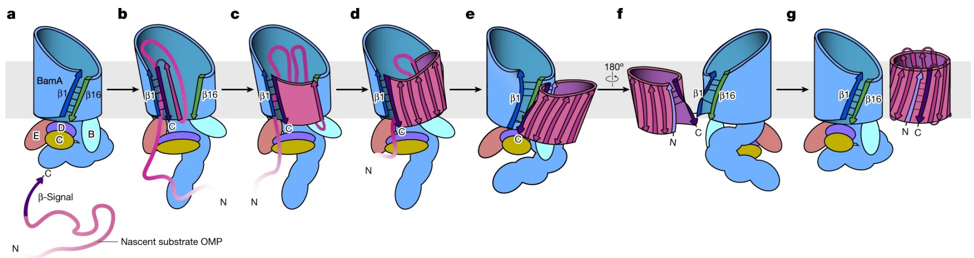

This is a summary of: Shen, C. *et al.* Structural basis of BAM-mediated outer membrane β-barrel protein assembly. *Nature* https://doi.org/10.1038/s41586-023-05988-8 (2023).

Courtesy H. Wacklin-Knecht

Acknowledgements

Colleagues at ILL and ESS


LSS group at ILL outing 2022

Students

Laurence Perino-Gallice
Barry Stidder
Audrey Schollier
Alexis de Ghellinck
Robin Delhom
Loic Joly
Krishna Batchu
Tetiana Mukhina
Ernesto Scoppola
Sebastain Kölher
Giacomo Corucci
Andreas Santamaria
Rachel Morrison
Ida Berts
Jonathan Talbot
Emanuel Schneck
. . .

Collaborators

Thierry Charitat
Jean Daillant
Hanna Wacklin-Knecht
Yuri Gerelli
Laura Cantù
Valeria Rondelli
Alessandra Luchini
Lionel Porcar
Anne Martel
Arnaud Hemmerle
Patricia Bassereau
Debora Berti
Marco Maccarini
Francesca Baldelli Bombelli
Debora Berti
Giuseppe Vitiello
Luigi Paduano
Valerie Laux
Michael Haertlein
Jayne Lawrence
Tommy Nylander
Jian Ren Lu
Michele Sferrazza
Beate Kloesgen
. . .

ILL NEUTRONS FOR SCIENCE
PSCM PARTNERSHIP FOR SOFT CONDENSED MATTER
ess EUROPEAN SPALLATION SOURCE
nmi3
SINE2020
LENS